Targeting the unfolded protein response as a potential therapeutic in prion disease

Mark Halliday

Thesis submitted for the degree of

Doctor of Philosophy

to the University of Leicester

MRC Toxicology Unit

University of Leicester

2014

For my parents, Colin and Ann

Abstract

Many neurodegenerative disorders, including Alzheimer's (AD), Parkinson's (PD) and prion diseases, are associated with the accumulation of misfolded disease-specific proteins. During prion disease, an increase in misfolded prion protein (PrP) generated by prion replication leads to sustained overactivation of the branch of the unfolded protein response (UPR) that controls the initiation of protein synthesis. The UPR is a protective cellular mechanism that is induced during periods of cellular and endoplasmic reticulum stress. UPR activation aims to restore protein homeostasis, by reducing protein translation, and up-regulating chaperone proteins that assist with proper protein folding. However, sustained activation of this pathway results in persistent repression of translation, resulting in the loss of critical proteins that leads to synaptic failure and neuronal death. Inhibiting the UPR by genetic means has recently been shown to be neuroprotective in prion disease (Moreno et al., 2012).

A drug screen was performed in the model organism *C. elegans* to search for inhibitors of the UPR. 34 compounds were identified, of which five were selected for further analysis in *C. elegans* before being tested as a potential treatment in prion diseased mice. Two compounds, dibenzoylmethane and trazodone hydrochloride displayed efficacy against prion disease, and represent novel therapeutic targets. GSK2606414, a specific inhibitor of PERK (protein kinase RNA-like endoplasmic reticulum kinase), a key mediator of the UPR induced translational repression was also tested in prion diseased mice. It restored protein synthesis and prevented the development of clinical prion disease. These data validate the UPR as a viable target in prion disease, and uncover promising potential therapeutics.

Acknowledgements

First and foremost I would like to thank my supervisor Giovanna Mallucci for the opportunity to undertake this work, and for her continued support, mentoring and enthusiasm during my PhD. Special thanks also goes to the members of the Mallucci lab, Julie Moreno, Nick Verity, Helois Radford, Colin Molloy and Diego Peretti, who's friendship and guidance will always be appreciated. Without you all my PhD would not have been such a positive experience, so cheers!

I would also like to thank a number of people in the MRC Toxicology unit and the University of Leicester for guidance and technical assistance. I am grateful to my secondary supervisor Jonathan McDearmid, and my thesis committee, Flaviano Giorgini and Martin Bushell, for helpful comments and suggestions. I am extremely grateful to Jenny Edwards for processing a mountain of brain slices, and to Alison Smart and David White in the CRF for always trying to accommodate my experiments, usually without enough prior warning. I am also thankful to Maria Guerra Martin for various technical assistance and words of encouragement, to David Read for help with microscopy and to John Nellis for too many jobs to list. I would also like to thank our collaborators at the University of Nottingham, Catharine Ortori, Dave Barret and Peter Fischer, for help with pharmacokinetics and for performing the LC-MS/MS experiments.

I would also like to thank my friends in Leicester who have also made my stay here so memorable, especially Matthew Adamson, Paul Ainsworth, Paul Gunderson, Jim Sinclair, Asha Akram, Franco Moreno and Emma Kelsall for all the good times we've had here.

Finally I would like to thank all my family and friends for their love and support, in particular Mum, Dad and Elaine, I couldn't have done this without you.

This work was funded by the Medical Research Council, UK.

Table of contents

List of abbreviations

Aβ	Amyloid β
AD	Alzheimer's disease
ATF4	Activating transcription factor 4
ATF6	Activating transcription factor 6
BACE1	Beta site APP cleaving enzyme 1
BAX	BCL-2 antagonist/killer
BCL-2	B cell lymphoma 2
BPSD	Behavioral and Psychological Symptoms of Dementia
BSE	Bovine spongiform encephalopathy
CHOP	C/EBP homologous protein
CJD	Creutzfeldt-Jakob disease
CNS	Central nervous system
COPAS	Complex Object Parametric Analyzer and Sorter
CREB	cAMP response element-binding protein
DAS	Diallyl sulfide
DBZ	Dibenzoylmethane
DMSO	Dimethyl sulfoxide
DPL	Doppel
EEG	Electroencephalogram
eIF2α	Eukaryotic initiation factor 2α
eIF2α-P	Phosphorylated eiF2α
ER	Endoplasmic reticulum
ERAD	Endoplasmic reticulum associated protein degradation
EV	Estradiol valerate
fCJD	Familial Creutzfeldt-Jakob disease
FFI	Fatal familiar insomnia
GCN2	General control nonrepressed 2
GFP	Green fluorescent protein
GRP78/BiP	78 kDa glucose-regulated protein/ Binding immunoglobulin protein
GSS	Gerstmann-Straussler-Scheinker syndrome

HD	Huntington's disease
H&E	Haematoxylin and eosin
HRI	Heme-regulated inhibitor kinase
IMS	Industrial methylated spirits
IRE1	Inositol-requiring enzyme 1
LC-MS	Liquid chromatography–mass spectrometry
LC-MS/MS	Tandem Liquid chromatography–mass spectrometry
LRRK2	Leucine-rich repeat kinase 2
iCJD	Iatrogenic Creutzfeldt-Jakob disease
IP	Intraperitoneal
kDa	Kilodaltons
mRNA	Messenger RNA
mTOR	Mammalian target of rapamycin
NBH	Normal brain homogenate
NGM	Nematode growth medium
NINDS	National Institute for neurological disorders and stroke
NRF2	Nuclear factor (erythroid-derived 2)-like 2
ORF	Open reading frame
PBS	Phosphate buffered saline
PD	Parkinson's disease
PERK	Protein kinase RNA like endoplasmic reticulum kinase
PERK-P	Phosphorylated PERK
PKR	Protein kinase RNA-activated
PrP	Prion protein
PrP^{C}	PrP cellular
PrP^{Sc}	PrP scrapie
PVDF	Polyvinylidene difluoride
RML	Rocky mountain laboratory
RT	Room temperature
SC	Subcutaneous
sCJD	Sporadic Creutzfeldt-Jakob disease
SEM	Standard error of the mean
SERCA	sarco/endoplasmic reticulum Ca^{2+} ATPase

TBS	Tris buffered saline
TCA	Trichloroacetic acid
Tm	Tunicamycin
Traz	Trazodone hydrochloride
Tri	Trifluoperazine hydrochloride
tRNA	Transfer RNA
TSE	Transmissible spongiform encephalopathy
vCJD	Variant Creutzfeldt-Jakob disease
w.p.i	Weeks post inoculation
XBP1	X box-binding protein 1
[^{35}S]	Radioactive methionine

List of figures

List of tables

Chapter 1: Introduction

1.1 Prion Disease

Prion diseases are rare neurodegenerative disorders, but importantly, they allow access to fundamental mechanisms of neurodegeneration. They are one of a group of neurodegenerative disorders associated with protein misfolding, and uniquely amongst mouse models of neurodegenerative diseases, prion-diseased mice completely recapitulate human disease. This thesis has used mice with prion disease as a means to access basic cellular pathways in neurodegeneration for therapeutic targets.

1.1.1 Background: Neurodegenerative diseases

Neurodegeneration is the progressive loss of the structure and function, and eventual death, of neurons. Neurodegenerative diseases include a plethora of disorders that vary in their incidence, severity, pathology and etiology. They pose an enormous social and economic burden upon society, and by 2040 are predicted to surpass cancer as the second most common cause of death behind heart disease. Dementia is a syndrome characterized by a progressive global cognitive decline and deterioration in intellectual function, and is the most insidious consequence of neurodegeneration. Alzheimer's disease (AD) is the most common cause of dementia, accounting for 50% to 75% of cases. Other important neurodegenerative diseases include Parkinson's disease (PD),

Huntington's disease (HD) and the rarer prion diseases, in which various levels of cognitive impairment are displayed, and are often associated with movement disorders, paralysis or ataxia. Recent estimates for the number of people with dementia worldwide suggest that 18–25 million people were affected in 2000 and that this number will double to 32–40 million by 2020 (Wimo et al., 2003). The largest risk factor for dementia is old age, as only 2% of cases occur in people under 65 years of age. After this point, the prevalence doubles with every five-year increment in age. Prevalence remains constant throughout the world, affecting approximately 1.5% of the population at 65–69 years, and rising to 45% for those aged 95 years or over (Wimo et al., 2003). Treatments for neurodegeneration are scarce and non-curative, so much research effort is being directed to the greater understanding of neurodegenerative diseases and new potential therapeutic options.

Despite having distinct clinical, pathological and biochemical signatures, neurodegenerative diseases such as AD, PD, HD, and prion disease, all share remarkable similarities, including protein aggregation in the brain and neuronal loss. The build up of misfolded proteins on neuropathological examination is the major common feature; this group of diseases is often referred to as protein misfolding disorders. Each disorder exhibits a build up of disease-specific misfolded proteins, amyloid-β (Aβ) in AD, α-synuclein in PD, huntingtin in HD or the prion protein (PrP) in prion disease. Much effort has been directed into elucidating how the build up of these specific misfolded proteins contributes to the pathology of their respective diseases. Aβ is known to be toxic to synapses, reducing synaptic transmission as well as the number of dendritic spines (Yu and

Lu, 2012). The accumulation of α-synuclein can damage mitochondria, leading to cell death in the substantia nigra (Cookson, 2009). Expanded Huntingtin can form inclusion bodies that interfere with normal cellular processes and induce the misfolding of proteins (Hatters, 2008). But as well as these disease-specific toxic mechanisms, are there more general similarities between these neurodegenerative diseases? Neurodegeneration starts with synaptic dysfunction, which leads to the loss of dendritic spines and the postsynaptic density, and ultimately to the failure of neuronal networks and neuronal cell death. Cellular processes such as protein recycling (Rubinsztein, 2006) and mitochondrial dysfunction (Lin and Beal, 2006) have already begun to explain some of the common footprints of neurodegeneration. There are also likely to be other shared features, such as dysregulation of protein synthesis (Halliday and Mallucci, 2014), between theses diseases that can be exploited for therapeutic value, that are only recently being elucidated.

1.1.2 Types of prion disease

Prion diseases, or transmissible spongiform encephalopathies (TSEs), are fatal neurodegenerative diseases that affect humans and animals. Known types of prion disease include scrapie in sheep, bovine spongiform encephalopathy (BSE) in cattle (Hope et al., 1989), chronic wasting disease in mule deer and elk (Williams and Young, 1993), and in humans Creutzfeldt-Jakob disease (CJD), Gerstmann-Straussler-Scheinker syndrome (GSS), fatal familiar insomnia (FFI), kuru and variant CJD (vCJD) (Collinge and Palmer, 1994). They are characterized by the presence of spongiform change, gliosis, amyloidosis and neuronal loss.

Spongiform change appears as a series of holes in brain tissue fixed for histological examination. Astrocyte proliferation and neuronal cell death are other common features, and insoluble amyloid plaques containing aggregates of protease resistant prion protein (PrP^{Sc}) are often correlated with prion diseases. Uniquely in the field of neurodegeneration, prion diseases are transmissible between members of the same species, and often between (mammalian) species, although not freely as species barriers do exist. Transmission can occur by intracerebral or peripheral inoculation, or orally by the transmission of contaminated material.

1.1.3 The history of prion disease

Scrapie was the first prion disease to be described, having been recognized in sheep since 1755 by a Parliamentary inquiry. Affected animals develop a loss of coordination, an uncontrollable urge to itch, ataxia and a progressive paralysis that leads to death. The transmissibility of the disease was demonstrated by Cuillé and Chelle, who succeeded in 1936 in transmitting scrapie to two healthy sheep by intraocular inoculation of brain tissue from an affected animal (Cuillé and Chelle, 1936). Later, ironically, the transmissible nature of the scrapie agent was further established beyond any doubt by the accidental inoculation of hundreds of sheep with scrapie by a vaccine targeted against looping ill virus, which was developed by using lymphoid tissue for animals that were later discovered to have scrapie (Gordon, 1946). The vaccine was formalin treated but failed to prevent scrapie transmission, giving the first insight into the resistance of the infectious agent to chemical treatments. In combination with

the observation that infectivity survived after a dose of ionizing radiation that was incompatible with the biologic integrity of nucleic acids (Alper et al., 1967), a protein only hypothesis of infectivity was proposed (Griffith, 1967), an almost heretical proposition at the time.

Interest in prion diseases took a more human turn when it was recognized that kuru, a fatal neurodegenerative disease that was devastating the Fore people of Papua New Guinea resembled scrapie pathologically (Gajdusek and Zigas, 1957). It was proposed by Hadlow that kuru was an infectious disease (Hadlow, 1959), which was confirmed by the successful transmission to chimpanzees (Gajdusek et al., 1966). It was believed that ritualistic cannibalism was transmitting the disease, which led to a ban on the practice in the late 1950s and an almost complete disappearance of the disease.

The emergence of the bovine spongiform encephalopathy (BSE) epidemic in the UK during the mid 1980s brought prion diseases back to the fore of public and scientific interest, helped (or hindered) by the nickname “mad cow disease”. It is unknown if BSE crossed the species barrier from sheep or if it first occurred sporadically, but its initial impact was amplified by the reprocessing of infected carcasses into cattle feed, leading to a full-blown epidemic. The contaminated cattle fodder was also fed to a variety of other animals, leading to new TSEs in animals such as cats (Wyatt et al., 1991), Arabian oryx and greater kudu (Kirkwood et al., 1990) and a variety of zoo animals, including cheetahs, pumas and ostriches (Kirkwood and Cunningham, 1994). The ease of transmission raised concerns that BSE might be transmissible to humans, and indeed a new

form of CJD, variant CJD (vCJD) was described in 1996 (Will et al., 1996). This aggressive new disease was subsequently proven to be due to BSE exposure (Collinge et al., 1996; Hill et al., 1997), igniting research into the pathogenesis and etiology of prion disease.

1.1.4 Human prion diseases

Human prion diseases share many characteristics with their animal counterparts, such as pathology and disease progression. Prion disease is rare in humans, with an annual incidence of around one case per million worldwide. Despite their rarity, they have been the source of intense interest since the 1960s, because of the phenomenon of kuru and its transmissibility, the emergence of BSE and because of the highly novel biological concepts associated with them. Intense research into human prion diseases has revealed a range of closely related, yet distinct, disorders. They can be sporadic, inherited or acquired in origin, and are characterised as the clinicopathological syndromes of CJD (and its subtypes), GSS, FFI and kuru. Prion disease can only be definitively diagnosed with histopathological examination, but predictive testing for the inherited forms can be performed for specific mutations, by sequencing of the gene that encodes the prion protein, *PRNP*.

Sporadic CJD (sCJD) accounts for 85% of cases of human prion disease, in around one in a million people over the age of 65. Early onset cases are extremely rare. The disease presents with a rapidly progressive dementia with myoclonus and development of movement disorders such as tremor and rigidity. Associated

neurological symptoms include cerebellar ataxia, pyramidal and extra pyramidal signs, and cortical blindness. Most cases have a characteristic electroencephalogram (EEG) that includes periodic sharp-wave complexes. Death occurs after an average of 4 months, making it one the most aggressive forms of neurodegeneration (Gambetti et al., 2003).

Mutations in the gene that encodes the endogenous prion protein, *PRNP*, causes inherited prion disease that accounts for approximately 15% of prion disease cases. There are over 30 different mutations have been described which can produce a wide spectrum of clinical phenotypes (Mallucci et al., 1999) but generally have an earlier onset, but slower disease progression than sporadic cases. These mutations are autosomal dominant, and can result in either an expanded octapeptide repeat in the normal sequence of the prion protein, a non-conservative point mutation or a stop mutation in the *PRNP* open reading frame (ORF). This can lead to familial CJD (fCJD), GSS and FFI. fCJD causes a rapidly progressive dementia with myoclonus and unusual EEG recordings, GSS is characterised by a slow progressive of ataxia and late onset dementia, and FFI is unique with its refractory insomnia, dysautonomia and motor dysfunction. These disease syndromes are not absolute, however: the same mutation can lead to highly divergent phenotypic and pathological variation between individuals (Collinge et al., 1992; Mallucci et al., 1999).

Acquired prion diseases include kuru, iatrogenic CJD (iCJD) and vCJD. Kuru is characterised by progressive cerebellar ataxia, mood and personality changes, and a late onset dementia (Gajdusek and Zigas, 1957). Death occurs after

approximately one year after the emergence of the disease. iCJD is rare, and has occurred after the exposure of patients to contaminated medical treatments or equipment. Contaminated dura matter and corneal grafts, inoculation with human pituitary-derived growth hormone and gonadotrophins have all been reported (Gibbs et al., 1985). Improperly sterilized surgical equipment has also led to iCJD after brain surgery. iCJD caused by intracerebral infection is relatively rapid in onset and duration, with prominent early dementia. Peripheral inoculation is associated with a prolonged incubation time and late onset dementia.

In the mid 1990s, in the wake of the UK BSE epidemic, a new neurodegenerative illness emerged in the UK. Clinically and pathologically it resembled sCJD, but the disease had a longer duration with a protracted neuropsychiatric syndrome, and critically, only affected young people (Batemann et al., 1995: Britton et al., 1995). It was termed new variant, or variant CJD (vCJD). The age of onset was much earlier than sporadic CJD, with a mean age of 29, and patients as young as 16 were diagnosed. The initial symptoms are mainly behavioural, followed by ataxia and movement disorders. Dementia occurs at a much later point in the disease than CJD, with EEG abnormalities frequently absent. It also progresses slower than sporadic CJD, with a mean duration of 14 months. As none of the patients had *PRNP* mutations and were at a very low risk of iatrogenic exposure, BSE was considered to be the most likely cause. Molecular studies on vCJD tissue showed that the biochemical properties of the protease resistant prion protein found in these patients were distinct from other human prion diseases (Collinge et al.,

1996), but similar to that of BSE (Hill et al., 1997), leading ultimately to the acceptance that vCJD is caused by BSE exposure.

1.1.5 The protein only hypothesis of prion infection

The unusual characteristics of the infectious prion agent were first noted by its resistance to formaldehyde degradation (Gordon, 1946), and later its resistance to temperature and ultraviolet radiation (Alper et al., 1966). This led to the hypothesis that prion disease was not caused by bacteria or a virus, but instead consisted entirely of protein that didn't include any nucleic acids (Alper et al., 1967). Griffith suggested how a protein might be able to self replicate and become infectious (Griffith, 1967). The idea didn't gain any traction until Stanley Prusiner purified the scrapie agent, and established that it shared the properties of proteins and not nucleic acids (Prusiner, 1982). Prusiner termed the disease causing agent a "prion", for proteinaceous infectious particle. He expanded on Griffith's theory and developed the protein only hypothesis, that stated that prions can replicate independently of nucleic acids in vulnerable host cells, where the accumulation of replicating proteins leads to the development of prion disease. The causative infectious agent in scrapie was later found to be aggregated, highly insoluble in non-ionic detergents and partially protease resistant, with a relative molecular mass of 27-30kDa (McKinley et al., 1983). This concurred with the protein only hypothesis, so the major constituent of the scrapie agent was designated the prion protein, or PrP. PrP was found to be encoded for by the *PRNP* gene, which interestingly was equally expressed in both infected and uninfected animals (Chesebro et al., 1985). The normal product of

the *PRNP* gene is a protease sensitive protein of 33-35kDa, was designated PrP^{C}, for cellular prion protein, while the previously isolated disease specific protein was called PrP^{Sc} for scrapie associated prion protein.

These two isoforms of PrP share identical primary structures, but differ in secondary and tertiary structure, prompting Prusiner to update his protein hypothesis by proposing that the central mechanism of infectivity involved a change in the normal cellular isoform, PrP^{C}, into PrP^{Sc} (Prusiner, 1989). This conversion is thought to be a post-translational change in conformation that initiates the catalytic conversion of PrP^{C} into more PrP^{Sc}, by the interaction of existing PrP^{Sc} molecules. The brain would become depleted of normal PrP^{C}, stimulating synthesis of more PrP^{C} that would only provide more substrate for the pathological conversion (Figure 1.1.5). This hypothesis shows how sporadic, acquired or inherited forms of prion disease can all develop via the same basic mechanism. In sporadic disease, spontaneous conversion of PrP^{C} into PrP^{Sc} would seed the disease process, while in acquired disease, introduced PrP^{Sc} would begin the catalytic conversion of host PrP^{C}. Familial disease would arise from mutations that increase the likelihood of spontaneous conversion of PrP^{C} to PrP^{Sc}.

Although this model of prion disease transmission is widely accepted, the identity of the actual infectious agent even in purified scrapie infectious fractions remains a source for debate. Only 1 in 10^5 particles appear to be infectious (Bolton and Bendheim, 1991), so the structure of the infectious agent cannot be definitively inferred. The most infectious particles have been shown to be

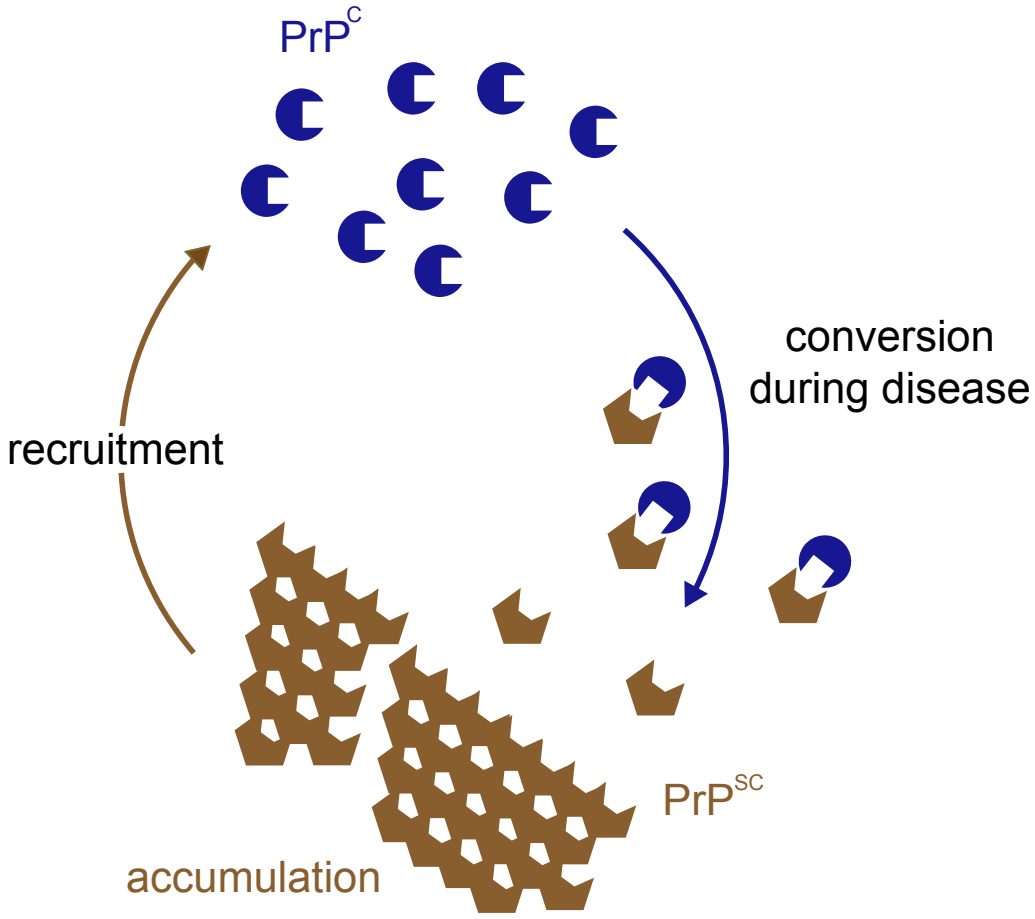

Figure 1.1.5 Model of prion conversion. *PrP^{Sc} causes the catalytic conversion of host PrP^{C}, leading to a buildup of PrP^{Sc}. Due to falling levels of PrP^{C}, more PrP^{C} is produced, providing more substrate for the conversion process.*

non-fibrillar in nature, and comprised of 14-28 PrP molecules, with infectivity significantly reduced in oligomers larger or smaller than this (Silveira et al., 2005). Partial protease resistance is not consistently correlated with infectivity, and non-infective protease resistant PrP can be produced (Riesner et al., 1996). In FFI, PrP^{Sc} is often not detectable in the brain, despite the disease being transmissible (Tateishi et al., 1995). However, it is still likely that PrP is the essential, and probably only component of the infectious agent (Weissmann, 1996).

1.1.6 PrP function

Despite extensive research, the function of PrP^{C} is still unknown. The *PRNP* gene is highly conserved between mammalian species, and is tightly regulated developmentally (Manson et al., 1992), suggesting an essential biological function. Surprisingly, however, knockout mouse models of the mouse *Prnp* gene are developmentally and phenotypically normal (Bueler et al., 1992; Manson et al., 1994a). The possibility that functional compensation was occurring in these knockout models was eliminated by the creation of adult onset, conditional knockout mouse (Mallucci et al., 2002). Here, Cre-mediated excision of the *Prnp* gene occurred around 9-10 weeks after birth. The mice remained healthy after neuronal PrP depletion, confirming PrP's non-essential role and demonstrated that prion neurodegeneration is not caused by loss of PrP function.

Despite the lack of gross abnormalities in PrP null mice, there are some subtle phenotypic differences. Both synaptic function (Collinge et al., 1994) and the

intrinsic properties of hippocampal cells (Mallucci et al., 2002) are altered upon PrP knockout. PrP null mice also have altered circadian rhythms (Tobler et al., 1996), reminiscent of what is observed in FFI. PrP has been shown to be cytoprotective i*n vitro,* reviewed in (Lo et al., 2007). The protein protects human fetal neurons in culture against apoptosis induced by Bax. Bax is a pro-apoptotic member of the Bcl-2 family that plays a major role in postmitotic neurons of the central nervous system (van Delft and Huang, 2006). When human fetal neurons in culture were microinjected with a plasmid encoding Bax, approximately 90% of the neurons underwent apoptosis; but when the neurons were co-injected with both Bax and PrP encoding plasmids, the percentage of apoptotic cells was reduced to ~10% (Bounhar et al., 2001). PrP has also been found to rescue cultured cerebellar granule neurons (Drisaldi et al., 2004) and N2a neuroblastoma cells (Qin et al., 2006) from apoptosis induced by doppel (Dpl). Dpl is a PrP paralog which causes a neurodegenerative phenotype when ectopically expressed in the CNS of $Prnp^{0/0}$ transgenic mice (Moore et al., 1999).

Several lines of evidence suggest that PrP may play a role in protecting cells from oxidative stress. Cerebellar granular and neocortical neurons cultured from $Prnp^{0/0}$ mice are more susceptible than neurons from wild-type mice to treatments with agents that induce oxidative stress, including hydrogen peroxide, xanthine oxidase and copper ions (Brown et al., 2002; Brown et al., 1997). Brain tissue from $Prnp^{0/0}$ mice exhibits biochemical changes indicative of oxidative stress, such as increased levels of protein carbonyls and lipid peroxidation products (Wong et al., 2001). In addition, brain lesions induced by hypoxia and ischemia are larger in $Prnp^{0/0}$ compared to $Prnp^{+/+}$ mice (Spudich et

al., 2005) implicating PrP in protection from oxidative stress. PrP binds to copper with femtomolar affinity (Jackson et al., 2001), leading to its endocytosis, suggesting it may act as a copper transporter in the brain (Brown, 1999).

Several experimental observations suggest that PrP could play a role in synaptic structure, function or maintenance. Incubation of cultured hippocampal neurons with recombinant PrP induces rapid elaboration of axons and dendrites, and increases the number of synaptic contacts (Kanaani et al., 2005), suggesting that PrP plays a regulatory role in synapse formation. It has also been reported that PrP is concentrated at the neuromuscular junction where it is localized in the sub-synaptic sarcoplasm, possibly associated with endosomal structures (Gohel et al., 1999). In addition, nanomolar concentrations of recombinant PrP have been found to potentiate acetylcholine release at the neuromuscular junction (Re et al., 2006). PrP has also been discovered to be necessary for peripheral myelin maintenance in aged mice in several knockout mouse models (Bremer et al., 2010).

1.1.7 Prion disease in mice

There are currently many animal models available to researchers that aim to recapitulate the symptoms and pathology of neurodegenerative disease. Most rely on the introduction of known mutations that have been shown to increase the risk of disease, or the overexpression of the disease related misfolding protein. Although these models have proved to be extremely useful in understanding some aspects of specific disorders, they often do not produce

neuronal cell death, the major pathological event in diseases such as AD, PD and HD, see for review (Jucker, 2010). Prion infected mice do develop stereotypical prion disease with the resultant symptoms and neuronal cell death, making them an extremely important and useful model.

Prion disease in mice begins with a reduction in the number of synapses. Later, behavioural signs such as decreased burrowing activity and loss of object recognition memory, as well as a reduction in hippocampal synaptic transmission and the first neuropathological changes, are all established. Extensive neuronal degeneration follows, with the animals becoming clinically ill several weeks later, the timing depending on the strain of both the infectious prions and that of the recipient mice. In particular, the incubation period and onset to death is inversely related to levels of PrP in the infected mice (Bueler et al., 1993; Manson et al., 1994b).

In this thesis tg37 mice were used. They over-express PrP at around 3 fold wild type levels, and succumb to Rocky Mountain laboratory (RML) prion infection at around 12 weeks post infection (w.p.i) (Mallucci et al., 2002), but are otherwise phenotypically equivalent to wild-type mice. They demonstrate an abrupt reduction in the number of synaptic proteins at 9 w.p.i, with a concurrent decrease in translation. This correlates with increasing accumulation of the misfolded prion protein, a further decrease in synaptic number and a critical decline in neurotransmission (Figure 1.1.7) (Moreno et al., 2012). Control mice are injected with normal brain homogenate (NBH).

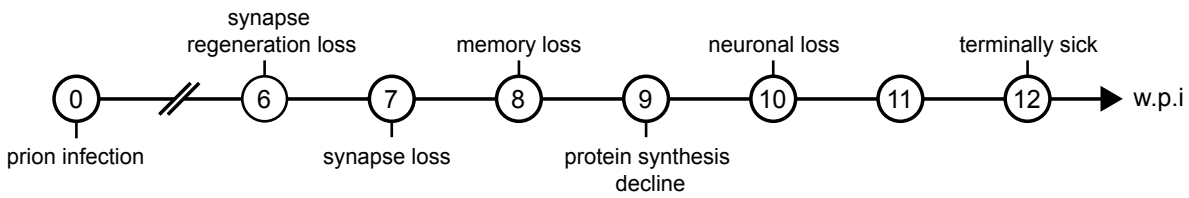

Figure 1.1.7 Time course of prion disease in tg37 mice*. The first pre-symptomatic changes occur at 7 w.p.i, with cognitive deficits developing at 8 w.p.i. Neuronal death occurs at 10 w.p.i, and clinical signs of terminal disease emerge at 12 w.p.i.*

Prion disease in mice is diagnosed via the observation of a variety of signs of varying severity. Early indicator signs of prion disease are a rigid, raised tail, hind limb clasping when the animal is held by the tail, piloerection, mild loss of co-ordination or an unsustained hunched posture. Confirmatory signs of prion disease include ataxia, impairment of the righting reflex, dragging of limbs, sustained hunched posture or significant abnormal breathing. The presence of two early indicator signs and one confirmatory sign, or two confirmatory signs is used to diagnose prion disease. The time to confirmation of prion disease is termed the scrapie incubation time.

1.1.8 Models of prion disease in lower organisms

Genetic experiments in mice, which are central to the study of the molecular basis of neurodegenerative disorders, have certain limitations that include slow

pace and high costs. Therefore, neurodegeneration is often modeled in genetically tractable organisms, including yeast, and *C. elegans*. Yeast have proven especially useful in the study of prion replication and propagation. An analogous mechanism for prion propagation has been discovered and elucidated, after the discovery of a group of proteins that have so-called prion domains, characterized by enrichment of glutamines and asparagines (Michelitsch and Weissman, 2000). With low probability, these proteins can change conformation to form self-propagating aggregates, which can be transmitted to daughter cells, and like PrP^{Sc} in humans and mice, yeast prions efficiently recruit soluble molecules of the same species, thus inactivating them (Wickner et al., 2001).

Mammalian PrP expressed in yeast also has a tendency to aggregate and can acquire the protease-resistant prion conformation (Ma and Lindquist, 1999). Normally PrP is synthesized in the ER, where it is folded and further transported to the plasma membrane (Lehmann et al., 1999). However, experiments with yeast demonstrated that a small fraction of PrP is transported from the ER lumen back to the cytosol where it is rapidly degraded by the proteasome (Ma and Lindquist, 2001). Importantly, there is a fraction of molecules in the cytosol that escape degradation and convert to the prion state. This implies there are conditions, or perhaps the presence of other proteins, that promote PrP misfolding in the cytosol. This is corroborated by experiments in mammalian cell culture that removed the PrP membrane signaling sequence and observed a large increase in the levels of misfolded PrP (Ma and Lindquist, 2002), which when performed in mice, led to a rapid neurodegeneration (Ma et al., 2002).

C. elegans models of prion disease have also been developed. Park and Li expressed the cytosolic fragment of the mouse prion protein in the worm, eliciting a range of toxic phenotypes that differed in their severity but not in the levels of the prion fragment, which the authors suggested may be due to differing folding states of the fragment (Park and Li, 2008). The expression of octarepeat-expanded PrP in *C. elegans* mechanosensory neurons led to partially protease resistant protein aggregates and progressive loss of response to touch without causing cell death, whereas wild-type PrP expression did not alter behavior (Bizat et al., 2010). This phenotype was found to be protected by the activation of sirtuins induced by the polyphenol resveratrol (Bizat et al., 2010). Expression of the yeast prion like protein Sup35 in *C. elegans* can also induce protein misfolding, aggregation and toxicity (Nussbaum-Krammer et al., 2013). The toxic aggregates co-localized to autophagy-related vesicles that transport the prion-like protein from the site of expression to adjacent tissues. This was associated with cell autonomous and cell non-autonomous disruption of mitochondrial integrity and loss of proteostasis, suggesting how prions can transmit between neurons by co-opting the autophagy-lysosome pathway (Nussbaum-Krammer et al., 2013).

1.1.9 Mechanisms of neurotoxicity in prion disease.

It is still unknown how conversion of PrP^{C} to PrP^{Sc} causes prion disease. The conversion needs to occur within neurons for it to be toxic, as extraneuronal conversion can occur with no obvious detrimental effects (Chesebro et al., 2005; Mallucci et al., 2003). It was long assumed that PrP^{Sc} was directly toxic to

neurons, but this has only been demonstrated *in vitro*, not *in vivo*. The weak correlation between PrP^{Sc} deposition and clinical signs also agues against this. Indeed, there are some prion diseases in which PrP^{Sc} levels are low, and subclinical disease states with high levels of PrP^{Sc} deposition (Hill and Collinge, 2003).

PrP null mice do not develop prion disease, demonstrating that prion disease is not caused by the loss of function of PrP^{C} (Bueler et al., 1993). But importantly, PrP null mice are resistant to scrapie (Bueler et al., 1993), indicating that PrP^{C} is required for prion disease. Brandner and colleagues grafted neural tissue overexpressing PrP^{C} into the brain of PrP null mice (Brandner et al., 1996). After inoculation with prions, the grafts accumulated high levels of PrP^{Sc} and developed the severe histopathological changes characteristic of prion disease. Substantial amounts of graft-derived PrP^{Sc} migrated into the surrounding areas of the host brain, but even 16 months after inoculation no pathological changes were seen in PrP null tissue (Brandner et al., 1996). Therefore, in addition to being resistant to scrapie infection, brain tissue devoid of PrP^{C} is not damaged by exogenous PrP^{Sc}, providing further evidence that PrP^{Sc} is not directly toxic *in vivo*. Critical evidence came from experiments in which PrP^{C} was depleted during the course of prion infection (Mallucci et al., 2003). Double transgenic mice were generated that had floxed PrP transgenes, from which PrP coding sequence is deleted by neuronal Cre recombinase expression at 9 weeks of age. When these mice are inoculated with prions before PrP knockout, they develop the initial stages of prion disease, including spongiosis and hippocampal shrinkage. When the Cre-mediated excision of the *Prnp* gene occurred, prion disease was

prevented from developing and the early spongiform changes were reversed, despite continued prion replication in non-neuronal cells and further astrocytic extra-neuronal PrP^{Sc} deposition. The mice lived for the normal lifespan, and remarkably, they never developed further clinical disease. These results also argue against direct neurotoxicity of PrP^{Sc}, because the continued non-neuronal replication and accumulation of PrP^{Sc} throughout the brains of scrapie-infected mice is not pathogenic.

It is clear that the major pathological changes in prion disease do not result from the loss of PrP^{C}, and PrP^{Sc} is not enough by itself to cause disease, and is absolutely dependent on the presence of PrP^{C} for neurotoxicity. This has led to the hypothesis that a neurotoxic intermediate is formed during the conversion of PrP^{c} to PrP^{Sc} (Hill and Collinge, 2003). This mirrors the potential mechanisms of neurotoxicity of amyloid β (Aβ) in Alzheimer's disease (Hardy and Selkoe, 2002) and other protein misfolding disorders (Kayed et al., 2003).

Even if the identity of a toxic intermediate remains elusive, it is clear that the process of prion replication does induce toxic processes in neurons. It has recently been demonstrated that the induction of the unfolded protein response (UPR) by prion replication contributes to the neurotoxicity of prion disease (Moreno et al., 2012). These findings and the UPR will be discussed in more detail in section 1.2.

1.1.10 Therapeutic approaches to prion disease

Uncertainties around the identity of the neurotoxic species and the mechanisms of neurodegeneration in prion disease have hindered therapy, and unfortunately prion diseases are invariably fatal due to there being no available effective treatments. The lack of preclinical diagnostic testing for sporadic and acquired prion disease compounds the problem, as diagnosis relies on clinical symptoms that reflect an advanced stage of neurodegeneration.

Most treatment options in the past have focused on targeting PrP^{Sc}, due to its association with pathology and infectivity. Several compounds have been found to reduce PrP^{Sc} accumulation, but most perform much better in *in vitro* assays compared to *in vivo* experiments, see Trevitt and Collinge for review, (Trevitt and Collinge, 2006). Many of the substances only work when administered with, or soon after, the prion inoculation, because they reduce prion titre. Pentosan polysulphate was one of the most promising compounds previously tested (Doh-ura et al., 2004), but tests in humans have been disappointing (Todd et al., 2005). Phosphorothioate oligonucleotides have been shown to inhibit PrP^{Sc} formation (Kocisko et al., 2006), but they do not readily cross the blood-brain barrier, and intracerebral infusion was not well tolerated.

As the conversion of PrP^{C} to PrP^{Sc} is now known to be central to the pathogenesis of prion disease, and prion toxicity is abrogated by the depletion of neuronal PrP^{C} (Mallucci et al., 2003), therapeutics inhibiting this process either directly or

by targeting PrP^{C} are now the focus. Ligands that bind to PrP^{C} directly may prevent its conversion to PrP^{Sc} by blocking the catalytic conversion or stabilizing the molecule. The maintenance of effective brain levels of drugs that reduce prion propagation rates to below those of natural clearance mechanisms could plausibly cure prion infection, but to date none have been discovered, see for review (Mallucci and Collinge, 2005)

Antibodies that bind to PrP^{C} are also theoretical therapeutic options. Antibodies raised against several PrP epitopes can inhibit replication in vitro, and mice expressing anti-PrP μ chains are protected against peripheral, but not central prion infection (Heppner et al., 2001). Passive immunisation of peripherally infected mice with anti-PrP antibodies markedly reduced PrP^{Sc} accumulation, but again failure to cross the blood brain barrier prevented a central therapeutic effect (White et al., 2003). However, intracerebral administration of the antibodies was reported to cause severe neuronal apoptosis (Solforosi et al., 2004). This finding was challenged in 2012, when humanized anti PrP antibodies were stereotaxically injected into mouse hippocampi, and found not to induce any observable apoptosis (Klohn et al., 2012). However, Sonati et al., observed rapid neurotoxicity in mice and cerebellar organotypic cultured slices exposed to several anti PrP antibodies (Sonati et al., 2013). Humanized anti-PrP monoclonal antibodies might still find use for post-exposure prophylaxis of particular at-risk groups.

To date, the only approach that is effective for the prevention of clinical disease in animals with established prion disease is the removal of neuronal of PrP^{C}

through genetic knockout (Mallucci et al., 2003) or RNA interference (RNAi) (White et al., 2008). Genetic knockout effectively cured prion disease by removing the substrate of the PrP^{C} to PrP^{Sc} conversion, identifying PrP^{C} as a valid and important therapeutic target (Mallucci et al., 2003). Importantly, this knockout was still effective even after the onset of the disease, offering hope that prion disease in humans will be able to be cured even after diagnosis via the observation of symptoms. This was strengthened by the observation that cognitive and behavioral deficits and impaired neurophysiological function that accompany early hippocampal spongiform pathology could also be reversed (Mallucci et al., 2007). This demonstrated that early functional impairments precede neuronal loss in prion disease and can be rescued. However, this work relied on genetic engineering that is not possible in humans. RNA interference is a method of gene knockdown that may be of therapeutic value to humans. White et al., injected lentivirus containing PrP RNAi into the hippocampi of mice with prion disease (White et al., 2008). They observed increased lifespan, a prevention of the onset of behavioral deficits associated with early prion disease, reduced spongiform degeneration, and reduced neuronal loss. This approached relied on sterotaxic injection of lentivirus into the brain, which is many years away from becoming a regular treatment in humans, due to potential immune reactions and the possibility of insertional mutagenesis (Pauwels et al., 2009). Small molecules are still that most desirable form of treatment, especially when treating disorders of the central nervous system.

Recent evidence has revealed the effector pathway downstream of prion replication that mediates prion neurotoxicity: over-activation of the unfolded

protein response (Moreno et al., 2012). Further, targeting this pathway is therapeutically beneficial in prion disease (Moreno et al., 2013; Moreno et al., 2012). Thus the unfolded protein response has recently emerged as a new therapeutic target in prion disease, and possibly other neurodegenerative disorders, as discussed in section 1.2.

1.2 The unfolded protein response (UPR)

The UPR is a protective cellular mechanism that is induced during periods of cellular and endoplasmic reticulum (ER) stress. Secreted and transmembrane proteins enter the ER as unfolded proteins to be properly assembled, or to be targeted for degradation. The UPR maintains the protein-folding homeostasis within the ER, ensuring the proper functioning of the produced proteins, and therefore the cell. A variety of conditions can interfere with this process and cause ER stress, including amino acid deprivation, viral replication and, as the name suggests, the presence of unfolded proteins (Ron and Walter, 2007). This activates the UPR, which seeks to restore the normal functioning of the ER, using multiple strategies that act individually and in synergy. Chaperone proteins are produced to prevent protein aggregation and facilitate correct protein folding (Sitia and Braakman, 2003). Protein translation is temporarily reduced to lower the amount of proteins present in the ER (Zhao and Ackerman, 2006). Lipid synthesis is also stimulated to increase ER volume, and the degradation of unfolded proteins is induced by activating the endoplasmic reticulum-associated protein degradation (ERAD) pathway (Meusser et al., 2005).

1.2.1 The three arms of the UPR

When misfolded proteins accumulate within the ER, GRP78/BiP dissociates from three proteins that mediate the UPR stress response: protein kinase RNA like endoplasmic reticulum kinase (PERK), inositol-requiring enzyme 1 (IRE1) and activating transcription factor 6 (ATF6) (Lai et al., 2007). Dissociation of

GRP78/BiP from PERK, IRE1 and ATF6 allows the activation of these factors resulting in the induction of three UPR-related pathways (Figure 1.2.1).

Activation of PERK leads to a reduction in global protein synthesis via the phosphorylation of eukaryotic initiation factor 2α (eIF2α) (Harding et al., 1999). This phosphorylation causes an eIF2α-mediated translational repression, which halts protein synthesis, helping to alleviate the overload of unfolded proteins inside the ER. There are also three other kinases that can phosphorylate eIF2α, each of which is activated by a different cellular stress: Protein kinase RNA-activated (PKR) responds to viral infection (Clemens, 2004), general control nonrepressed 2 (GCN2) is activated during amino-acid starvation (Deng et al., 2002), and the heme-regulated inhibitor kinase (HRI) represses protein synthesis in heme-deficient erythroid cells (Han et al., 2001). Once the ER stress has been resolved and any unfolded proteins have been removed, the translational repression is reversed by dephosphorylation of eIF2α by the phosphatase GADD34 (Novoa et al., 2001). Although the phosphorylation of eIF2α causes the reduction in the synthesis of most proteins, some are upregulated like transcription factor 4 (ATF4) (Blais et al., 2004). ATF4 is a key transcription factor involved in the regulation of genes related to protein folding, amino acid metabolism and redox control (Ma and Hendershot, 2003). Important targets of ATF4 include Nrf2, which regulates the functions of a variety of antioxidant genes (He et al., 2001), and CHOP, which conversely is key in the activation of apoptotic pathways and cell death (Han et al., 2013).

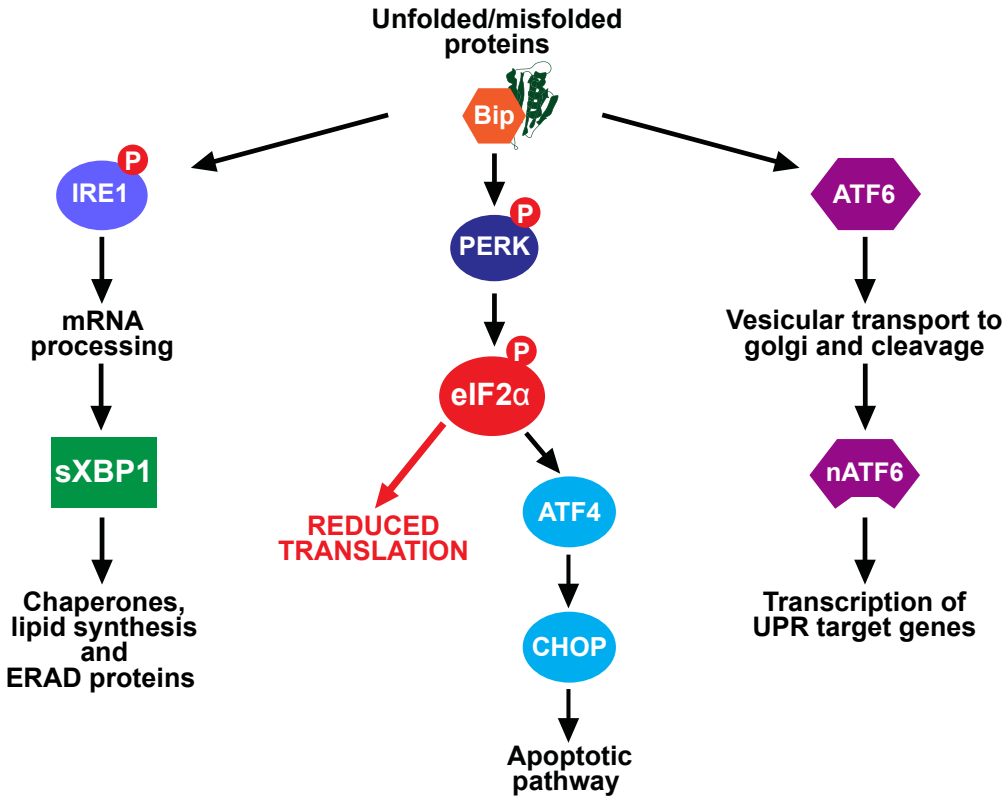

Figure 1.2.1 Schematic of the unfolded protein response. *After the detection of unfolded proteins by GRP78/BiP, the three arms of the UPR (PERK, IRE1 and ATF6) are activated. The PERK arm causes a reduction in global protein synthesis via the phosphorylation of eIF2α. Activation of IRE1 leads to XBP1 splicing and the transcription of chaperones and ERAD proteins. ATF6 is cleaved to nATF6, which leads to the expression of a variety of UPR target genes.*

There are two paralogs of IRE1: IRE1α and IRE1β (Wang et al., 1998). IRE1α is a kinase and endoribonuclease, that when activated, catalyzes the splicing of the mRNA encoding the transcription factor X box-binding protein 1 (XBP1), removing a 26 base-pair intron (Calfon et al., 2002). This splicing changes the reading frame of the XBP1 mRNA, resulting in a potent transcription factor that regulates a subset of UPR targets genes involved in ER protein synthesis and folding, ERAD, autophagy and redox metabolism (Acosta-Alvear et al., 2007). IRE1β controls the site-specific cleavage of 28S rRNA, which contributes to translational repression (Iwawaki et al., 2001).

ATF6 has a CREB/ATF bZIP transcription factor domain at the amino terminus. Upon accumulation of unfolded proteins in the ER, ATF6 is released from Grp78/BiP, and is trafficked to the Golgi apparatus where it is cleaved by site 1 and site 2 proteases at the transmembrane site, yielding a cytosolic fragment known as ATF6 p50 (or nATF6), which migrates to the nucleus to activate UPR gene expression (Haze et al., 1999). The chaperones GRP78/BiP and GRP94, the transcription factors CHOP and XBP1 as well as other proteins such as p58IPK/DNAJC3 and SERCA are all induced by ATF6 (Bravo et al., 2013). ATF6 also plays a role in regulating ER volume increases and stimulates cellular adaptation to chronic ER stress (Ron and Walter, 2007).

1.2.2 The UPR in prion disease

Recent evidence has demonstrated the importance of the UPR in prion disease (Moreno et al., 2012) and Figure 1.2.2). The authors observed that during the

course of prion infection there was an abrupt marked reduction in synaptic protein levels. This could result from increased degradation, or decreased synthesis. The ubiquitin proteasome pathway is known to be inhibited in prion disease, causing a reduction, not an increase, in protein degradation (Andre and Tabrizi, 2012). In contrast, Moreno and co-workers found that protein synthesis was reduced through dysregulated translational shutdown mechanisms, due to over-activation of the UPR. They showed a progressive increase in phosphorylated PERK (PERK-P) and eIF2α (eIF2α-P) as prion replication and prion disease progresses, with uncompensated shutdown in translation, causing a catastrophic reduction in the levels of protein synthesis (Moreno et al., 2012). Preventing the effects of this branch of the UPR from being terminated, by using the drug salubrinal that prevents dephosphorylation of eIF2α-P, accelerated the disease, while genetic manipulation of the UPR protected against neuronal death and increased lifespan. Overexpression of GADD34, the phosphatase that dephosphorylates eIF2α-P and restores protein translation was found to be protective in prion disease, demonstrating that inhibiting the UPR is a viable therapeutic target (Moreno et al., 2012). RNAi of PrP that had previously been established as neuroprotective (White et al., 2008) was also shown to lead to a reduction in UPR activation, as upstream protein load was reduced and UPR activation abrogated, with the associated benefits of increased translation and lifespan.

There is also other evidence for a role of the UPR in prion disease. Upregulation of several chaperones and ER stress proteins such as GRP78/BiP, GRP94 and GRP58/ERp57 is observed in patients with CJD, as well as in some mouse models

of prion disease (Hetz et al., 2003; Yoo et al., 2002). This suggests ER stress and abnormal homeostasis is a feature of prion disease. One of the ER's most important roles is in calcium homeostasis and signalling, and the ER contains the largest intracellular store of calcium in the cell. Disruption of calcium homeostasis, and the resulting ER stress, has emerged as another component of the development of prion disease. Exposing N2A cells to purified PrP^{Sc} from the brain of scrapie-infected mice induces the release of calcium from the ER stores as well as ER stress. This is associated with the upregulation of several chaperones that are involved in the UPR, that are also found in the brains of CJD patients, such as GRP78/BiP, GRP94 and GRP58/ERp57 (Torres et al., 2010). Cells chronically infected with prions are more susceptible to ER stress mediated cell death, linked with a stronger UPR activation after exposure to ER stress-inducing agents such as tunicamycin and thapsigargin (Torres et al., 2010).

ER stress can also facilitate the generation of intermediary misfolded forms of the prion protein, increasing its vulnerability to conversion into the misfolded PrP^{Sc} form *in vitro* (Orsi 2006). PrP^{Sc} has also been shown to result in the accumulation of proteins in the ER, which can lead to ER stress induced apoptosis (Wang et al., 2011).

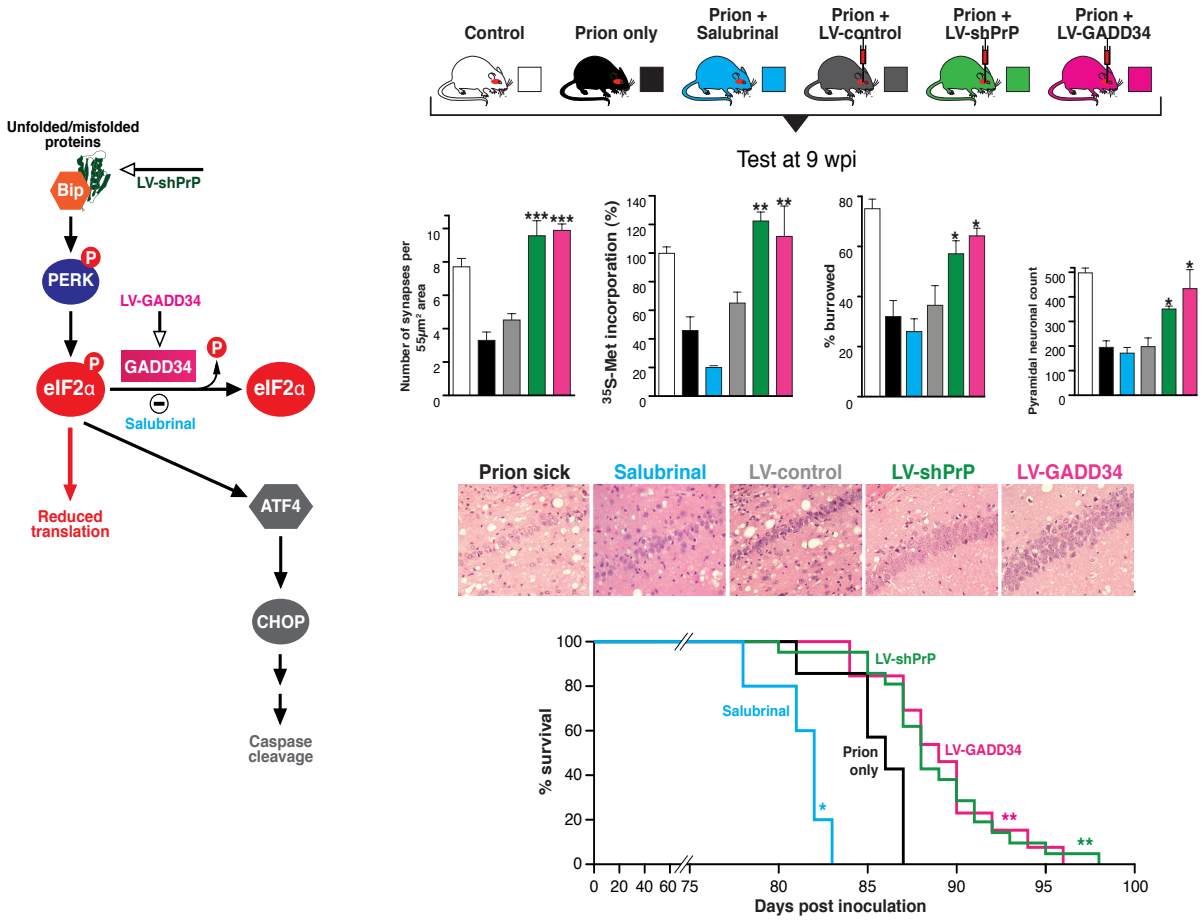

Figure 1.2.2. Manipulation of the UPR changes the progression of prion disease*. RNAi against PrP (green), or overexpression of GADD34 (pink) restored synaptic protein levels, synaptic transmission, burrowing behaviour, synapse number and neuronal pathology, while also increasing lifespan in prion disease when compared to untreated prion diseased mice (black) or empty vector controls (grey). Salubrinal (blue) had a detrimental effect in the same experiments. Reproduced from Moreno et al., 2012.*

1.2.3 The UPR in Alzheimer's disease

There have been multiple reports of UPR activation in the brains of Alzheimer's patients (Hamos et al., 1991; Hoozemans et al., 2009; Hoozemans et al., 2005). Importantly, PERK-P and eIF2α-P are also widely reported to be associated with AD post mortem brains (Chang et al., 2002; Nijholt et al., 2011; O'Connor et al., 2008). eIF2α-P levels correlate with elevated BACE1 (an enzyme that cleaves the amyloid precursor protein into Aβ) levels in transgenic mice as well as AD patient brains (O'Connor et al., 2008). Levels of GRP78/BiP, the ER stress sensor and UPR activator, are increased in the temporal cortex and the hippocampus of AD cases compared to non-demented control cases (Hoozemans et al., 2005). A comparison of the expression of GRP78/BiP in the different Braak stages of AD suggests that UPR activation occurs early in AD.

Treatment of cells with Aβ peptides leads to the activation of ER specific caspases, that correlates with the induction of apoptotic cell death (Nakagawa et al., 2000). Exposing cells to Aβ oligomers or fibrils in different experimental models can also trigger ER stress, which has been shown to lead to the phosphorylation of eIF2α, PERK and other indicators of UPR activation (Katayama et al., 2004).

UPR activation is also associated with hyperphosphorylated Tau. PERK-P has been observed in neurons and glia that exhibit tau pathology (Nijholt et al., 2011). IRE1 and PERK phosphorylation have also been observed in patients affected with AD, as well as a wide range of frontotemporal dementias that

exhibit tau pathology (Nijholt et al., 2012). *In vitro* studies suggest that the induction of ER stress by the exposure of cells to Aβ oligomers correlates with the induction of Tau phosphorylation, suggesting a link between ER stress, Aβ mediated neurotoxicity and Tau hyperphosphorylation (Resende et al., 2008). Importantly, induction of UPR signalling has been shown to induce Tau phosphorylation, possibly via the activation of glycogen synthase kinase 3β (GSK-3β) (Sakagami et al., 2013), demonstrating a direct link between UPR activation and neurodegenerative processes. Neurons displaying PERK-P co-express active GSK-3β in AD brains, suggesting a possible mechanism (Hoozemans et al., 2009). ERAD has been shown to be blocked by tau accumulation, leading to UPR activation in the tg4510 mouse model of tau pathology (Abisambra et al., 2013), demonstrating a novel mechanism of tau toxicity via the disruption of normal proteostasis.

1.2.4 The UPR in Parkinson's disease

The UPR has been shown to be activated in dopaminergic neurons of the substantia nigra bearing α-synuclein inclusions in the brain of patients affected by Parkinson's disease (PD), suggesting that the UPR may be involved in dopamine neuron degeneration (Hoozemans et al., 2007). α-synuclein has also been shown to accumulate within the ER, directly activating the PERK arm of the UPR by binding to GRP78/BiP (Bellucci et al., 2011). Additionally, the accumulation of α-synuclein in dopaminergic cells increased the expression of GRP78/BiP and induced the expression of the UPR-related transcription factor

ATF4. The authors also suggested that activation of the UPR pathway in cells by α-synuclein, coincided with pro-apoptotic changes (Bellucci et al., 2011).

The A53T missense mutations in the gene coding for α-synuclein causes dominant familial PD. This mutation is associated with UPR activation, as observed by an increase in CHOP and GRP78/BiP expression, and increased phosphorylation of eIF2α, suggesting the UPR is active in these cells (Smith et al., 2005). ER stress leads to mitochondrial dysfunction, but inhibition of caspase-12, a downstream caspase of UPR activation (Nakagawa et al., 2000), protected the A53T α-synuclein overexpressing cells from cell death, suggesting that the activated UPR was inducing apoptosis (Smith et al., 2005).

LRRK2 mutations also cause dominant familial PD, by impairing protein degradation pathways in an age dependent manner. This leads to the build up of α-synuclein and ubiquitinated proteins, impairment of autophagy, and increased apoptosis, which is likely to lead to the build up of unfolded proteins (Tong et al., 2010).

Mutations in Parkin result in an impairment of the ubiquitin proteasome pathway, which can result in the accumulation of misfolded proteins within neurons and may underpin the development of PD in people with this mutation (Imai et al., 2000). Parkin has been shown to be upregulated via ATF4, following ER stress and this event is associated with neuroprotection. It was also found that CHOP could down-regulate Parkin expression. These findings suggest wild-type Parkin plays a protective role following ER stress by preventing stress

induced mitochondrial damage, and the loss of function of Parkin due to mutation can be a factor in the development of PD.

1.2.5 Current treatments targeting the UPR

There are several points in the UPR pathway that allow access to potential therapeutic modulation. As reducing eIF2α-P levels by genetic means was found to be neuroprotective in prion disease (Moreno et al., 2012), achieving the same reduction using a drug is also predicted to be neuroprotective. Blocking the formation of misfolded PrP that causes the phosphorylation of eIF2α, inhibiting eIF2α phosphorylation directly, or increasing the amount of dephosphorylation by modulating GADD34 would accomplish this. Targeting PrP has been the subject of intense research, but so far none of the drugs tested have found much efficacy in the clinical setting (Trevitt and Collinge, 2006), so exploring other approaches will be valuable. Increasing the activity of GADD34 would require allosteric modulation of the protein or an increase in its transcription, both of which are hard to stimulate via a drug. Inhibiting PERK is an attractive target as it is "druggable". Indeed, protein kinases have become the second most important class of drug targets after G-protein coupled receptors (Cohen, 2002). Importantly, compounds for pharmacological inhibition of PERK have recently been developed for use as anti-tumour agents (Atkins et al., 2013; Axten et al., 2012). It is possible that these, or related compounds optimised for penetration of the blood brain barrier, would be potential therapeutic agents or allow for the development of compounds for treatment of the over-activation of the PERK

branch of the UPR. This thesis tests one such compound as a possible therapeutic agent in prion disease (see chapter 5).

Indeed, recent evidence is demonstrating the efficacy of targeting the UPR in neurodegenerative disease. Ma et al., deleted the PERK and GCN2 genes in a mouse model of Alzheimer's disease, causing a reduction in the amount of phosphorylated eIF2α (Ma et al., 2013). This reduced deficits in synaptic plasticity and memory exhibited by these mice. Sidrauski et al., screened for inhibitors of PERK signaling, and identified a small molecule, ISRIB, that potently reverses the effects of eIF2α phosphorylation, although the exact mechanism of action is not clear (Sidrauski et al., 2013). ISRIB-treated mice display significant enhancement in spatial and fear-associated learning, making it a promising potential therapeutic.

1.3 Using *C. elegans* to screen for inhibitors of the unfolded protein response

Given that the UPR is a target in neurodegenerative disease, screening for and testing drugs that inhibit the UPR is likely to be a useful approach in the search for potential new therapies. The nematode worm *C. elegans* is an extremely useful model organism for the screening of a large number of compounds, and due to its highly homologous UPR, it is likely that it can provide a useful tool in the search for therapeutics that target the UPR.

1.3.1 The model organism *C. elegans*

In the late 1960s, Sydney Brenner began the search for a new invertebrate model organism with the dedicated goal of studying the genetics of its development, the nervous system and how its nervous system controls behaviour. He chose the soil dwelling nematode worm *Caenorhabditis elegans*, one of the simplest multicellular organisms in existence. Despite containing fewer than a thousand somatic cells, and measuring barely a millimeter, *C. elegans* has a multitude of cell types and a fully functioning nervous system. His choice was vindicated when he demonstrated the ease with which *C. elegans* could be grown, maintained and genetically manipulated in *The genetics of Caenorhabditis elegans* (Brenner, 1974) after which *C. elegans* research took off in earnest.

There are many advantages to studying *C. elegans* as a model organism. It is transparent throughout its life span, allowing non-invasive observations of cell

development and gene expression via fluorescent markers. Each worm grows and develops in a stereotypical and conserved fashion, with each animal containing an identical number of cells – 959 in the hermaphrodite and 1031 in the male, allowing the easy identification of genetic defects between animals. It has a short life span of two to three weeks, and the hermaphrodites can self fertilise or be crossed with male worms, making it very amenable to genetic study. It can be grown easily like a microorganism on agar plates and fed with a bacterial lawn of *E. coli*, and also frozen for long-term storage and recovery. Most importantly, it also contains approximately 20,000 genes, of which 6000 have direct human homologues.

1.3.2. The *C. elegans* nervous system

The nervous system of *C. elegans* has been studied intensively, which at 302 neurons is complex for such a small organism but simple enough to allow the exact role of each neuron to be determined. The exact connectivity of the nervous system has been mapped out (White, 1986), revealing 118 neuron classes and 5000 synapses that control a surprisingly complex set of behaviours (Thomas, 2001). These include the sensation and distinction of diverse mechanical, chemical, olfactory and thermal stimuli and complicated patterns of movement during mating and, most surprisingly for such a small number of cells, various forms of associative learning. By using mostly genetic approaches, a plethora of components of synaptic neurotransmission has been linked to the individual neurotransmitters that have been identified in the worm. The study of the behavioural consequences of perturbations in the function of these

components and neurotransmitters is currently only paralleled by similar approaches carried out in the fruitfly *Drosophila melanogaster*.

1.3.3. Genetics and life-cycle

C. elegans has two sexes: hermaphrodites and males. Individuals are almost all hermaphrodite, with males comprising just 0.05% of the total population on average. The basic anatomy of *C. elegans* includes a mouth, pharynx, intestine, gonad, and a thick cuticle. After hatching, *C. elegans* pass through four juvenile stages (L1–L4). They can also enter an alternative third larval stage called the dauer state if the environment become crowded or there is a lack of food (Figure 1.3.3). Dauer larvae are stress-resistant and do not age. When self-inseminated the hermaphrodite worm will lay approximately 300 eggs. When inseminated by a male, the number of progeny can exceed 1,000. At 20°C, the laboratory strain of *C. elegans* has an average life span of approximately 2–3 weeks and a generation time of approximately 3 days. *C. elegans* has five pairs of autosomes and one pair of sex chromosomes. Sex in *C. elegans* is based on an X0 sex-determination system. Hermaphrodite *C. elegans* have a matched pair of sex chromosomes (XX); the rare males have only one sex chromosome (X0).

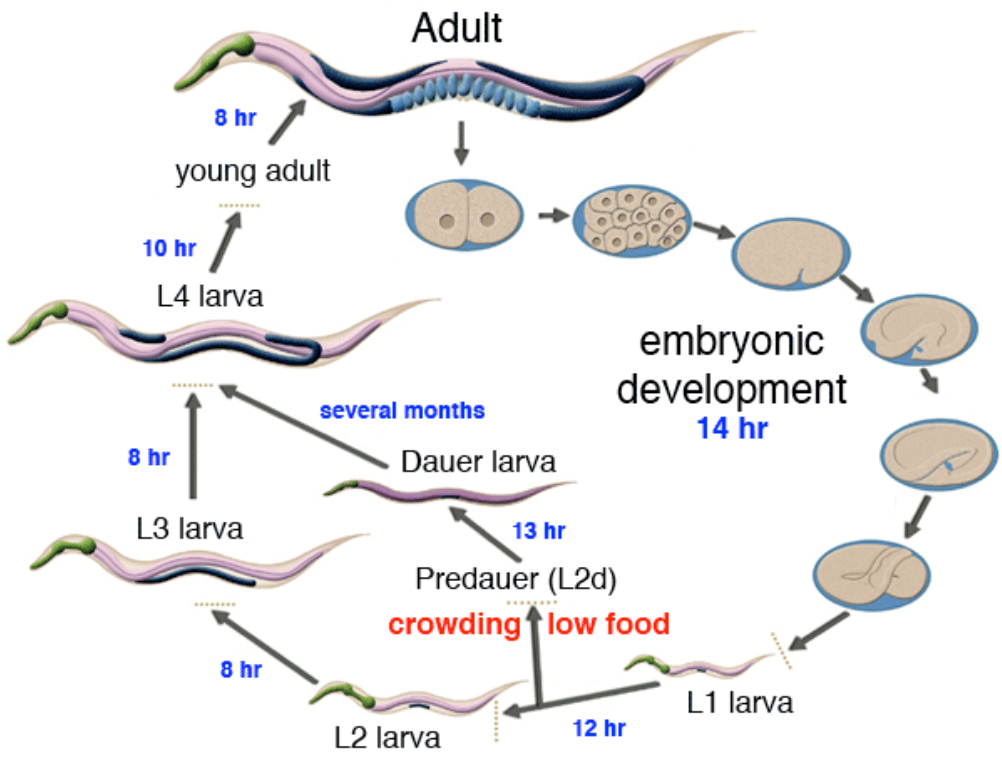

Figure 1.3.3. The life-cycle of C. elegans. *C. elegans pass through four developmental stages (L1-L4) before reaching adulthood three days after hatching. An alternative, developmental stage, called the Dauer stage can be induced during periods of stress or low food (reproduced from wormatlas.org).*

1.3.4 *C. elegans* nomenclature

In *C. elegans* nomenclature, gene names are usually designated by three letters followed by a hyphen and a number, and are always italicized. Proteins are named after the gene that codes for them, and are written in capitals without italics. A mutant is a worm strain with a specific nonfunctioning gene, produced either through knockout or mutation, and the strain of worm is named after the

nonfunctioning gene. For example, *pek-1* worms have a nonfunctioning *pek-1* gene.

1.3.5 The UPR in *C. elegans*

The *C. elegans* UPR is very similar to its mammalian counterpart. It contains the PERK (*pek-1*), IRE1 (*ire-1*) and ATF6 (*atf-6*) arms, which perform the same roles in the worm as it does in mammals (Shen et al., 2005; Sood et al., 2000) (figure1.3.5 B), with XBP-1 splicing occurring after IRE-1 activation (Shen et al., 2001). There are orthologues of all the major UPR genes except GADD34; dephosphorylation of eIF2α is performed by protein phosphatase 4. In *C. elegans*, the UPR is required for normal larval development (Shen et al., 2001) and the proper trafficking of glutamate receptors (Shim et al., 2004). Exposing worms to tunicamycin, an antibiotic that prevents the formation of N-linked glycoproteins and induces the formation of unfolded proteins, leads to activation of the UPR. This causes a developmental arrest at the L3 stage of larval development, and provides a way to examine the effects of UPR activation in an *in vivo* system (Figure 1.3.5 A).

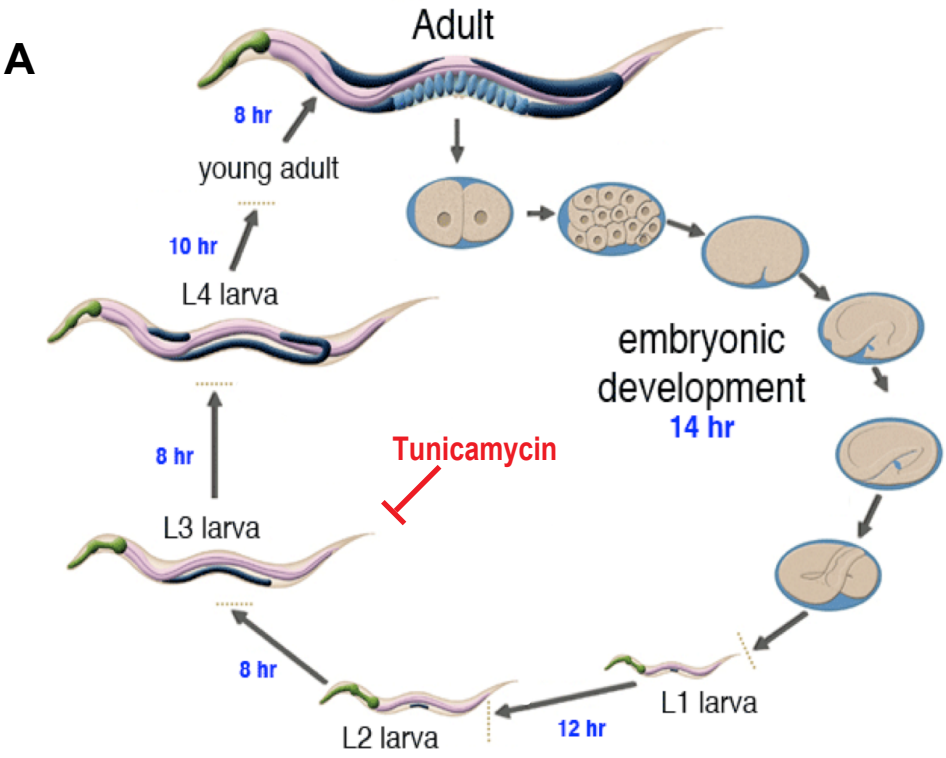
A
Adult
8 hr
young adult
10 hr
L4 larva
embryonic
development
14 hr
8 hr
Tunicamycin
L3 larva
8 hr
L2 larva
12 hr
L1 larva

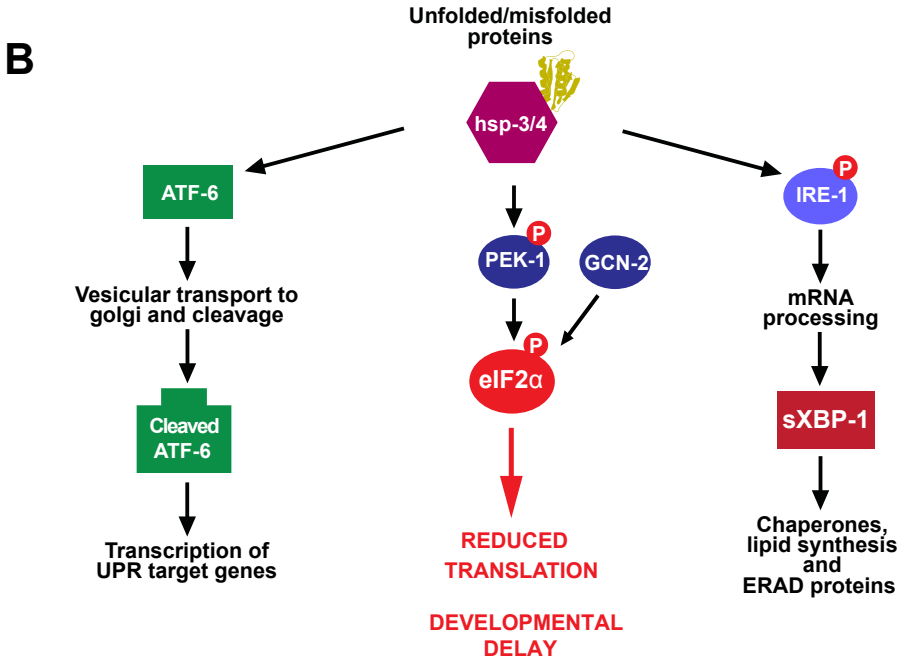
B
Unfolded/misfolded
proteins
hsp-3/4
ATF-6
Vesicular transport to
golgi and cleavage
Cleaved
ATF-6
Transcription of
UPR target genes
PEK-1
P
GCN-2
eIF2α
P
REDUCED
TRANSLATION
DEVELOPMENTAL
DELAY
IRE-1
P
mRNA
processing
sXBP-1
Chaperones,
lipid synthesis
and
ERAD proteins

Figure 1.3.5 The C. elegans UPR*. A. Exposing worms to tunicamycin stalls development at the L3 larval stage (adapted from wormatlas.org). B. C. elegans contain orthologs of the major components of the mammalian UPR.*

1.3.6 Drug Screening in *C. elegans*

The development of experimental models amenable to live animal compound screening is an attractive approach to discovering effective pharmacological therapies for disorders caused by misfolded and aggregation-prone proteins. However, live animal drug screening is labour and resource intensive, and has been hampered by the lack of robust assay designs and high throughput approaches. Based on their small size, tissue transparency and ease of cultivation, the use of *C. elegans* should remove many of the technical hindrances associated with live animal drug screening. Moreover, their genetic tractability and accomplished record for providing insights into the molecular and cellular basis of human disease, makes *C. elegans* an ideal model system for *in vivo* drug discovery efforts. Many fully automated screens have been performed in the worm, making use of automated worm handling equipment such as the Complex Object Parametric Analyzer and Sorter (COPAS) biosorter. Gill et al., identified compounds that extend life span through enhanced resistance to oxygen radicals or other stressors, and increased throughput by combining automated worm-handling technology with automated real-time fluorescence detection (Gill et al., 2003). Gosai and colleagues used transgenic worms expressing fluorescently-tagged proteins to developed a high-throughput screen using automated

fluorescence microscopy to conduct a small molecule screen to identify compounds that altered the intracellular accumulation of the human aggregation prone mutant that causes liver disease in α1-antitrypsin deficiency (Gosai et al., 2010). A microfluidic platform for high-sensitivity, real-time drug screening in *C. elegans* has also been developed (Carr et al., 2011). An ultra high-throughput screen has also been performed using 1536-well plates, which screened approximately 364,000 compounds (Leung et al., 2013).

In contrast to traditional biochemical assays that focus on specific molecular targets, a screen based on a phenotypic observation has the advantage of being independent of the specific molecular target involved. Then, depending on the readout, a large variety of bioactive molecules may be detected in the same screen. Additionally, experiments could further lead to the identification of unsuspected targets. An example of this approach is well illustrated by the screen made by Kwok et al. (Kwok et al., 2006) which screened 14,100 small molecules for bioactivity in wild-type *C. elegans* and identified 308 compounds that induced a variety of phenotypes, including slow growth, uncoordinated movements and morphology defects. One of these compounds, nemadipine-A, induces morphology and egg-laying defects. Through a genetic suppressor screen using the mutant *egl-19*, a calcium channel inhibitor was identified as the sole candidate target of this compound in *C. elegans*. Moreover, by showing that nemadipine-A can also antagonize vertebrate L-type calcium channels, they demonstrated the relevance of this approach for drug discovery (Kwok et al., 2006).

1.4 Aim of the thesis

Due to the scarcity of available treatments for neurodegeneration, searching for new treatments is of the upmost importance. The UPR has recently emerged as a new and exciting target for therapeutics in neurodegenerative disease, especially in prion disease. Genetic approaches to modulating the UPR in prion disease have proved successful, but small molecules provide a more attractive target for therapy. This thesis uses a dual approach to searching for new small molecule therapeutics:

1. Screening approach: Using the model organism *C. elegans*, the effects of unfolded proteins and UPR overactivation will be modeled, and then used to screen for drugs that can inhibit the UPR using the NINDS custom collection 2. Any hits will be validated in the worm, then tested in a mouse model of prion disease as potential treatments.

2. Targeted approach: A newly described PERK inhibitor, GSK2606414, will also be tested in mice with prion disease to determine its efficacy and toxicity profile.

Chapter 2: Materials and Methods

2.1 Maintenance of *C. elegans*

C. elegans were maintained under standard conditions, as outlined by Brenner (Brenner, 1974). Worms were grown on 6cm Petri dishes filled with 10 ml nematode growth medium (NGM). 200 µL of *E. coli* strain OP50 was used as a food source. A starter culture of OP50 was obtained from the *C. elegans* genetics center (CGC). Worms were transferred to fresh plates every 3-5 days. *C. elegans* was visualized using a dissecting stereomicroscope equipped with a transmitted light source (Leica model M165 FC) with standard 10X eyepieces and objectives that range from 0.6X to 5X (total magnification of 6X to 50X).

2.2 *C. elegans* egg extraction

Large numbers of *C. elegans* eggs were extracted by performing an egg extraction. Worms were washed off NGM plates with sterile H_20 three days after the last transfer to gather large numbers of gravid hermaphrodites. The collected worms were centrifuged for 1 minute at 1300rpm to pellet the worms, and the supernatant aspirated off. The pellet was re-suspended in a solution of 1ml 5% sodium hypochlorite, 0.5ml 5M sodium hydroxide and water up to 5ml. The sodium hypochlorite solution was vortex/shaken until the worms had dissolved (approximately 5-10 minutes), leaving behind the eggs. As above, the eggs were centrifuged at 1300rpm for 1 minute to collect the eggs, and the supernatant aspirated off again. The eggs were washed with 5ml water and re-centrifuged 3-

5 times. 1-2ul of eggs were pipetted onto a glass slide and counted to work out a concentration of eggs. The desired amount of eggs were then pipetted onto a fresh NGM plate, usually around 100.

2.3 Inducing unfolded proteins in *C. elegans* with tunicamycin.

The desired concentration of tunicamycin was added to NGM plates before pouring (usually 1-5 μg/ml). Approximately 100 eggs prepared from a *C. elegans* egg extraction (section 2.2) were pipetted onto each plate, and allowed to develop for 3 days (the normal generational time of *C. elegans*). After three days the proportion of worms at the L4 stage of development or older, between the L1-L3 stages or dead was recorded.

2.4 The drug screen.

The 1040 compounds of the NINDS custom collection 2 drug library were screened in *C. elegans*. Eggs from gravid hermaphrodites were extracted, and approximately 100 were placed onto each test plate. Each plate contained 2 μg/ml Tunicamycin, 10 μM of the drug tested and a final concentration of 1% dimethyl sulfoxide (DMSO), as the NINDS library was supplied dissolved in 100% DMSO. The eggs were allowed to grow for 3 days, and the change in the percentage of worms reaching the L4 stage of development or older was semi-quantitively recorded, with a score of 3 to -3 (Table 2.4). Any plates scored 2 or three were counted, and the fold difference in the percentage of worms reaching L4 or adulthood was calculated. A hit was defined as a drug that caused a 3-fold

or greater increase in the percentage of worms reaching L4 or adulthood. Each drug was tested in duplicate. Control plates containing 2 µg/ml Tunicamycin and 1% DMSO were counted everytime plates were examined to account for day-to-day variability.

Score	Relative change in worm development compared to controls
3	Large increase in L4 or adult worms
2	moderate increase in L4 or adult worms
1	Small increase in L4 or adult worms
0	No change in L4 or adult worms
-1	Small decrease in L4 or adult worms
-2	Large increase in L4 or adult worms
-3	No worms alive

Table 2.4 Scoring of the drug screen*. The change in the percentage of worms reaching the L4 stage of development or older was semi-quantitively recorded, with a score of 3 to -3.*

2.5 Testing ER stress in *C. elegans*

The *hsp-4::GFP* strain of worm expresses GFP during periods of ER stress. hsp-4::GFP eggs were extracted by *C. elegans* egg extraction (section 2.2) and placed onto NGM plates containing 5µg/ml Tunicamycin and 10 µM of the drug to be

tested. After three days, the worms were washed off with sterile water, and immobilized in 1 mg/ml levamisole. The immobilized worms were placed onto a 3.5% agarose pad that had been made on glass microscope slides, and a cover slip added on top. GFP expression was observed using a Zeiss LSM510 Meta NLO confocal microscope, and ZEN 2009 acquisition software. The same exposure and laser power settings setting were used for each worm to allow comparison of GFP levels.

2.6 List of *C. elegans* strains

N2 (wild-type), *ire-1*(v33), *pek-1*(ok275), *atf-6*(ok551), *xbp-1*(zc12), gcn-1(nc40), and zcIs4[*hsp-4::GFP*]. All strains were acquired from the *C. elegans* genetics center (CGC), University of Minnesota.

2.7 Mouse strains

Hemizygous tg37 mice (Mallucci et al., 2003) were used for all experiments. tg37 mice express PrP at approximately three times wild-type levels on a FVB background (Mallucci et al., 2002).

2.8 Scrapie transmissions

Designated staff, according to established local protocols, performed inoculation of mice with RML prions. Three to four week old mice were anaesthetised with isofluorane in an inhalation chamber until pinch reflexes were absent. They were

then inoculated with 20µl of 1% brain homogenate of RML (Rocky Mountain Laboratory) mouse-adapted scrapie strain in PBS using a 1ml insulin syringe and a 26-gauge hypodermic needle inserted 3- 4 mm into the right parietal lobe. Mice were allowed to recover in a cage placed on a heated pad prior to being replaced in their home cage. Control mice were inoculated with 1% normal brain homogenate (NBH).

2.9 Diagnosis of scrapie symptoms

Mice were examined daily for appearance of scrapie symptoms or other illness. Prion disease in mice is diagnosed via the observation of a variety of signs of varying severity. Early indicator signs of prion disease are: rigid tail, hind limb clasping (when the animal is held by the tail), piloerection, mild loss of co-ordination or an unsustained hunched posture. Confirmatory signs of prion disease are: ataxia, impairment of the righting reflex, dragging of limbs, sustained hunched posture or significant abnormal breathing. The presence of two early indicator signs and one confirmatory sign, or two confirmatory signs is used to diagnose prion disease (see appendix 2 for prion symptom sheets). The time to confirmation of prion disease is termed the scrapie incubation time.

2.10 Dosing of mice

GSK2606414 treatment: Mice were orally gavaged twice daily with GSK2606414 at 50 mg/kg suspended in vehicle (0.5% HPMC + 0.1% Tween-80 in H2O at pH 4.0), or with vehicle alone from 7 w.p.i. or from 9 w.p.i.

Trifluoperazine and Trazodone treatment: Mice were intraperitoneally dosed once daily with 10 mg/kg trifluoperazine or 40 mg/kg Trazodone dissolved in vehicle (Sterile saline) from 7w.p.i..

Estradiol Valerate treatment: Mice were injected subcutanously once daily with 50 µg/kg estradiol valerate dissolved in vehicle (sesame oil) from 7 w.p.i.

Diallyl sulfide treatment: Mice were orally gavaged once daily with 10mg/kg diallyl sulfide dissolved in vehicle (sesame oil) from 7.wp.i

Dibenzoylmethane treatment: Mice were fed powdered diet containing 0.5% Dibenzoylmethane from 7 w.p.i. Vehicle treated mice received powdered diet only.

2.11 Novel object recognition

Novel object recognition assays were performed by Colin Molloy, University of Leicester. Male mice were tested in a black cylindrical arena (69 cm diameter), mounted with a 100 LED cluster infra-red light source and a high resolution day/ night video camera (Sony). The mice were acclimatized to the arena five days prior to testing. During the learning phase, two identical objects were placed 15 cm from the sides of the arena. Each mouse was placed in the arena for two blocks of 10 min for exploration of the objects with an inter-trial interval of 10 minutes. Two hours later, one of the objects was exchanged for a novel one, and

the mouse was replaced in the arena for 5 minutes (test phase). The amount of time spent exploring all objects was tracked and measured for each animal using Ethovision software (Tracksys Ltd.). During the test phase, healthy mice will explore the novel object more as they remember the non-novel object, while mice with memory deficits explore both objects equally as they do not remember the non-novel object. All objects and the arena were cleansed thoroughly between trials to ensure the absence of olfactory cues.

2.12 Burrowing assay

Female mice were placed in a large cage with a perspex tube full of food pellets. The natural tendency of rodents is to displace (burrow) the food pellets. The percentage of burrowing activity is calculated from the difference in the weight of pellets in the tube before and after two hours

2.13 ^{35}S-Methionine incorporation

Global translation levels were detected using ^{35}S-Methionine incorporation into protein acute hippocampal slices, as described (Moreno et al., 2012). Hippocampi were dissected in oxygenated sucrose artificial cerebral spinal fluid (ACSF), then ~5-6 slices were incubated for 1 hour to recover in normal ACSF and oxygenated in 95% O_2/5% CO_2. Slices were then incubated in 5.7 mBq of [^{35}S] Methionine for 1 hour. Samples were then washed, homogenized in 1X passive lysis buffer (PLB; Promega) and protein precipitated with 25% Trichloroacetic acid (TCA) (Sigma). TCA lysates were then placed on Whatmann

filters, washed with 70% industrial methylated spirits (IMS) and acetone and then placed into scintillation cocktail buffer. Scintillation counts were performed on the samples and CPM recorded (Winspectal, Wallac Inc.).

2.14 Histology

Tissue preparation: Tissue (brain or pancreas) was extracted from mice and placed into 10% formalin for at least 3 days to ensure fixation. Following fixation tissue was placed into pre-labeled histological cassettes and incubated in 70% IMS to dehydrate tissue for dehydration. Cassettes were then added to the automated paraffin embedded machine. Once tissue was embedded it was sectioned at 4 μm prior to staining.

NeuN staining: Paraffin embedded brains were sectioned at 4 um and stained with NeuN antibody (1:200; Millipore) for neuronal counts. CA1 pyramidal neuron counts were determined using three serial sections from three separate mice. A biotinylated secondary antibody (Invitrogen) was used and the stain visualised by diaminobenzidine reagent. All images were taken on using a wide-field Zeiss Axiovert 200M with Axiovision 4.9 software (Zeiss) and counted using volocity imaging system.

Astrocyte staining: Astrocytosis was detected using anti-GFAP polyclonal antibody (1:500; Dako).

H&E staining: Paraffin embedded brains and pancreases were sectioned at 4 μm and then placed into an automated Haematoxylin and Eosin (H&E) staining machine (Shandon Varistain 24-4) (see appendix 3 for a full schedule).

2.15 Western blotting

Mice to be tested were culled using appropriate schedule 1 methods, and the brain removed. The hippocampus was then removed from the brain by dissection in PBS. Hippocampi were homogenized using a handheld homogenizer in 200 μl homogenization buffer. After homogenization, 200μl 2x superstrong lysis buffer was added, and incubated on ice for 10 minutes. The solution was then centrifuged at 14000rpm for 20 minutes, and the supernatant removed to a clean test tube. Protein concentration was determined by using Bradford protein assay (Biorad), and the samples diluted to the desired concentration in water and 5x SDS-loading buffer. Samples were heated to 95^0C for 5 minutes to denature proteins, and 5-40 μg of protein was loaded onto 8, 10 or 12% polyacrylamide gels for electrophoresis. Separated protein bands were transferred by wet transfer to 0.2 μm nitrocellulose or 0.45 μM PVDF, using a constant 350 mA current for 1.5 hours. Transfer was confirmed by using a Ponceau S stain (0.25% Ponceau S + 1% acetic acid). Non-specific binding sites were blocked by incubating the membrane for 1 hour at room temperature (RT) with 5% non-fat dry milk or 5% BSA in 1x TBS + 0.1% tween-20 (TBST). The membrane was incubated with the appropriate primary antibody diluted in the blocking solution overnight at 4OC. The membrane was washed (3 X 10 min) in TBST before being incubated with the HRP secondary antibodies for 1 hour at

RT, followed by (4 X 10 min) final washes. Immunoreactive proteins were detected by enhanced chemiluminescence plus western blotting detection system. Immunoreactivity was analysed using image J software. All secondary antibodies were purchased from Dako except donkey anti-rabbit (Promega).

2.16 List of antibodies and western blotting conditions

Antibody	Company	Membrane	Dilution	Block with	Secondary
ATF4	Santa Cruz	Nitrocellulose	1:1000	5% Milk	1:1000 Goat anti rabbit
ATF6	Abcam	Nitrocellulose	1:1000	5% Milk	1:1000 Goat anti rabbit
β-tubulin	Cell signalling	Nitrocellulose	1:5000	5% BSA	1:5000 goat anti mouse
CHOP	Thermoscientific	Nitrocellulose	1:1000	5% BSA	1:1000 Goat anti mouse
eIF2α	Cell signalling	PVDF	1:1000	5% BSA	1:5000 goat anti mouse
eIF2α-P	Cell signalling	PVDF	1:1000	5% BSA	1:5000 donkey anti rabbit
GAPDH	Santa Cruz	Nitrocellulose	1:5000	5% Milk or BSA	1:5000 goat anti mouse
PERK	Cell signalling	Nitrocellulose	1:1000	5% BSA	1:5000 goat anti rabbit
PERK-P	Cell signalling	Nitrocellulose	1:1000	5% BSA	1:5000 goat anti rabbit
PrP^{c}	Abcam (8H4)	Nitrocellulose	1:10,000	PBST	1:10,000 Goat anti mouse
PrP^{Sc}	D-Gen (ICSM34)	Nitrocellulose	1:1000	PBST	1:10,000 Goat anti mouse
PSD-95	Millipore	Nitrocellulose	1:1000	5% Milk	1:5,000 goat anti rabbit
SNAP-25	Abcam	Nitrocellulose	1:10,000	5% Milk	1:5,000 goat anti rabbit

2.17 Proteinase K digestion of brain homogenates

This was performed to detect protease resistant PrP in homogenates of prion-inoculated mouse brains. Proteinase K at was added to homogenates at a final concentration of 50 μg/ml for 1 hour at 37°C in a water bath followed by a quick centrifugation, addition of 5X SDS- loading buffer and denaturation of the proteins at 95^0C for 5 min. The sample was then loaded onto gels for electrophoresis.

2.18 XBP1 splicing assay.

Total RNA was extracted from hippocampi using the mirVANA RNA/miRNA isolation kit (Ambion, Inc). RNA samples were reverse-transcribed with ImProm II Reverse Transcriptase (Promega) by priming with oligo(dT). XBP1 mRNA was amplified with primers flanking the 26bp intron (5' – GGAGTGGAGTAAGGCTGGTG and 5' -CCAGAATGCCCAAAAGGATA) using Phusion High Fidelity taq polymerase (New England Biolabs). PCR products were resolved on 3% agarose gels. Mouse neuroblastoma cells (N2A) were treated with 5 μg/ml tunicamycin for 8 hours and used as a positive control for XBP1 splicing.

2.19 LC-MS/MS.

Blood and brain tissue were collected 2, 14 or 24 hours post dosing from mice treated drug or vehicle. Blood was extracted by cardiac puncture using a 25G

needle while mice were under anaesthesia and blood centrifuged for 1 hour at 1400rpm and saved at -80C until used. Blood plasma (0.025-0.95 mL, exact volume measured) was diluted with water to 0.1 mL and extracted with 0.4 mL of isopropanol. Following vortex mixing (10 min) and centrifugation (10,000g, 10 min), the supernatant was dried using vacuum centrifugation and reconstituted in 50µl methanol: isopropanol (3:1). Brain tissue (one complete half, approximately 0.2 g) was homogenised in 0.8 ml isopropanol and further processed exactly as the plasma samples. GSK2606414 quantitative analysis (using external standards) was by liquid chromatography tandem mass spectrometry (LC-MS/MS) using a 4000 QTRAP (Applied Biosystems, Foster City, CA, USA) equipped with a TurboIon source and LC series 10 AD VP (Shimadzu, Columbia, MD, USA). The mobile phase was a water: acetonitrile gradient modified with 0.1% formic acid using a Phenomenex Gemini column (100 x 3mm 3 µm particle size) which was maintained at 40°C. LC-MS/MS multiple reaction monitoring used a precursor ion of m/z 452 and a product ion of m/z 265 in positive electrospray ionisation mode (ES+). Data analysis was performed using the Quantitate mode of Analyst 1.4.1.

2.20 Statistical analysis

Data is presented as a mean ± standard error of the mean (SEM), unless otherwise stated. Statistical significance was tested using an unpaired t-test (Graphpad Prism, Graphpad software). Statistical significance was accepted at $p<0.5$. * denotes $p<0.05$, ** denotes $p<0.01$ and *** denotes $p<0.001$ unless otherwise stated.

2.21 List of solutions

NGM media
NaCl 3 g
peptone 2.5 g
agar 17 g
H2O 975 ml
Autoclaved, and cooled to 55°C, then the following is added:
1M CaCl2 1 ml
1M MgSO4 1 ml
1M Potassium Phosphate pH 6.0 25 ml
Cholesterol (5mg/ml in EtOH) 1 ml

Sucrose ACSF buffer

Sucrose	250 mM,
KCL	2.5 mM,
$NaHCO_3$	26 mM,
Glucose	10 mM,
NaH_2PO_4	1.25 mM,
Sodium pyruvate	2 mM,
Myo-inositol	3 mM,
CaCl	0.1 mM,
$MgCl_2$	4 mM,
Ascorbic Acid	0.5 mM,
L-arginine	0.1 mM

Normal ACSF buffer

NaCl	125 mM,
KCL	2.5 mM,
$NaHCO_3$	26 mM,
Glucose	10 mM,
NaH_2PO_4	1.25 mM,
Sodium pyruvate	2 mM,
Myo-inositol	3 mM,
CaCl	2 mM,
$MgCl_2$	1 mM,
Ascorbic Acid	0.5 mM,
L-arginine	0.1 mM

Hypotonic Homogenisation Buffer
0.25M Sucrose
50mM TRIS pH 7.4
1mM EDTA

Add one Phos-STOP tablet (Roche) to 10 ml of buffer
Add protease inhibitor cocktail (Roche) to final 1x concentration

2x 'Superstrong' Lysis Buffer
100mM TRIS pH 8.0
300mM NaCl
4mM EDTA
2mM $MgCl_2$
200mM NaF
20% Glycerol
2% TRITON X-100
2% Na Deoxycholate
0.2% SDS
0. 25M Sucrose

2X SDS loading buffer
125mM Tris
4% SDS
20% Glycerol
10% β-mercaptoethanol
0.005% bromophenol blue

Chapter 3: Using *C. elegans* to screen for modulators of the unfolded protein response

3.1 Introduction

Recently, it has been shown that in the brains of prion-diseased mice, the accumulation of misfolded PrP due to prion replication causes sustained over-activation the PERK/eIF2α branch of the UPR. The resulting persistently high levels of eIF2α-P lead to neurodegeneration through sustained repression of protein synthesis, which is catastrophic in this context due to the critical decline in the levels of key proteins, such as synaptic proteins (Moreno et al., 2012). Genetic manipulation of this pathway by stereotaxic delivery of lentiviruses to the hippocampus, upstream and downstream of eIF2α-P in prion-diseased mice, reduced eIF2α-P levels and restored vital translation rates, allowing recovery of synaptic protein levels, resulting in marked localised neuroprotection and a significant increase in survival (Moreno et al., 2012). It is hypothesised that a drug that can mimic these results, either by reducing eIF2α-P or by restoring translation via other mechanisms would also be neuroprotective. There has been little drug development targeted against proteins in the UPR, and what there has been has focused on potential cancer therapies. This is because the conditions of hypoxia and restricted nutrient delivery in the tumour microenvironment lead to UPR activation in cancerous cells, so inhibiting the UPR has been predicted to disrupt cancer cell viability. However, as sustained activation of the UPR can lead to apoptosis, a beneficial outcome in cancer but not in neurodegeneration, drug

discovery efforts have been tempered until a better understanding of the divergent roles of UPR activation in cancer are better understood, see for review (Ma and Hendershot, 2004). The emerging role of the UPR in prion disease has highlighted a more urgent need for suitable UPR inhibitors. Drug development is a long and costly process, estimated to take 15 years and cost $800 million to bring a single drug to market (DiMasi et al., 2003). One solution is to identify new uses for existing drugs. As current drugs have known pharmacokinetics and safety profiles, and are often approved by regulatory agencies for human use, any newly identified uses can be rapidly evaluated in phase II clinical trails, which typically only cost $2 million (DiMasi et al., 2003). Screening for drugs that inhibit the UPR might uncover an existing drug that has efficacy as a potential treatment, greatly speeding up the process of discovering a therapeutic for use in prion disease.

This chapter details the screening of the National Institute for Neurological Disorders and Stroke (NINDS) custom collection 2 drug library in *C. elegans* for potential modulators of the UPR. The NINDS custom collection 2 contains 1040 off patent compounds, three quarters of which are FDA-approved and the rest are known to influence brain activity.

3.2 Developing the drug screen

The model organism *C. elegans* was chosen for the drug screen due to its numerous experimental advantages (see section 1.3). Before performing the drug screen, a model of UPR activation in *C. elegans* needed to be developed. Once a basic platform of UPR activation has been established, it will be used to screen for modulators of the UPR. Tunicamycin is a drug that is often used experimentally to induce the production of unfolded proteins and hence activation of the UPR. It inhibits the formation of N-linked glycoproteins, disrupting protein secondary structure and causing protein misfolding. In *C. elegans*, exposure to tunicamycin strongly activates the UPR. If exposure to tunicamycin occurs from hatching, development is stalled at the L3 stage of development (Shen et al., 2001). This is because compensatory UPR activation prevents the production of new proteins, stopping an additional increase in size and stalling any further development. It is hypothesised that any drug that would inhibit the UPR, or allows the worms to cope with the presence of unfolded proteins and the associated ER stress would restore protein synthesis and allow the worms to develop into adulthood, thus providing an easily observable readout of UPR inhibition.

3.2.1 Experimental plan

The 1040 drugs from the NINDS custom collection 2 were chosen for screening in *C. elegans* as it exclusively contains compounds that influence brain activity. Eggs from gravid hermaphrodites were extracted and placed onto NGM agar

plates containing tunicamycin and a compound from the NINDS drug library. The eggs were allowed to develop for three days, the normal time for development into adulthood in wild-type worms. The number of worms at each developmental stage were counted, and the proportion of worms at the L4 stage of development or older, stages L1-L3, or that died were determined. Drugs that increased the proportion of worms reaching the L4 stage of development were further investigated in the worm, to determine if they reduce UPR activation. The hits were then tested in a mouse model of prion disease as a potential treatment (Figure 3.2.1). Before performing the drug screen a suitable concentration of tunicamycin was determined, and the effects of the solvent the drugs are stored in was investigated.

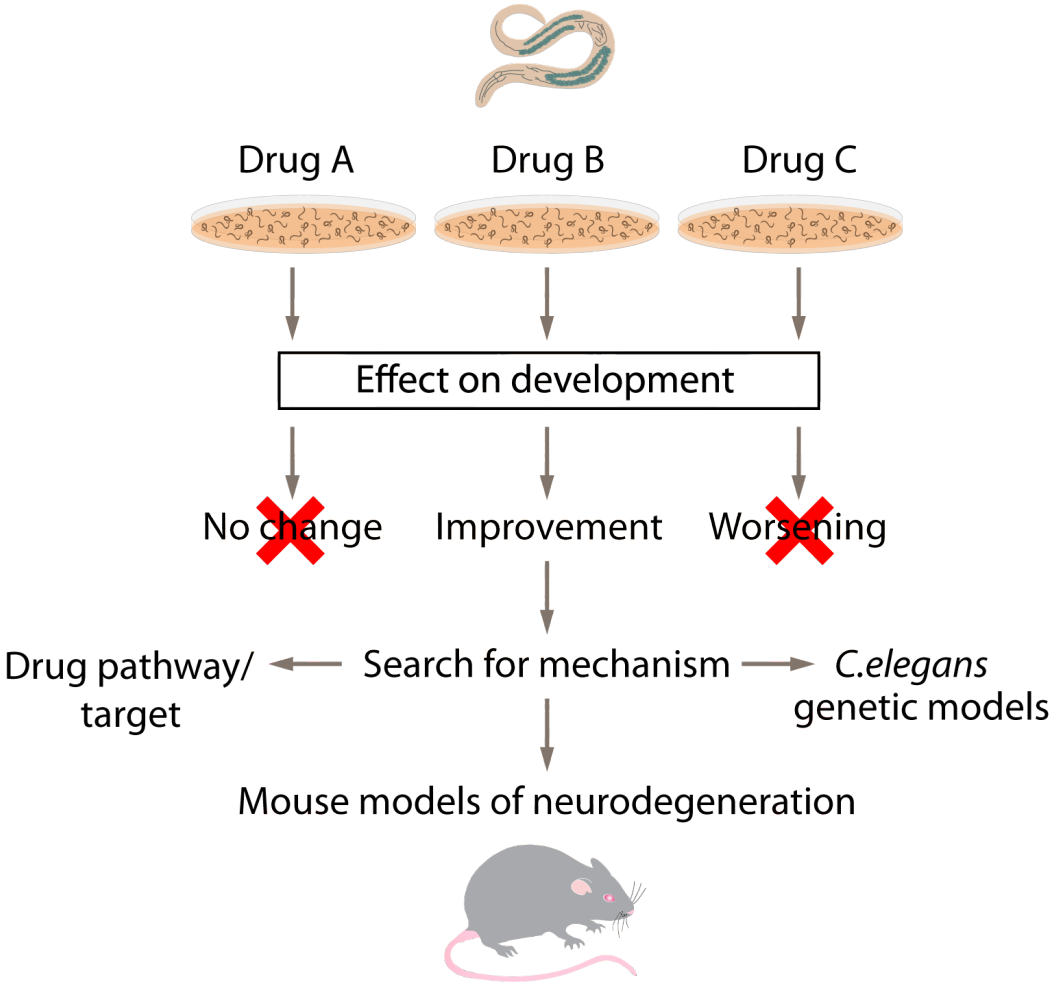

Figure 3.2.1 Schematic of the drug screen. *The 1040 drugs of the NINDS custom collection 2 were screened in a worm model of UPR activation. Any hits that restored normal development in tunicamycin exposed worms were further investigated in the worm before being tested in a mouse model of prion disease.*

3.2.2 The response of *C. elegans* to tunicamycin

The response of N2 (wild-type) *C. elegans* to chronic exposure of tunicamycin across a range of doses was tested, and the proportion of worms that developed to the L4 larval stage or further into adulthood, stalled at larval stage L1-L3, or

died was counted (Figure 3.2.2). Eggs were extracted from gravid hermaphrodites and placed on NGM agar plates containing tunicamycin. 100% of untreated worms reached the L4 stage of development or further, while increasing concentrations of tunicamycin induced developmental delay or death in a concentration dependent manner, confirming the predicted effects of tunicamycin on *C. elegans* development.

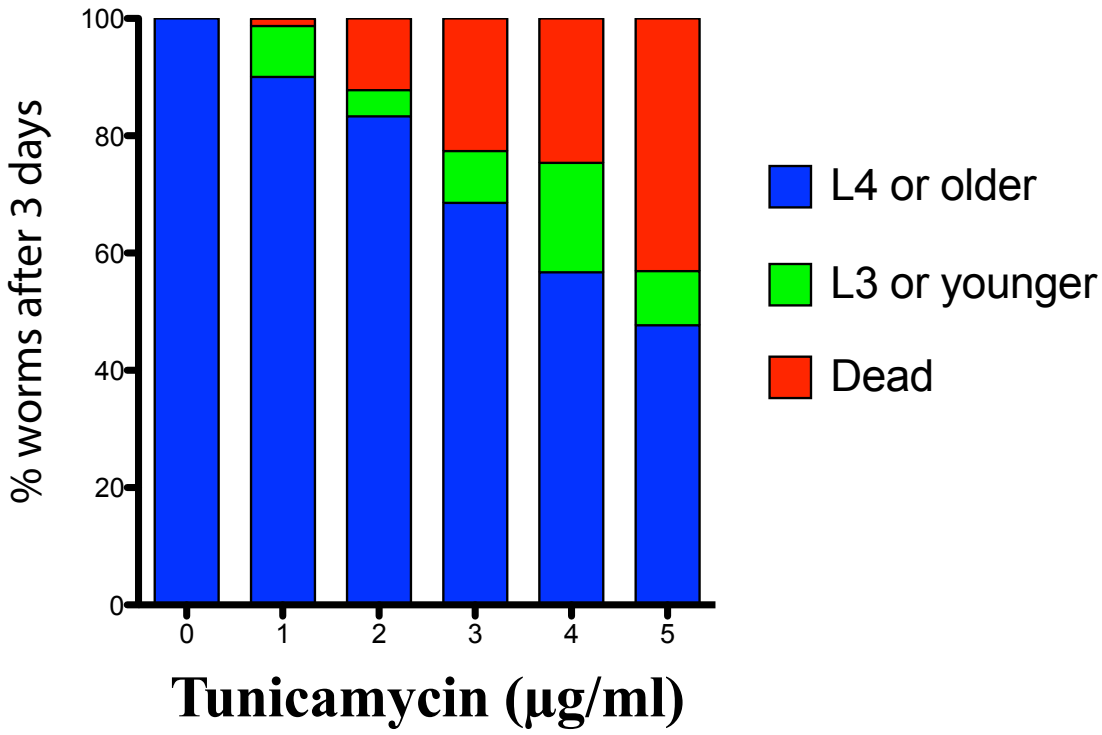

Figure 3.2.2 The response of C. elegans to increasing concentrations of tunicamycin*. Exposure to tunicamycin caused an increasing amount of developmental delay and death in the worms. Exposure time was three days, n=~100 for each group.*

3.2.3 The response of *C. elegans* mutant worms to tunicamycin.

The response of UPR mutant worms exposed to tunicamycin for three days was also tested. Mutant strains for the three arms of the UPR, PEK-1, IRE-1 and ATF-6 were tested, along with XBP-1 mutants (Figure 3.2.3A-E). At 2µg/ml^{-1} tunicamycin *pek-1*, *ire-1* and *xbp-1* worms were more sensitive than wild-type worms, and at 5µg/ml-1 *pek-1*, *ire-1, xbp-1* and *atf-6* worms were all more sensitive. *gcn-1* worms were also tested (Figure 3.2.3F). These worms are mutants for the *C. elegans* ortholog of GCN2, a kinase of eIF2α, and are reported to exhibit reduced eIF2α phosphorylation (Nukazuka et al., 2008). *gcn-1* worms were almost completely resistant to the effects of tunicamycin treatment at the doses tested. This is extremely important as it demonstrates that reducing eIF2α phosphorylation causes a recovery of the developmental phenotype, so any drugs tested in the screen that effect eIF2α will likely cause the same effect and show up as a hit. As the UPR mutant worms were all more sensitive, a functioning UPR is still required during periods of unfolded protein stress. It is likely that the downstream affects of UPR activation, such as XBP-1 splicing and the translation of ERAD genes are still important, and preserving these while still reducing eIF2α phosphorylation is the most desirable approach.

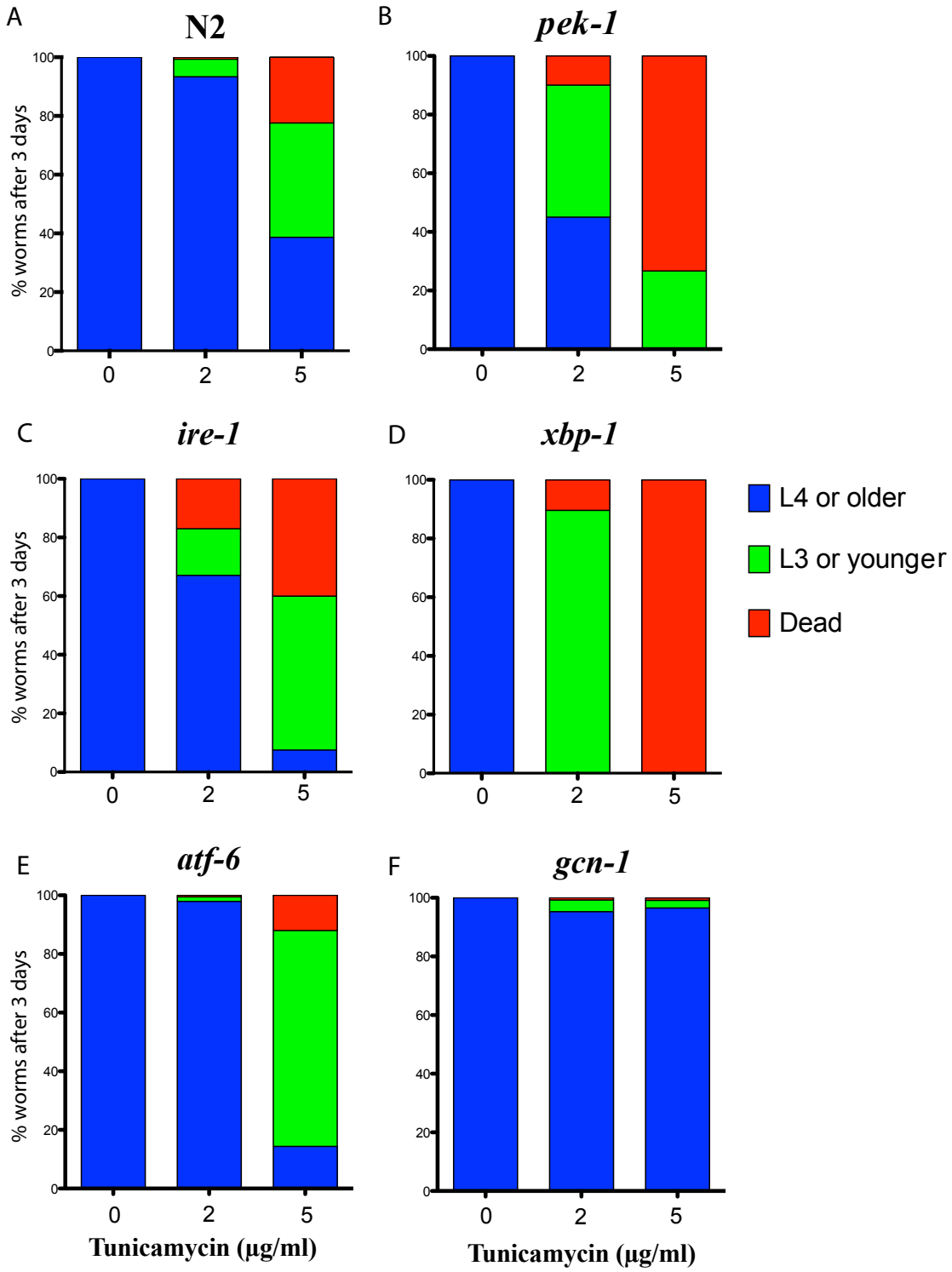

Figure 3.2.3 The response of various UPR mutants to tunicamycin. A-E) *ire-1, xbp-1, pek-1 and atf-6 worms are more sensitive to tunicamycin treatment,* ***F)*** *while gcn-1 worms are protected against the developmental delay observed. Exposure time 3 days, n=~100 for each group.*

3.2.4 The effects of Dimethyl sulfoxide on development

A concentration of 10μM was selected to test the drugs in the screen, as the NINDS drug library had previously been successfully screened at this concentration before in *C. elegans* (Sleigh et al., 2011). The library is supplied dissolved in 100% dimethyl sulfoxide (DMSO), and after the drugs are diluted to a concentration of 10μM for the drug screen, the final DMSO concentration would be 1%, so it was important to determine if 1% DMSO would effect the results of the experiment. DMSO has been reported to increase lifespan in *C. elegans* (Frankowski et al., 2013; Wang et al., 2010), possibly by affecting protein homeostasis (Frankowski et al., 2013) at concentrations of 0.5-2%, so has the potential to protect against unfolded protein stress. In fact, the opposite was observed; worms treated with 1% DMSO and tunicamycin were more sensitive to the effects of tunicamycin (Figure 3.2.4A). DMSO is a widely used solvent due to its ability to dissolve both polar and non-polar molecules, while remaining miscible in water. It can increase the rate of absorption of compounds across biological membranes, and has been used to increase the absorption of the large molecule icariin in *C. elegans* (Cai et al., 2011). DMSO caused a shift to the left in the dose response curve of the worms to tunicamycin (Figure 3.2.4B), suggesting an increase in its potency, meaning DMSO may be increasing the absorption of tunicamycin in a similar fashion. In light of these results, a concentration of 2 $\mu g/ml^{-1}$ Tunicamycin was chosen for the drug screen, as this produced a substantial enough developmental phenotype to allow for any rescue to be easily observable, while not making the worms so sick that rescue was impossible.

A)

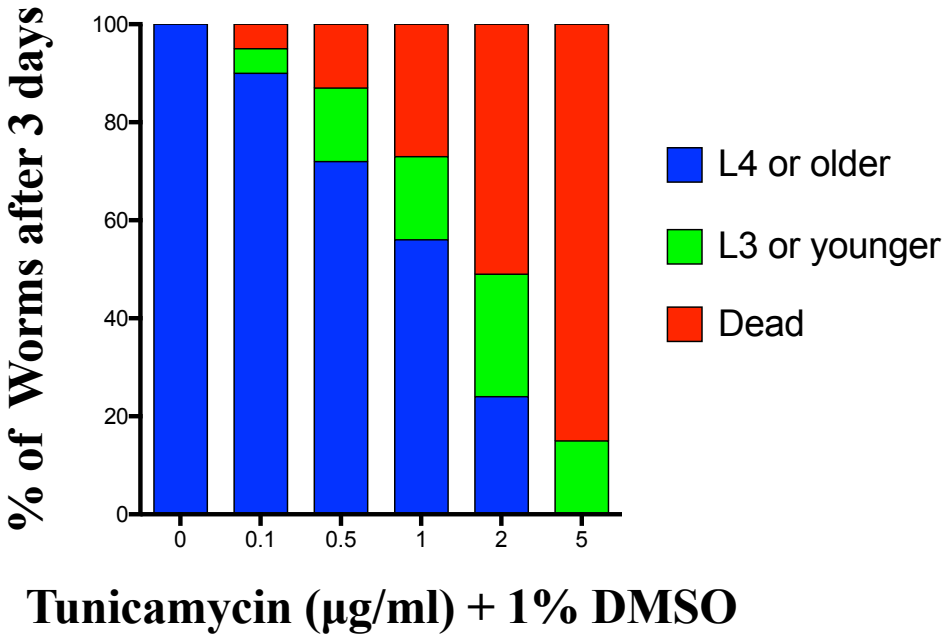

B)

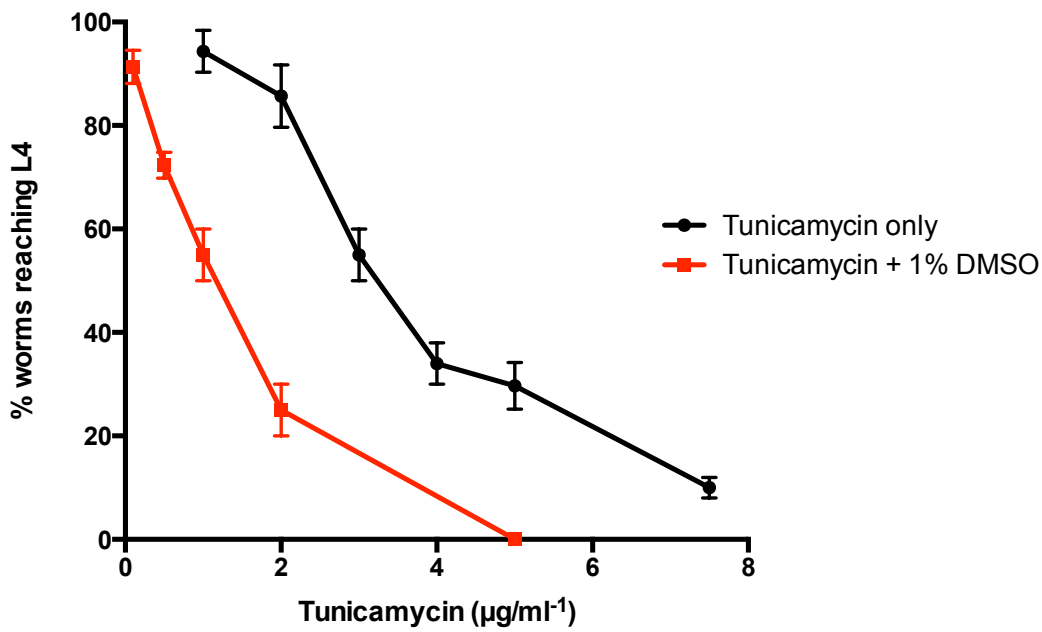

Figure 3.2.4 The effects of DMSO on the tunicamycin induced developmental phenotype. A *Worms exposed to 1% DMSO and tunicamycin are more sensitive to the developmental delay caused by tunicamycin alone (Figure 3.2.2).* ***B*** *1% DMSO caused a shift the left of the dose response curve of tunicamycin, suggesting an increased potency in its presence. (n=~300 for each group, three biological replicates, error bars = SEM). Exposure time was three days for both experiments.*

3.3 The UPR screen

3.3.1 The UPR screen resulted in 34 hits

The 1040 compounds of the NINDS custom collection 2 drug library were screened in *C. elegans*. Eggs from gravid hermaphrodites were extracted, and approximately 100 we placed onto each test plate. Each plate contained 2μg/ml^{-1} Tunicamycin, 10μM of the drug tested and a final concentration of 1% DMSO. The eggs were allowed to grow for 3 days, and the change in the percentage of worms reaching the L4 stage of development or older was semi-quantitively recorded, with a score of 3 to -3 (Table 2.4). Any plates scored 2 or three were counted, and the fold difference in the percentage of worms reaching L4 or adulthood was calculated. A hit was defined as a drug that caused a 3-fold or greater increase in the percentage of worms reaching L4 or adulthood. Each drug was tested in duplicate. Fold increase was used to express the results as control plates differed in the percentage of worms reaching L4 or older between different experimental days, allowing for an easier comparison of compounds. Out of the 1040 compounds tested, 34 fulfilled the criteria for a hit (Table 3.3.1.1 and appendix 1). Out of the 34 hits there were a range of different drugs, covering 17 different classes (Table 3.3.1.2)

ID	Molecular Name	Score	Fold increase in worms reaching L4 or older
01503973	2-THIOURACIL	3	3.36
01500618	ACRIFLAVINIUM HYDROCHLORIDE	3	6.17
01500127	ANTHRALIN	2	3.13
01503722	ATORVASTATIN CALCIUM	3	3.85
01503802	AZADIRACHTIN	3	7.75
01505309	BIFONAZOLE	2	3.49
01500623	BROXYQUINOLINE	3	5.14
01500173	CHLORAMPHENICOL HEMISUCCINATE	2	3.25
01500178	CHLOROCRESOL	2	3.00
01504211	CHLOROGUANIDE HYDROCHLORIDE	3	4.96
01500186	CHLORTETRACYCLINE HYDROCHLORIDE	2	3.55
01505293	DIALLYL SULFIDE	3	3.49
01505311	DIBENZOYLMETHANE	3	4.47
01500238	DICLOXACILLIN SODIUM	3	5.75
01504060	EMODIC ACID	3	3.94
01500283	ESTRADIOL CYPIONATE	2	3.00
01500284	ESTRADIOL VALERATE	3	6.10
01500285	ESTRIOL	3	8.50
01500303	FLUOCINONIDE	3	6.86
01500314	GENTAMICIN SULFATE	3	5.38
01500327	HETACILLIN POTASSIUM	3	5.15
01504098	PHENOTHRIN	3	7.83
01500490	PIPERAZINE	3	4.13
01504181	PRISTIMERIN	3	3.17
01503935	PROPAFENONE HYDROCHLORIDE	3	5.02
01500530	ROXARSONE	3	3.31

01500543	STREPTOZOSIN	3	3.39
01500545	SULFACETAMIDE	3	4.36
01500556	SULINDAC	3	4.97
01504105	TANNIC ACID	3	4.21
01500583	TOLNAFTATE	3	6.28
01503121	TRAZODONE HYDROCHLORIDE	3	4.20
01500591	TRIFLUOPERAZINE HYDROCHLORIDE	3	3.87
01504171	VENLAFAXINE	3	3.85

Table 3.3.1.1 Hits from screening the NINDS custom collection 2 drug library.

34 hits were discovered out of the 1040 drugs tested, a hit rate of 3.27%

Class of drug	Number of hits	Name of hit
Antibacterial	8	Diallyl sulfide, Dicloxacillin sodium, Gentamicin Sulphate, Hetacillin Potassium, Sulfacetamide, Roxarsone, Chlortetracycline Hydrochloride, Chloramphenicol hemisuccinate
Anthelmintic	1	Peperazine
Antiarrhythmic	1	Propafenone hydrochloride
Antidepressant	2	Trazodone Hydrochloride, Venlafaxine
Antifungal	2	Tolnaftate, Bifonazole
Antihyperlipidemic	1	Atorvastatin Calcium
Anti-infectant	3	Chlorocresol, Broxyquinoline, Acriflavinium hydrochloride
Anti-inflammatory	2	Sulindac, Fluocinonide
Antimalarial	1	Chloroguanide hydrochloride,
Antineoplastic	3	Dibenzoylmethane, Streptozosin, Pristimerin
Antipsoriatic	1	Anthralin
Antipsychotic	1	Trazodone hydrochloride
Insecticide	2	Phenothrin, azadirachtin
Oestrogen	3	Estriol, estradiol valerate, estradiol cypionate
Polyphenol	1	Tannic acid
Purgative	1	Emodic acid
Thyroid depressant	1	2-Thiouracil

Table 3.3.1.2 The classes of the 34 hits from the NINDS drug screen.

3.3.2 Selecting the compounds for further study

Compounds were then chosen for further experiments in *C. elegans*, before being tested in prion disease (Chapter 4). A range of compounds was selected to cover as much of the 17 different classes of drugs as possible, with more weight given to a class with multiple hits. The scientific literature was searched for compounds that had previously been given to mice for an extended period of time with little or no side effects. Predicted brain penetration was also used as a selection criterion, as although all of the compounds in the NINDS drug library influence brain activity, some are reported to have poor brain penetration *in vivo.*

Five compounds were chosen for further study: Dibenzoylmethane, Diallyl sulfide, estradiol valerate, trazodone hydrochloride and trifluoperazine hydrochloride (Figure 3.3.2). Dibenzoylmethane (DBZ) is a minor constituent of liquorice that has been found to have antineoplastic effects, with efficacy against prostate and mammary tumors (Huang et al., 1998; Khor et al., 2009). Diallyl sulfide (DAS) is an organosulfur compound derived from garlic that is an inhibitor of chemically induced carcinogenesis (Yang et al., 2001), and also has antibacterial properties (Tsao and Yin, 2001). Estradiol valerate (EV) is a synthetic ester of the naturally occurring sex hormone estradiol, which acts as a pro-drug, being cleaved in the body into estradiol and valeric acid. EV is used for hormone replacement therapy, and estradiol has been shown to be neuroprotective following ischemic stroke, reviewed in (Brann et al., 2012). Trazodone hydrochloride (Traz) is an antidepressant in the serotonin antagonist

and reuptake inhibitor class. It also has anxiolytic and hypnotic effects. Traz has been shown to reduce the Behavioral and Psychological Symptoms of Dementia (BPSD) in AD (Lopez-Pousa et al., 2008) and frontotemporal dementia (Lebert et al., 2004), but no studies have looked at the progression of neurodegeneration with Traz treatment. Trifluoperazine hydrochloride (Tri) is a typical antipsychotic that has antidopaminergic effects, and has been shown to increase the degradation of long lived proteins by increasing autophagy (Zhang et al., 2007), leading to the suggestion that it could be a possible treatment for ER stress disorders (Kim et al., 2008). Tri has also been shown to reduce the build up of PrP^{Sc} *in vitro* (Kocisko et al., 2003).

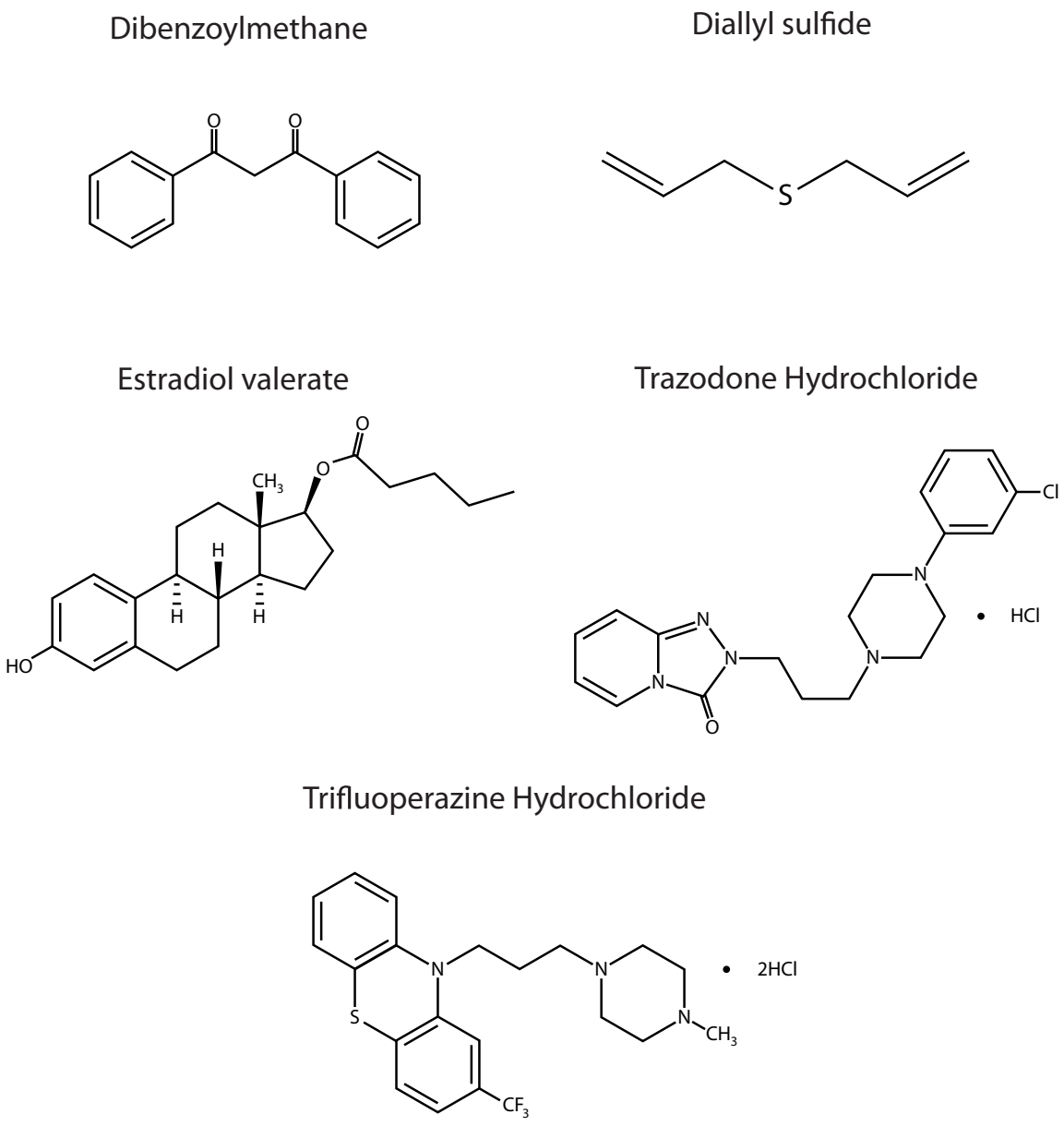

Figure 3.3.2 Molecular structure of the drugs to be studied.

3.3.3 The drugs to be tested are not false positives

False positives can be a problem when undertaking drug screens, especially when large numbers of molecules are involved. Each of the compounds that were selected for further testing was re-tested in the worm model of UPR stress, to allow statistical analysis and confirm they were true positive results. All of the drugs were found to be true positives, and consistently caused a statistically significant increase in the percentage of worms that developed to the L4 stage or further (Figure 3.3.3).

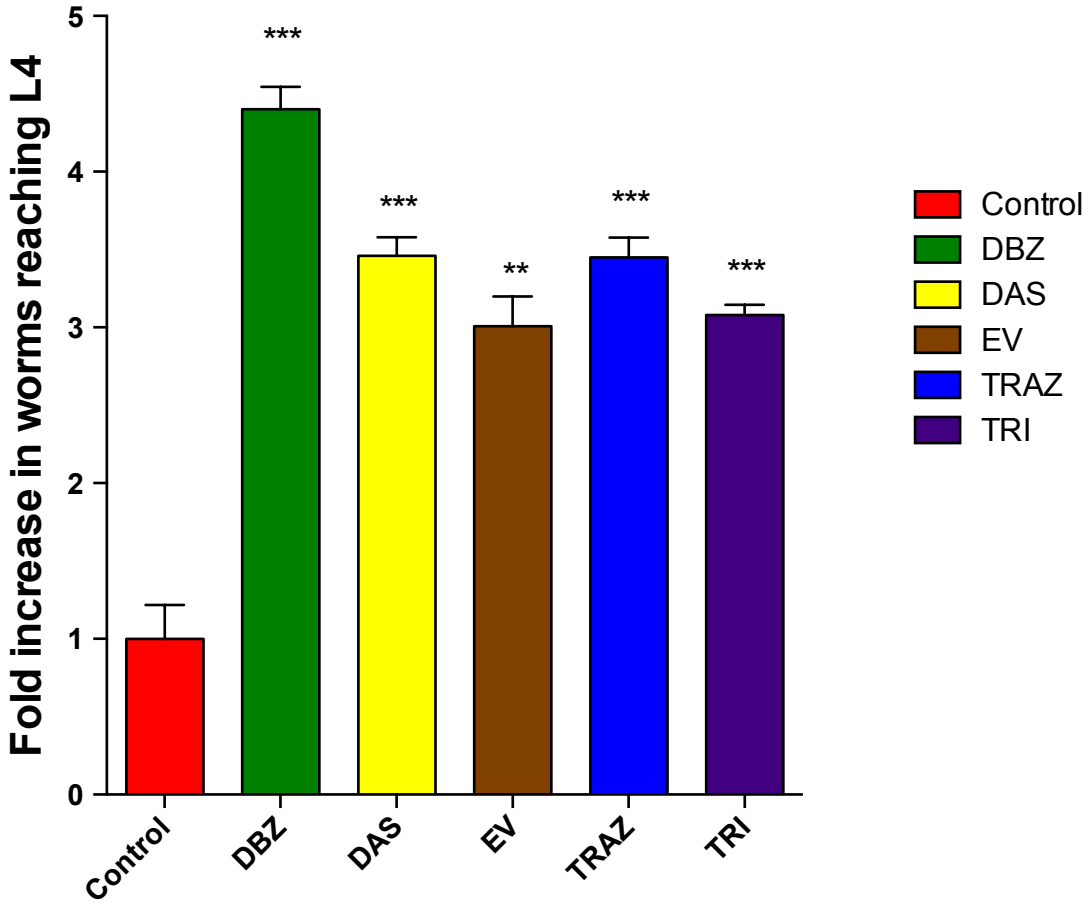

Figure 3.3.3. The drugs tested are not false positives*. DBZ, DAS, EV, Traz and Tri all cause an increase in the % of worms developing to L4 or older after stress induced by tunicamycin. N=~300 for each group, three biological replicates, error bars = SEM (* p < 0.05; ** p < 0.01; *** p < 0.001) All worms were exposed to tunicamycin for three days.*

3.4 Exploring the mechanism of action for the drugs to be tested

3.4.1 Testing the drugs in another readout of ER stress

The hits were tested to determine if they are beneficial in another model of ER stress. *hsp-4::GFP* worms express green fluorescent protein (GFP) tagged to HSP-4, the *C. elegans* ortholog of BiP. This worm strain has been used as a marker of ER stress in a number of studies, as GFP expression is induced during periods of ER stress from a variety of sources (Calfon et al., 2002; Urano et al., 2002; Yan et al., 2006). Control worms showed no GFP expression (Figure 3.4.1A and B), while tunicamycin treated worms expressed GFP throughout the hypodermis, intestine, and gonads (Figure 3.4.1C). EV and Traz reduced GFP expression across the whole worm (Figure 3.4.1F and G), while DAS, DBZ and Tri reduced GFP expression in the intestine and hypodermis, while maintaining patches of GFP expression in the spermatheca and below the pharynx in the head of the worms (Figure 3.4.1 D,E,H). An attempt was made to quantify GFP expression levels across the treatment groups by calculating the relative area of GFP expression (μm^3) from Z-stack 3-D images. Due to the drugs recovering the developmental phenotype of tunicamycin treatment, the worms were later developmental stages and hence a larger size in the treatment groups, leading to an increased area of GFP expression despite having a more diffuse and weaker signal compared to tunicamycin only treated worms, affecting the analysis.

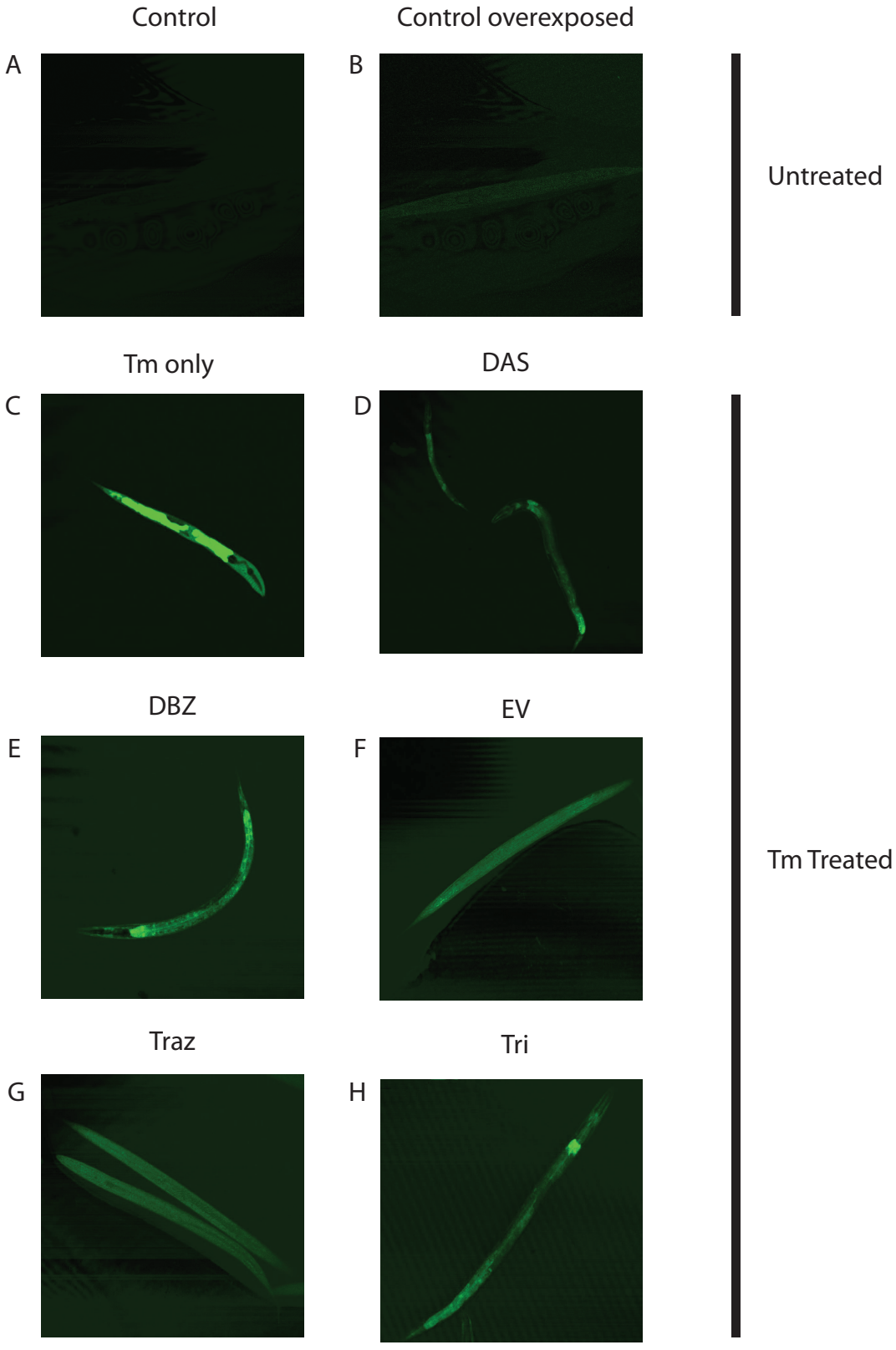
Control
Control overexposed
A
B
Untreated
Tm only
DAS
C
D
DBZ
EV
E
F
Tm Treated
Traz
Tri
G
H

Figure 3.4.1. The drugs reduce ER stress in hsp-4::GFP worms*. Representative images showing:* ***A)*** *Untreated worms show no GFP expression.* ***B)*** *Overexposed picture from A, showing the outline of the worm.* ***C)*** *Tunicamycin (Tm) treated worms express GFP throughout the hypodermis, intestines and gonads. EV,* ***F)****, and Traz,* ***G)****, show a reduction in GFP throughout the worms. DAS,* ***D)****, DBZ,* ***E)*** *and Tri,* ***H)*** *treated worms exhibit a reduction in GFP expression while maintaining some patches of GFP in the spermatheca and head region. All worms were exposed to tunicamycin for three days.*

3.4.2 The drugs do not act through PEK-1, IRE-1 or ATF-6

The drugs were then tested to see which arm of the UPR the act on, if any. The mutant worms for PEK-1, IRE-1 and ATF-6 introduced in section 3.2.2 were again used. It is known the drugs can restore normal development in wild-type animals (Figure 3.3.2), if they can also restore development in UPR mutant worms, it can be assumed the drugs do not act on the mutated protein in that strain. But, for example, if a drug doesn't restore development in *pek-1* mutant worms, it suggests the drug acts via PEK-1 in wild-type worms. Each of the drugs was found to increase the percentage of worms that develop to L4 or adulthood in *pek-1* (Figure 3.4.2 A), *ire-1* (Figure 3.4.2B) and *atf-6* (Figure 3.4.2 C) mutant worms. This suggests that although the drugs reduce ER stress (Figure 3.4.1), they do not act through any of the three arms of the UPR. It is not surprising the drugs do not act through IRE-1 or ATF-6, as they are transcription factors that induce chaperone expression without affecting global translation levels. It is more surprising the drugs do not act through PEK-1, as this arm controls protein translation and is the arm of the UPR shown to mediate prion neurotoxicity (Moreno et al., 2012). This does not rule out the possibility of the drugs acting upstream or downstream of PEK-1, or by increasing levels of translation via a separate mechanism.

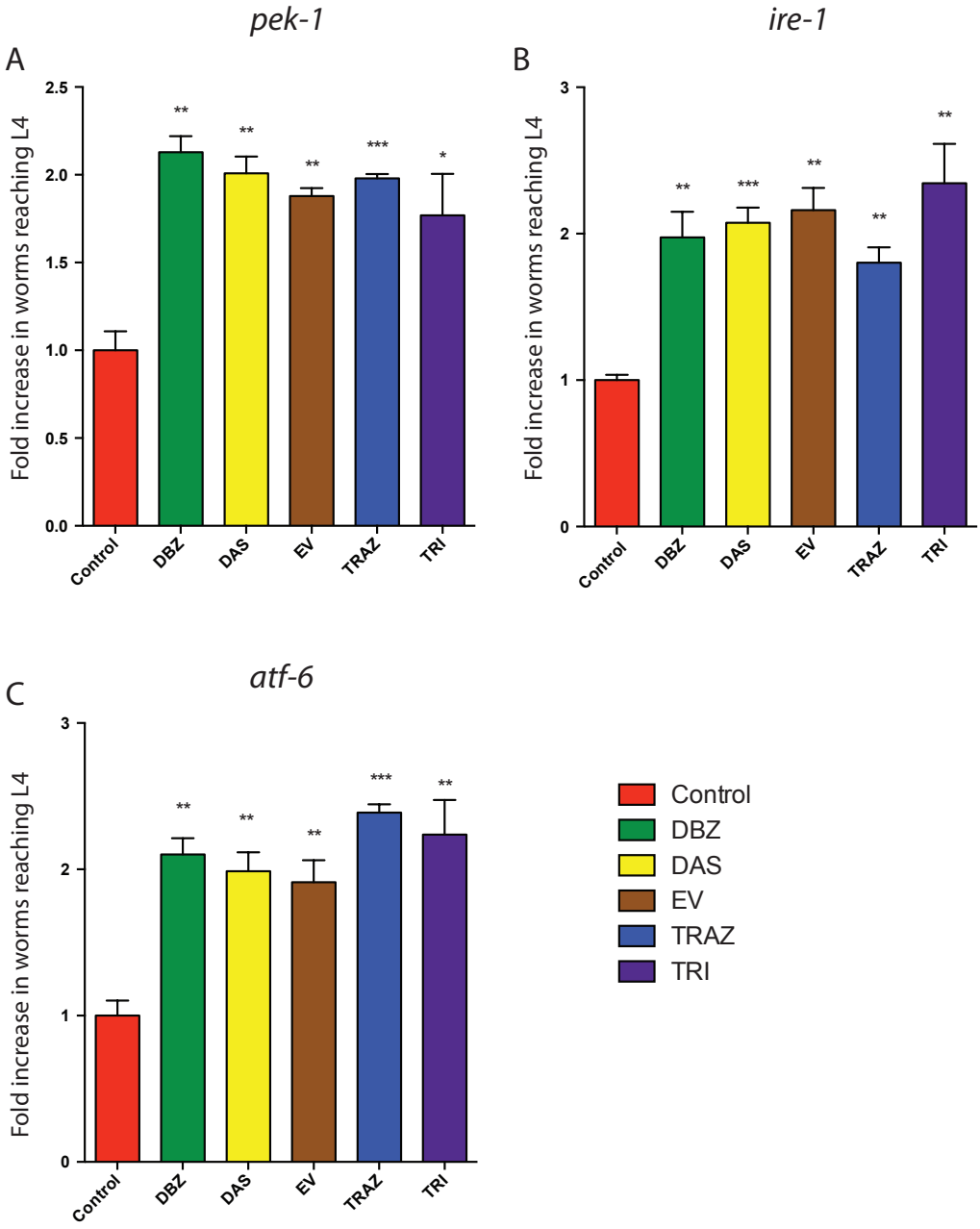

Figure 3.4.2 The hits recover the developmental phenotype in UPR mutant worms. *Each of the hits from the NINDS screen increase the percentage of worms developing to L4 or adulthood in pek-1,* ***A)****, ire-1,* ***B)****, and atf-6,* ***C)*** *mutant worms. n=~300, three biological replicates, error bars = SEM (* p < 0.05; ** p < 0.01; *** p < 0.001). All worms were exposed to tunicamycin for three days.*

3.5 Summary

A *C. elegans* model of UPR activation was developed, by exposing the worms to tunicamycin in their growth media for 3 days, from hatching until the normal age of adulthood. Exposure to tunicamycin results in a developmental delay in a dose dependent fashion, stalling development at the L3 stage or earlier. It is hoped exposure for 3 days, the usual generation time in *C. elegans* will produce an adequate chronic exposure to more accurately model extended UPR overactivation seen previously in mouse studies (Moreno et al., 2012) compared to shorter exposures. DMSO was found to enhance this phenotype of UPR activation, possibly by increasing the amount of tunicamycin being absorbed. The NINDS custom collection 2 drug library was then screened in this model of UPR activation, to search for drugs that can recover this phenotype. 34 hits were found, comprising 17 different classes of drugs. Five of these drugs, Dibenzoylmethane, Diallyl sulfide, estradiol valerate, trazodone hydrochloride and trifluoperazine hydrochloride were chosen for further study due to their known penetration into the brain, and previous experiments where they have been given to mice for extended periods of time with minimal side effects. The drugs all reduced ER stress in the worm, but this the developmental recovery was found to not be dependent on any of the PEK-1, IRE-1 or ATF-6 arms of the UPR when tested in mutant worms.

Chapter 4: Testing potential UPR inhibitors in prion diseased mice

4.1 Introduction and experimental plan

The five hits identified from the *C. elegans* UPR screen performed in chapter 3 were then tested in prion diseased mice as a potential treatment. tg37 mice were inoculated with RML prions at approximately 4 weeks of age. Treatment with each of the drugs was started at 7 w.p.i, when prion infection is established and synaptic loss has developed, but before neuronal loss and behavioural deficits are seen (see section 1.1.7). Morphological analysis of the brain was performed in terminally sick animals to check for spongiosis, cell death and possible neuroprotection. Behavioural assays, burrowing and novel object recognition, were performed to check for any recovery with drug treatment. Translational rates using [^{35}S] methionine labeling experiments were performed to determine if the drugs were restoring global protein synthesis levels, and if this correlated with a recovery in the levels of vital synaptic proteins. The levels of phosphorylated eIF2α were also determined as a possible mechanism for the recovery of protein translation levels. Finally, lifespan analysis was carried out to determine the overall efficacy of the drugs.

Due to the insolubility of DBZ, it was delivered as a 0.5% mixture into the standard mouse powdered diet. Tri and Traz were dissolved in saline and administered by intraperitoneal (IP) injection at a concentration of 10 mg/kg

and 40 mg/kg respectively. DAS was dissolved in sesame oil and orally gavaged at 10 mg/kg. EV was also dissolved in sesame oil and delivered by subcutaneous (SC) injection at 50 μg/kg. All drugs were administered once daily, except DBZ, which was present as a food source continuously.

4.2 Testing the drugs in prion disease

4.2.1 Determining if the drugs enter the brain.

Concentrations of Tri and Traz that enter the brain were determined by liquid chromatography dual mass spectrometry (LC-MS/MS), to confirm they could cross the blood brain barrier and determine the most effective concentration to deliver the drugs at. Tri was administered at 1, 5 or 10mg/kg and Traz was administered at 1, 10, 40 or 50 mg/kg, with samples taken 2 or 24 hours after injection. Both drugs were absorbed into the blood and entered the brain (Table 4.2.1). 10 mg/kg Tri and 40 mg/kg Traz were chosen as treatment concentrations as they resulted in the highest penetration into the brain. LC-MS/MS is still being performed on samples treated with DAS, DBZ and EV. LC-MS/MS analysis was kindly performed by Catharine Ortori and Dave Barrett, University of Nottingham.

Drug	Dosage	Sample time (Hours)	Mean ng/ml drug in Plasma	Mean ng/g drug in Brain
Trifluoperazine	Vehicle	2	0.00	0.00
	Vehicle	24	0.00	0.00
	1mg/kg Trifluoperazine	2	75.07	118.59
	1mg/kg Trifluoperazine	24	0.00	Trace
	5mg/kg Trifluoperazine	2	144.28	130.81
	5mg/kg Trifluoperazine	24	0.00	31.06
	10mg/kg Trifluoperazine	2	160.09	902.07
	10mg/kg Trifluoperazine	24	0.00	28.25
Trazodone	Vehicle	2	0.00	0.00
	Vehicle	24	0.00	0.00
	1mg/kg Trazodone	2	5.36	3.94
	1mg/kg Trazodone	24	0.00	0.40
	10mg/kg Trazodone	2	70.70	22.71
	10mg/kg Trazodone	24	0.01	0.21
	40mg/kg Trazodone	2	510.19	192.01
	40mg/kg Trazodone	24	N.D	
	50mg/kg Trazodone	2	349.67	81.24
	50mg/kg Trazodone	24	0.00	0.08

Table 4.2.1 Brain penetration of Tri and Traz. LC-MS/MS was performed to determine the concentration of Tri and Traz in brain and plasma. N.D = Not determined

4.2.2 Neuroprotection with Traz, DBZ and DAS treatment

Each cohort of mice was monitored until they succumbed to prion disease and the degree of spongiosis and neuronal loss was measured in terminal animals. Spongiosis appears as a series of circular holes when examined histopathologically. Cell death is readily observed in the CA1 region of the hippocampus, where the neuronal ribbon of cell bodies disappears in prion disease. Uninfected control animals display no spongiosis or neuronal death (Figure 4.2.2A,D), compared to prion infected only (Figure 4.2.2B,E) and vehicle treated animals (Figure 4.2.2C,F), which display extensive spongiosis and neuronal death. The five drugs caused varying degrees of neuroprotection. DBZ treatment was substantially neuroprotective, as animals displayed reduced spongiosis and a reduction in neuronal death (Figure 4.2.2G,J), although some dying neurons can be observed (appearing as darker, more cylindrical cells - Figure 4.2.2J). DAS treatment was slightly neuroprotective; although there was still significant spongiosis, cell death in the CA1 region was reduced (Figure 4.2.2H,K). EV treatment offered slight neuroprotection, as seen by the maintenance of the neuronal ribbon, but these cells were largely dying (Figure 4.2.2 L), again seen by the appearance of darker more cylindrical cells. Extensive spongiosis was still present (Figure 4.2.2I). Traz treatment was substantially neuroprotective. Slight spongiosis was still present but the neuronal ribbon was intact and CA1 neurons were healthy (Figure 4.2.2M,O). Tri treatment was not neuroprotective, these mice displayed extensive spongiosis and neurodegeneration (Figure 4.2.2N,P).

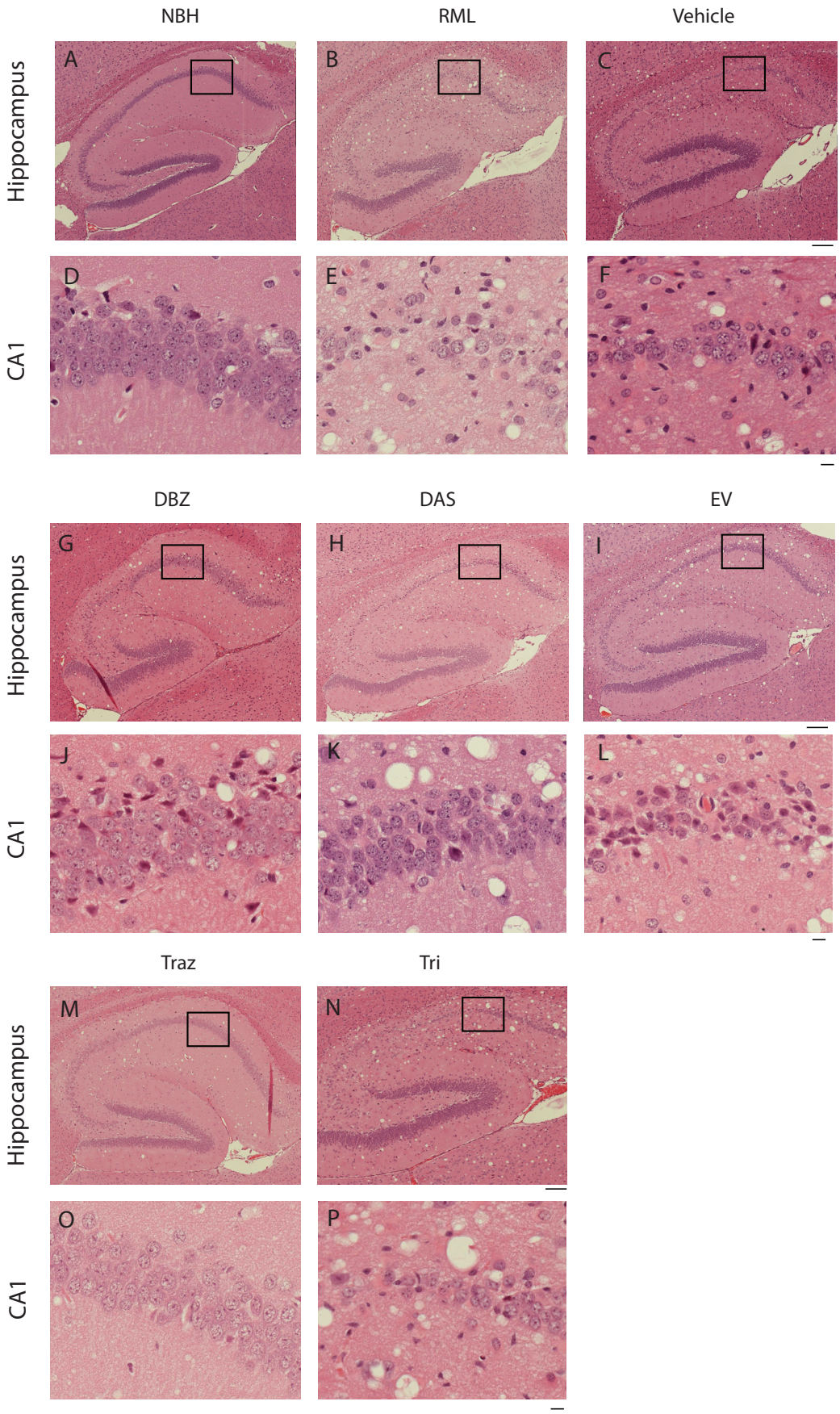
NBH
RML
Vehicle
Hippocampus
CA1
A
B
C
D
E
F
DBZ
DAS
EV
G
H
I
J
K
L
Traz
Tri
M
N
O
P

Figure 4.2.2 Histology of the hippocampus in each treatment group*.*

Representative images of haematoxylin and eosin stained hippocampal sections from uninfected control mice (A,D) prion-infected animals (B,E), vehicle treated (C,F), DBZ treated (G,J), DAS treated (H,K), EV treated (I,L), Traz treated (M,O) or Tri treated (N,P). RML only and vehicle treated animals have marked neuronal loss in CA1-4 region of hippocampus, with shrinkage of whole hippocampus and extensive spongiosis (B,C,E,F). Drug treated animals display varying levels of neuroprotection (G-P). Scale bar = 200 μm for A-C, G-I and M-N; Scale bar = 50 μm for D-F, J-L, and O-P.

4.2.3 DBZ, Traz and DAS improve cognitive deficits in prion-infected mice.

The drug treated mice were assessed using the burrowing and novel object recognition behavioural assays. The burrowing assay is a simple behavioural test that measures a rodent's natural tendency to empty a tube filled with food pellets. Damage to the hippocampus and prefrontal cortex has been shown to decrease burrowing activity in mice (Deacon et al., 2002; Deacon et al., 2003), and has been used previously to measure behavioural deficits in prion disease (Mallucci et al., 2007). The novel object recognition assay is a memory test that is performed in two stages. In the first training stage, a mouse is placed in an enclosure with two separate objects. The mouse explores both objects equally as they are both novel to the animal. In the second test stage, one object is replaced by a second novel object. Mice that remember the previous objects show preference for exploring the novel object, mice with memory deficits explore both the previously seen and novel object equally. Deficits in novel object

recognition begin at 8 w.p.i, and with burrowing begin at 9 w.p.i. DBZ and DAS treated animals both show significant increases in burrowing activity at 9 and 10 w.p.i compared to vehicle controls (Figure 4.2.3A). Tri and Traz treated animals could not be burrowed as they both experienced side effects from the drugs. Traz treated mice would often fall asleep after dosing, this likely reflects the sedative and hypnotic properties of the drug. Tri treated mice would become extremely lethargic after dosing, and would not burrow when placed in the burrowing cages. Both Tri and Traz treated mice would appear normal after the initial effects of the drug wore off, but this could take several hours. EV treated mice were all males to remove any endogenous estrogen effect and therefore were unable to be burrowed due to male mice fighting following the burrowing assay.

Vehicle treated mice lose preference for the novel object at 9w.p.i, as seen before with a preference ratio of 1, while DBZ and Traz treated animals displayed preference for the novel object, demonstrating improved memory in these animals (Figure 4.2.3B). DAS treated animals did not show a preference for the novel object (Figure 4.2.3B), reflecting impaired memory in theses animals despite improvements in burrowing activity (Figure 4.2.3A). Again Tri treated animals were too lethargic to be assayed. Novel object recognition assays where kindly performed by Colin Molloy, University of Leicester.

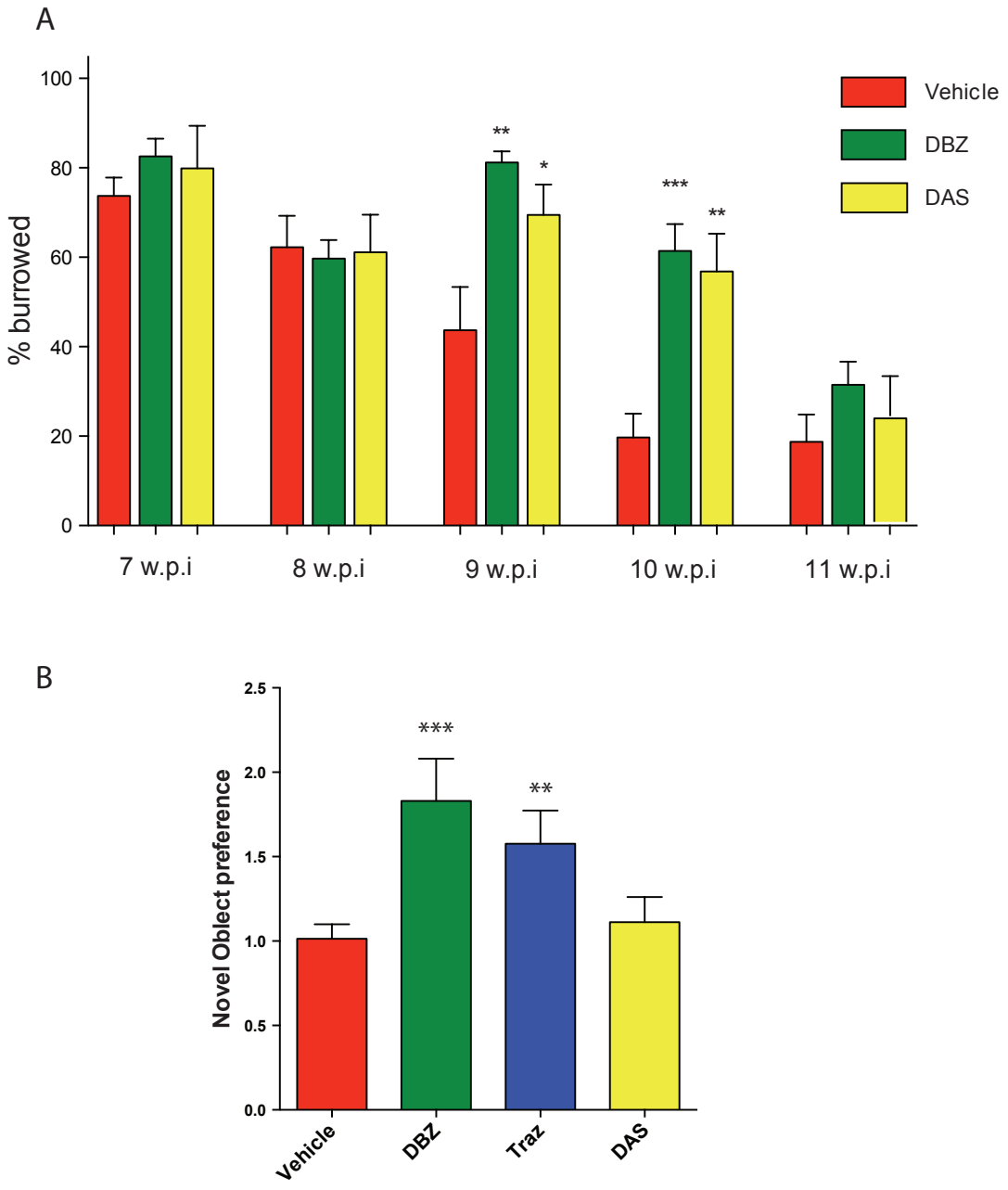

Figure 4.2.3 Recovery of behavioural deficits after drug treatment. A) *DBZ and DAS treated animals improve burrowing activity at 9 and 10 w.p.i compared to vehicle controls.* ***B)*** *DBZ and Traz treated animals retain preference for the novel object, while DAS treated mice do not. N=10 for all groups, error bars = ±SEM, (* p < 0.05; ** p < 0.01; *** p < 0.001).*

4.2.4 Restoration of global protein synthesis levels by treatment with DBZ, DAS, Traz and Tri

Global protein synthesis rates can be measured by [^{35}S] methionine labeling experiments. Acute hippocampal slices are generated from mice receiving drug treatment or vehicle, and incubated with radioactive methionine. The slices take up the methionine and incorporate them into any proteins being made that contain methionine. After homogenization of the slices and TCA precipitation of the proteins, the amount of radiolabel, and hence the rates of protein synthesis can be determined by scintillation counting. The drugs were tested to see if they restored protein synthesis levels, as predicted from the recovery of the *C. elegans* developmental phenotype observed in section 3.3.3. DBZ, DAS, Traz and Tri treatment all restored global protein synthesis levels at 10 w.p.i, while EV treatment did not (Figure 4.2.4).

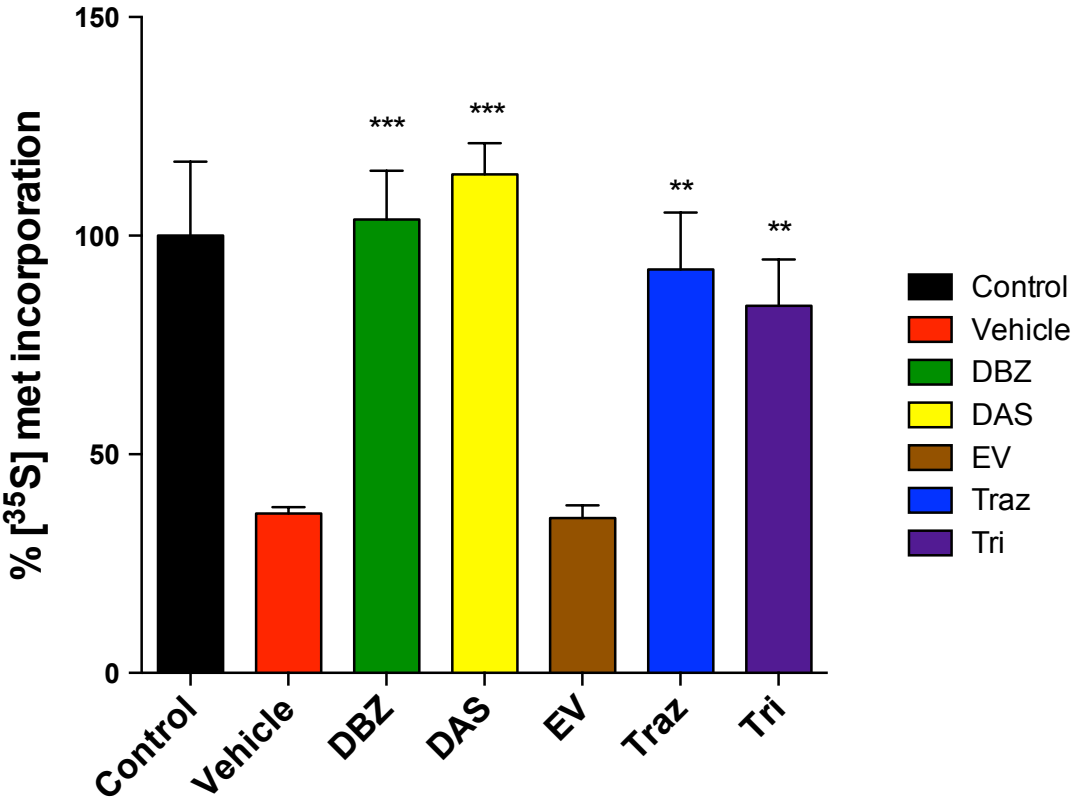

Figure 4.2.4 Measuring global protein synthesis in drug treated mice*. Protein synthesis rates in hippocampal slices at 10w.p.i, determined by ^{35}S-methionine incorporation into protein, showed ~60% reduction in prion-infected vehicle-treated mice compared to uninfected controls. DBZ, DAS, Traz and Tri treatment all restored protein synthesis rates, while EV did not. N=6 in each group, error bars = ±SEM, (* p < 0.05; ** p < 0.01; *** p < 0.001).*

4.2.5 The drugs do not effect eIF2α phosphorylation

During prion disease the levels of eIF2α-P steadily rise as the disease progresses, causing a reduction in global translation rates (Moreno et al., 2012). Due to four out of five of the drugs tested restoring global protein synthesis rates, the levels of phosphorylated eIF2α were determined, to ascertain if the recovery of protein synthesis rates was due to a reduction of eIF2α-P. The levels of eIF2α-P are determined by calculating the ratio of eIF2α-P to eIF2α as detected by western blotting (Figure 4.2.5). None of the five drugs tested caused a significant change in the levels of eIF2α-P after treatment. This indicates that other mechanisms are mediating the increase in protein synthesis observed. This is not the first instance of increased translation after treatment with a specific drug that is independent of eIF2α-P levels (Sidrauski et al., 2013), and will be discussed in greater detail in chapter 6.

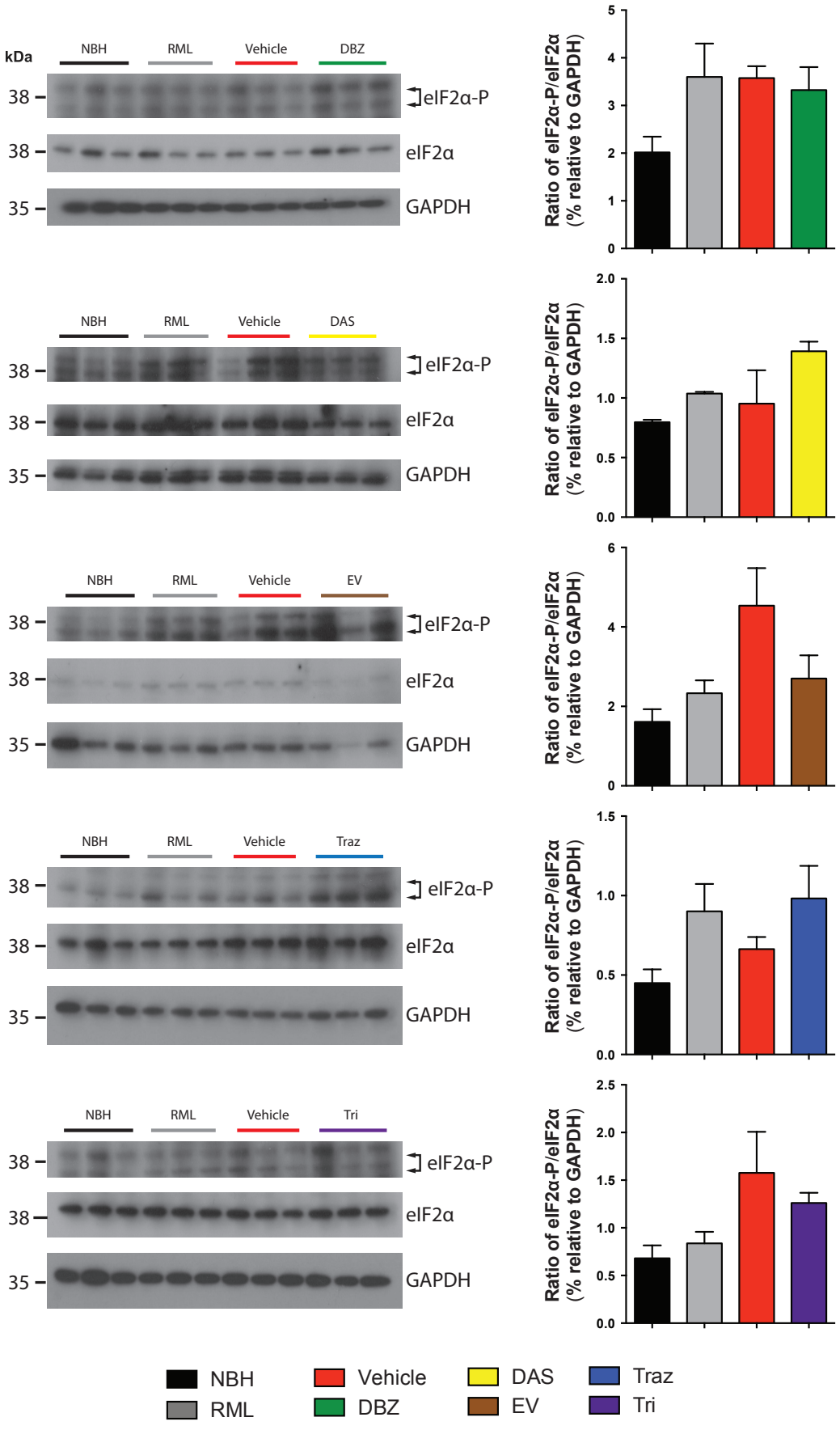
kDa
NBH
RML
Vehicle
DBZ
38
38
35
eIF2α-P
eIF2α
GAPDH
Ratio of eIF2α-P/eIF2α (% relative to GAPDH)
NBH
RML
Vehicle
DAS
EV
Traz
Tri

Figure 4.2.5 eIF2α-P levels do not change after drug treatment*. DBZ, DAS, EV Traz and Tri treatment do not alter levels of eif2α-P compared to vehicle treated or RML only animals. Control animals were inoculated with NBH. Three biological replicates were included for each treatment group. Samples were 10 w.p.i. error bars = ±SEM.*

4.2.6 Synaptic protein levels after drug treatment.

The levels of vital synaptic proteins decrease as prion disease progresses. Synaptic protein levels were determined by western blot to ascertain if the recovery of protein synthesis observed in section 4.2.4 was stimulating their transcription. If so, it would provide a possible mechanism for the neuroprotection exhibited after DBZ, DAS and Traz treatment. A pre-synaptic, SNAP25, and post-synaptic, PSD95, protein were chosen for analysis at 10 w.p.i. Treatment with DBZ or EV did not cause a significant change in the levels of SNAP25 or PSD95. DAS and Tri treatment stimulated an increase in SNAP25, but not PSD95 levels when compared to vehicle treated or RML only controls. Traz treatment caused an increase in PSD95 levels, but surprisingly decreased SNAP25 levels (Figure 4.2.6). Hence the translation of important synaptic proteins does not adequately explain the neuroprotection observed in DBZ, DAS and Traz treated mice. It is surprising that restoring protein synthesis has such a minor effect on synaptic protein levels. As the analysis took place at 10 w.p.i, it is possible the levels of synaptic protein take time to recover, further investigation at 11 or 12 w.p.i may explain the absence of recovery.

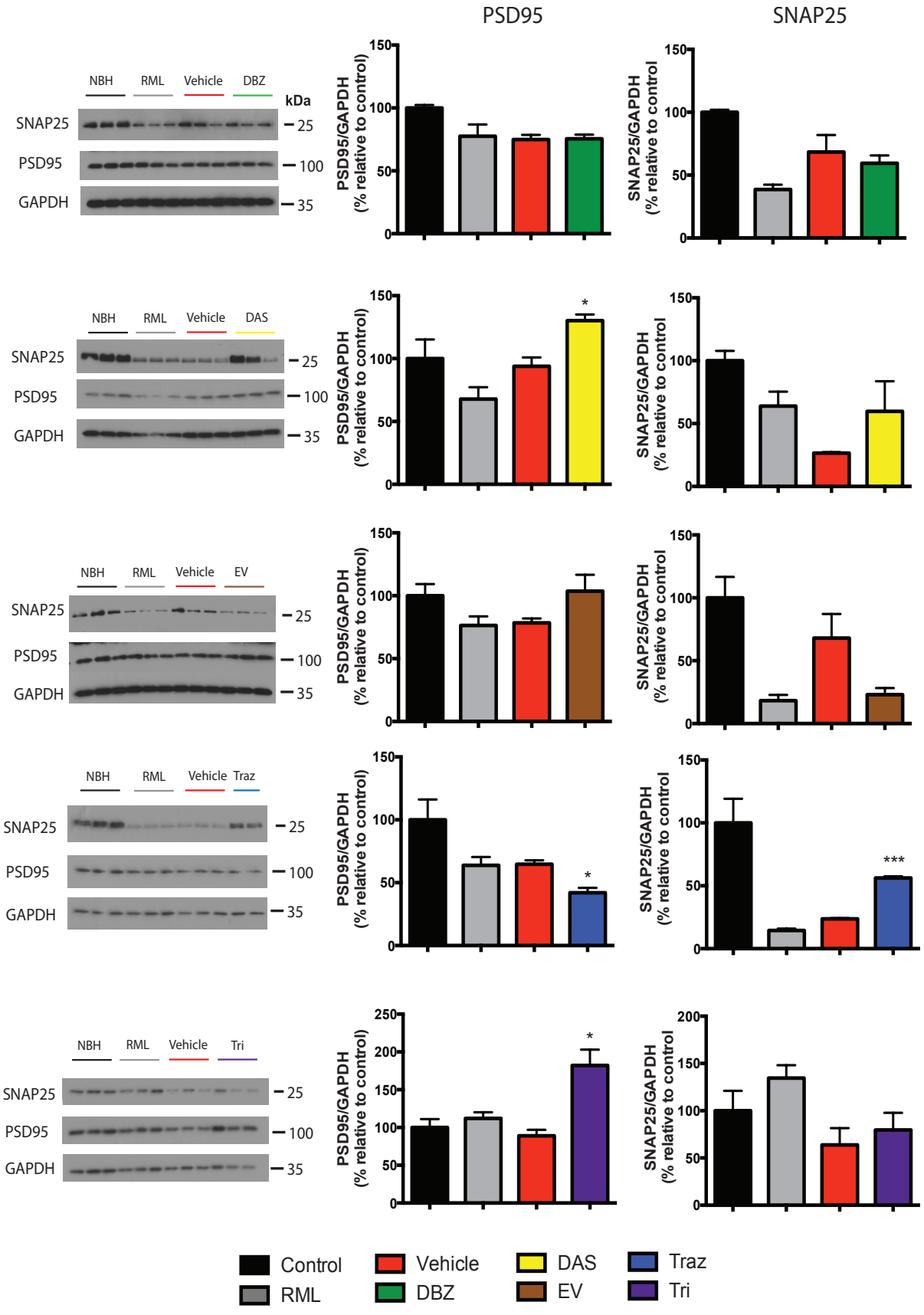
PSD95
SNAP25
NBH
RML
Vehicle
DBZ
DAS
EV
Traz
Tri
kDa
SNAP25
PSD95
GAPDH
25
100
35
PSD95/GAPDH (% relative to control)
SNAP25/GAPDH (% relative to control)
*
***
Control
RML
Vehicle
DBZ
DAS
EV
Traz
Tri

Figure 4.2.6 Synaptic protein levels after drug treatment*. Immunoblots of SNAP25 and PSD95 synaptic proteins. Treatment with DBZ or EV did not cause a significant change in the levels of SNAP25 or PSD95. DAS and Tri treatment stimulated an increase in SNAP25, but not PSD95 levels when compared to vehicle treated or RML only controls. Traz treatment caused an increase in PSD95 levels, but decreased SNAP25 levels. Control animals were inoculated with NBH. Three biological replicates were included for each treatment group. Samples were 10 w.p.i. error bars = ±SEM, (* $p < 0.05$; ** $p < 0.01$; *** $p < 0.001$).*

4.2.7 PrP^{C} and PrP^{Sc} levels after drug treatment

The levels of PrP^{C} and PrP^{Sc} after drug treatment were determined, to ascertain if the drugs were having a direct effect on the conversion of PrP^{C} to PrP^{Sc}. PrP^{C} levels increase during prion disease, this reflects increased production of PrP^{C} in response to its constant conversion to PrP^{Sc} as the disease progresses. Protease resistant PrP^{Sc} is deposited as prion disease progresses, and is observed as undigested fragments after digestion with proteinase K. In contrast, NBH samples contain no protease resistant fragments after proteinase K digestion. DBZ, EV and Traz treatment caused no significant difference in PrP^{C} levels compared to vehicle treated and RML only animals (Figure 4.2.7.1). Das treatment caused an increase in PrP^{C} levels compared to vehicle treated animals (but not RML only animals). Tri treatment caused an increase in PrP^{C} levels compared to RML only animals (but not vehicle treated animals). Strangely, in the DAS, EV, Traz and Tri immunoblots, a decrease in PrP^{C} levels compared to NBH controls was observed. It is not sure what caused this. Due to proteinase K

digesting all the reference proteins, it is not possible to quantify PrP^{Sc} immunoblots. However some conclusions about the levels of PrP^{Sc} can be drawn. DAS and Tri treatment appeared to reduce the levels of PrP^{Sc} (Figure 4.2.7.2). Taken together with the increase in PrP^{C} observed with DAS and Tri treatment, it is possible the drugs are reducing either PrP^{Sc} conversion or deposition. Tri has been reported to reduce PrP^{Sc} deposition *in vitro* (Kocisko et al., 2003), so may be having the same effect *in vivo*. DAS has no reported effects on prion conversion but may be working via a similar mechanism as Tri. It can also be concluded that the drugs do not act by reducing the levels of PrP^{C}, which has previously been shown to be protective (White et al., 2008).

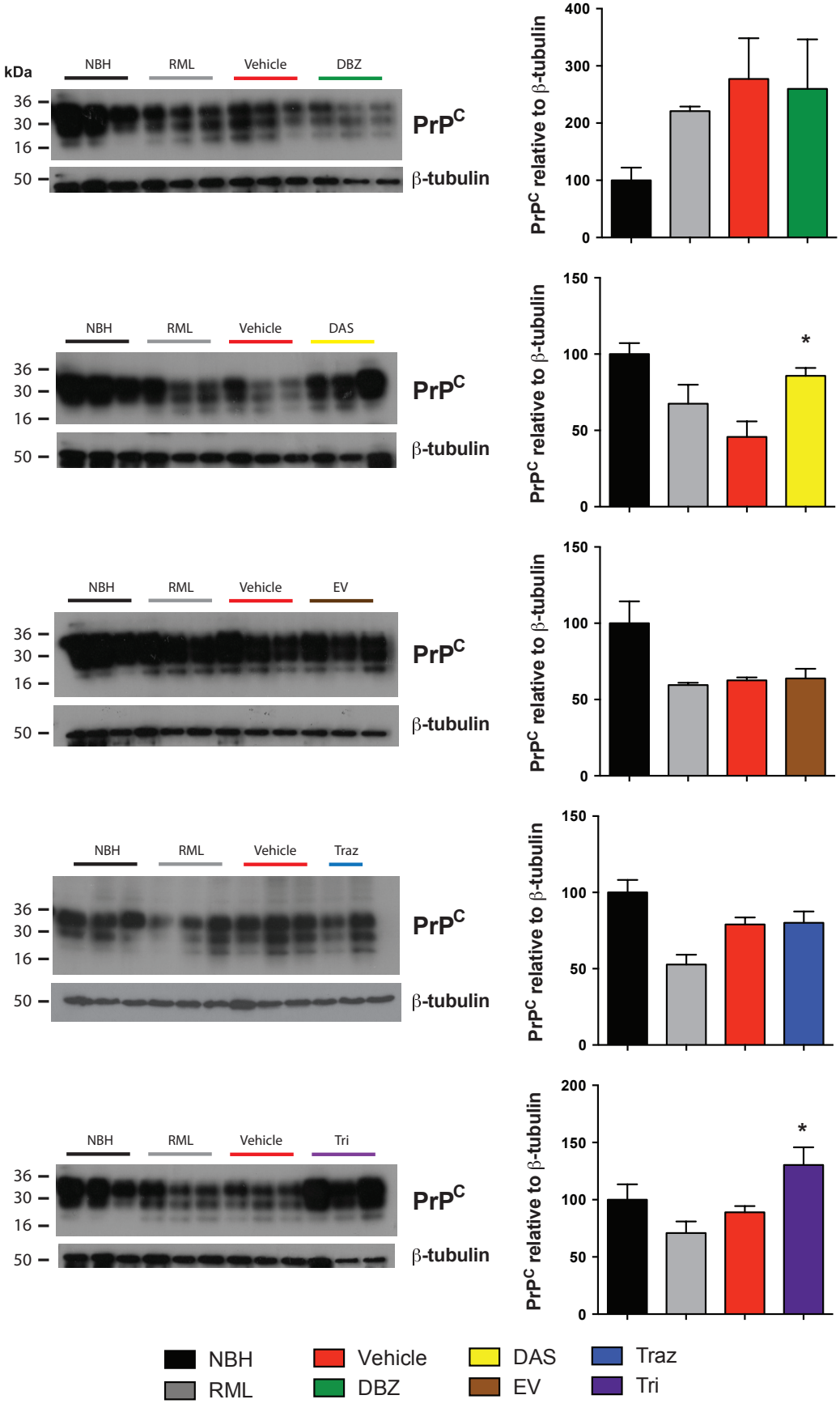
kDa
NBH
RML
Vehicle
DBZ
36
30
16
50
PrP^C
β-tubulin
PrP^C relative to β-tubulin
400
300
200
100
0
NBH
RML
Vehicle
DAS
150
100
50
*
NBH
RML
Vehicle
EV
NBH
RML
Vehicle
Traz
NBH
RML
Vehicle
Tri
200
150
NBH
RML
Vehicle
DBZ
DAS
EV
Traz
Tri

Figure 4.2.7.1 PrP^C levels after drug treatment. *Representative immunoblots and bar charts quantitating relative levels of proteins in 3 independent samples are shown. Samples are 10 w.p.i. Controls are NBH uninfected animals. error bars = ±SEM, (* $p < 0.05$).*

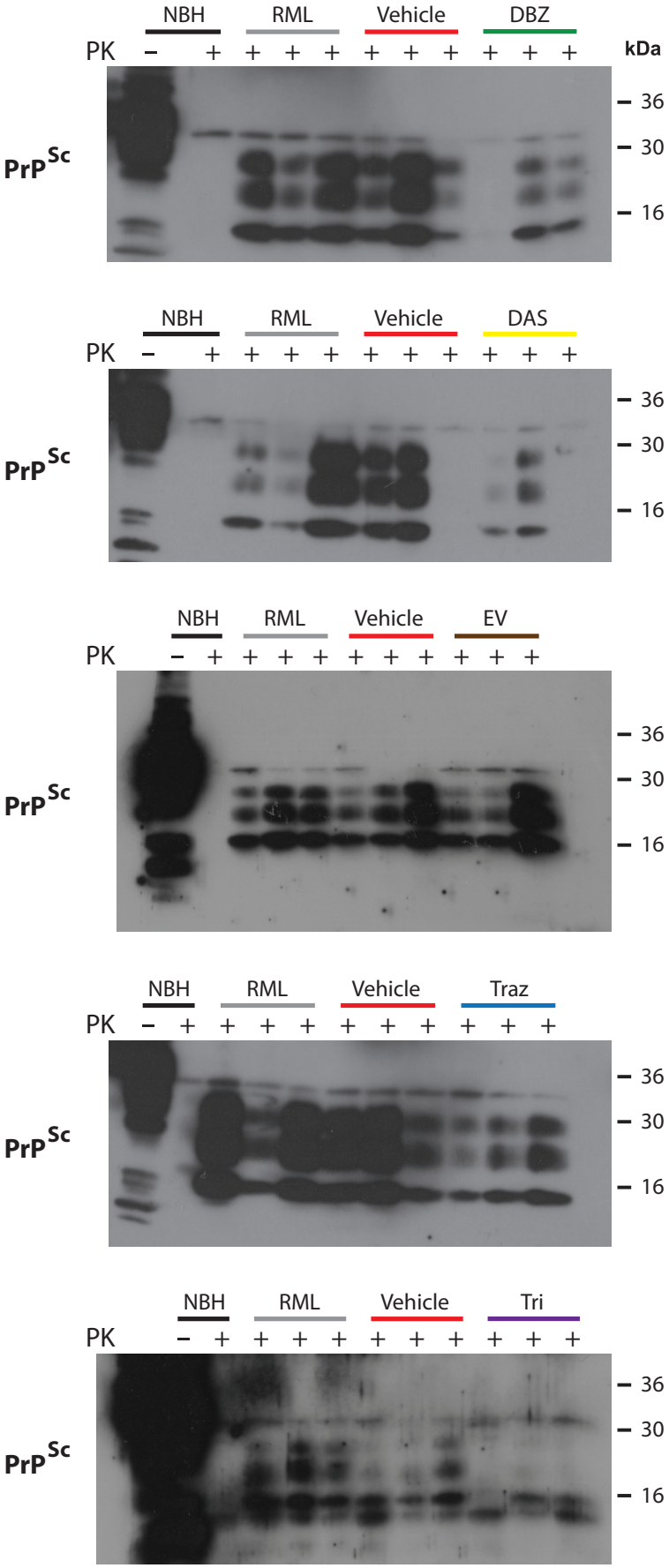
NBH
RML
Vehicle
DBZ
PK
kDa
PrP^Sc
36
30
16
NBH
RML
Vehicle
DAS
PK
PrP^Sc
36
30
16
NBH
RML
Vehicle
EV
PK
PrP^Sc
36
30
16
NBH
RML
Vehicle
Traz
PK
PrP^Sc
36
30
16
NBH
RML
Vehicle
Tri
PK
PrP^Sc
36
30
16

Figure 4.2.7.2 PrP^{Sc} levels after drug treatment. *Representative immunoblots and bar charts showing relative levels of proteins after proteinase K digestion in 3 independent samples are shown. Samples are 10 w.p.i. Controls are NBH uninfected animals.*

Figure 4.2.8 Lifespan analysis and overall efficacy of the drugs

Lifespan analysis of each drug treatment group was performed. DBZ and TRAZ treatment caused a significant increase in the lifespan of mice with prion disease (Figure 4.2.8). DAS, EV and Tri treatment had no effect on lifespan. Each group was compared to their relevant vehicle control. Out of the five drugs tested, DBZ and Traz are beneficial in the treatment of prion disease. Treatment with both drugs caused neuroprotection, increases in protein synthesis levels, prevention of behavioural deficits and increased lifespan. DAS treated mice showed benefits in burrowing, increased protein synthesis levels and a degree of neuroprotection, but the overall efficacy of the treatment was limited. Tri treatment restored protein synthesis levels, and possibly reduced PrP^{Sc} deposition, but didn't confer any neuroprotection. EV treatment was ineffective in the treatment of prion disease. It is unsure by which mechanism the drugs are exhibiting their neuroprotective effects, it is likely they act independently of the UPR as eIF2α-P levels are unchanged.

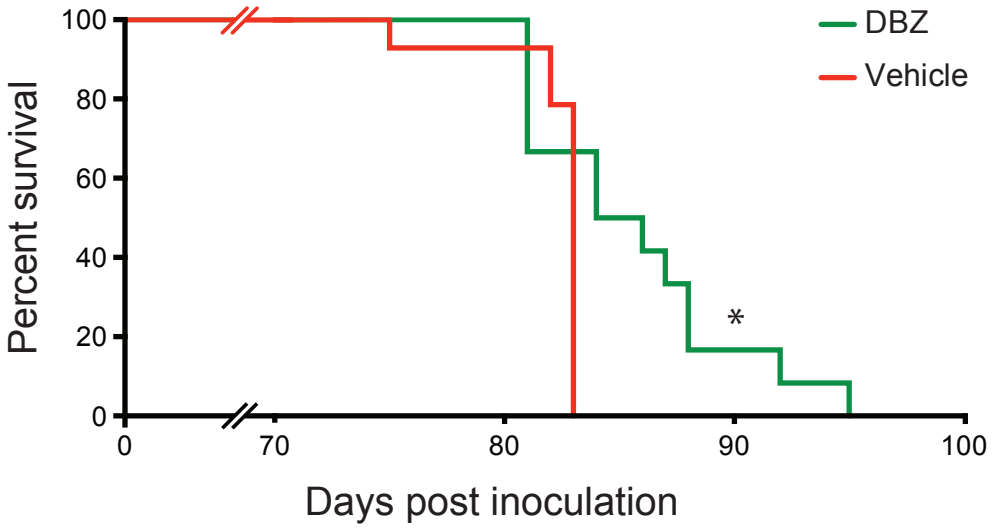
DBZ
Vehicle
Percent survival
100
80
60
40
20
0
0
70
80
90
100
*
Days post inoculation

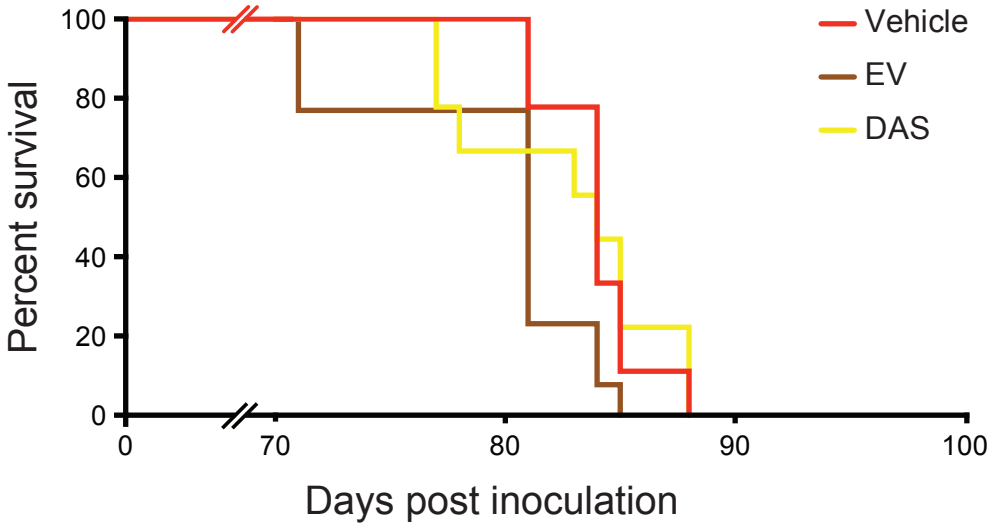
Vehicle
EV
DAS
Percent survival
100
80
60
40
20
0
0
70
80
90
100
Days post inoculation

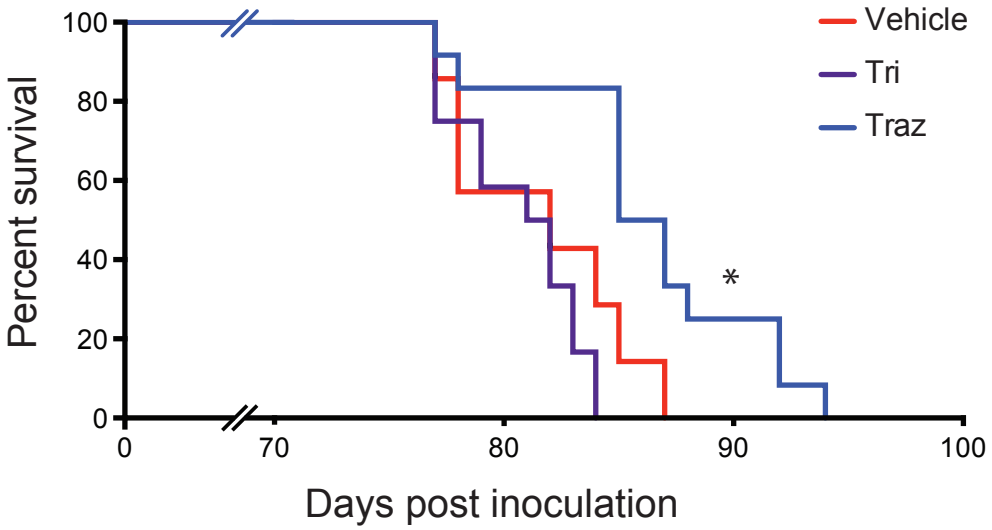
Vehicle
Tri
Traz
Percent survival
100
80
60
40
20
0
0
70
80
90
100
*
Days post inoculation

Figure 4.2.8 Kaplan-Meier survival plots for each treatment group. *DBZ and Traz treatment caused a significant increase in survival, while DAS, EV and Tri treatment had no effect. N=12, except for EV N=13, DAS and DAS vehicle N=9 and Tri vehicle N=7 (* $p < 0.05$, (Log-Rank, Mantel-Cox test)).*

4.3 Summary

Five hits from a drug screen in *C. elegans* to search for modulators of the unfolded protein response were tested in prion diseased mice as potential therapeutics. DBZ, DAS and Traz treated mice exhibited neuroprotection and prevention of behavioural deficits. DBZ, DAS, Traz and Tri treatment caused an increase in global protein synthesis rates, but this was not dependent on reduced eIF2α-P levels. The drugs had only minor effects on synaptic protein levels. PrP^{C} and PrP^{Sc} levels remained constant in DBZ, EV and Traz treated animals, but DAS and Tri possibly reduced PrP^{Sc} deposition. DBZ and Traz increased lifespan in prion diseased mice, and taken together with the other results, are newly identified potential therapeutic agents. It is unclear how the drugs elicit their neuroprotective effects, it is possible they act upstream or downstream of eIF2α-P, or stimulate translation via UPR independent methods. Off target effects are also a possibility. Potential mechanisms of action are discussed in greater detail in chapter 6. These results have validated the use of *C. elegans* as a tool for screening potential therapeutic compounds, and excitingly identified two novel targets for possible therapeutic use in prion disease.

Chapter 5: Testing a specific PERK inhibitor in mice as a treatment for prion disease

5.1 Introduction

In contrast to chapters 3 and 4, a more targeted approach was undertaken to modulate the UPR for therapeutic benefit. Pharmacological inhibition of PERK is predicted to be beneficial in prion disease. This chapter details the testing of a recently described, orally bioavailable, highly selective inhibitor of PERK, GSK2606414 (Axten et al., 2012), as a possible treatment for prion disease. This work was undertaken in collaboration with Dr Julie Moreno (University of Leicester), with technical assistance from Colin Molloy (University of Leicester – behavioural assays) and Catharine Ortori (University of Nottingham – pharmacokinetic assays). The data herein is published in *Science translational medicine: Oral treatment targeting the unfolded protein response prevents prion neurodegeneration and clinical disease in mice* (Moreno, Halliday et al., 2013).

5.1.1 GSK2606414

GSK2606414 is selective and potent inhibitor of PERK. It was developed through screening and lead optimization using the human PERK crystal structure, from an original lead molecule that had poor selectivity and pharmacokinetics, to the improved GSK2606414 molecule (Figure 5.1.1) that has excellent selectivity and oral efficacy (Axten et al., 2012). GSK2606414 has an IC_{50} of 0.4nM for PERK, and a much higher IC_{50} for the most similar kinases, HRI and PKR, of 420nM and 696nM respectively. It was originally developed as a possible cancer treatment, and it inhibits the development of human tumor xenografts in mice (Axten et al., 2012). GSK2606414 therefore has the required pharmacokinetics to be a useful experimental tool for the exploration of PERK inhibition in prion disease, and as a possible therapeutic.

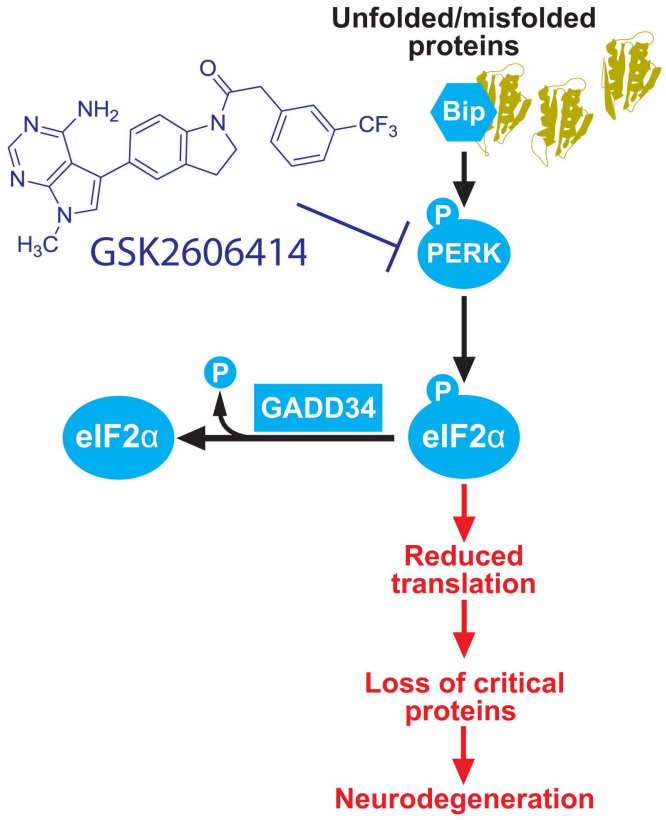

Fig. 5.1.1 Schematic showing the molecular structure of GSK2606414, and its point of action in the PERK arm of the UPR. *Misfolded proteins are detected by in the ER by BiP. BiP activates PERK, which dimerises and autophosphorylates. PERK phosphorylates eIF2α, leading to a shutdown of translation. This translational repression is reversed by GADD34, which dephosphorylates eIF2α. GSK2606414 inhibits PERK, preventing it from phosphorylating eIF2α and maintaining protein translation.*

5.2 Determining if GSK2606414 can penetrate the brain in sufficient quantities for PERK inhibition.

To date, GSK2606414 has only been tested *in vitro*. The potency of an inhibitory compound is often expressed as its IC_{50} – the concentration required to produce a 50% inhibition in the target protein. GSK2606414 has a PERK-P IC_{50} of 0.4 in a cell free assay, and higher IC_{50} of 30nM in a cellular assay (Axten et al., 2012). If this compound was to be used as a potential treatment, it was first important to confirm that GSK2606414 penetrated the blood brain barrier, and once this was confirmed, to select a dose that would deliver an appropriate amount of PERK inhibition in mice. To do this, liquid chromatography, dual mass spectrometry (LC-MS/MS) measurements were acquired from three separate doses of 10mg/kg, 50mg/kg or 150mg/kg (kindly performed by Catharine Otori, University of Nottingham). Due to the pharmacokinetics of the compound, twice daily oral dosing was administered approximately eight hours apart. Both 50mg/kg and 150mg/kg gave high brain levels of 7507 ± 2528 and 9539 ± 1516 ng/g respectively, and a ratio of 0.56 and 0.6 for brain:plasma levels of compound 14 hours after administration. The 10mg/kg dose resulted in a low brain level and brain:plasma ratio of 1227 ± 696 and 0.22 respectively. The unbound fraction of GSK2606414 in blood and brain ($F_{u,}$blood and F_{u},brain) and the ratios of F_{u},brain /cellular PERK IC_{50}, were also calculated. 50mg/kg and 150mg/kg dosing resulted in unbound brain levels of compound exceeding the cellular PERK IC_{50} value, at 43.2 nM and 54.9 nM respectively, while 10mg/kg dosing resulted in a ratio of 3.2 nM, much lower than the PERK IC_{50} (Table 5.2). Treatment with 50mg/kg of compound twice daily was chosen for subsequent

experiments as it resulted in sufficient quantities penetrating the brain, but with hopefully lower side effects than the higher 150mg/kg dose.

Dose (mg/kg)	**Plasma mean (ng/ml±SD)**	**Brain Mean (ng/g ±SD)**	**Mean ratio Brain:plasma**	**Plasma Mean (µM)**	**Brain Mean (µM)**	**F_u, blood (nM)**	**F_u Brain (nM)**	**F_u Brain/ IC_{50} PERK**
Vehicle	NQ	NQ	-	-	-	-	-	-
10	1227±696	557±292	0.22	2.72	1.23	71	32	3.2
50	13912±5914	7507±2528	0.56	30.81	16.63	801	432	43.2
150	16002±453	9539±1516	0.6	35.44	21.13	921	549	54.9

Table 5.2 Brain penetration of GSK2606414 at a range of doses.

Concentrations of GSK2606414 in the brain and plasma in mice were measured by LC-MS/MS 14 hours after oral administration of 10, 50 and 150 mg/kg of compound. The brain:plasma ratio of the compound, concentration of unbound fraction (F_u)in blood and brain, and ratio $F_{u\ brain}$ to cellular PERK inhibition IC_{50} were calculated. Doses of 50 mg/kg and 150 mg/kg twice daily gave good brain penetration (brain: plasma ratios >0.5) and F_u brain/$IC_{50,\ PERK,\ cell}$ greater than the known effective IC_{50} value (~30nM). n = 5 for all doses. NQ = not quantifiable.

5.3 Testing GSK2606414 in prion disease

5.3.1 Experimental design

Tg37 mice were inoculated with 1% RML prions at approximately 4 weeks of age, as in chapter 4. Again treatment was started at 7 w.p.i (n=20), when prion infection is established and synaptic loss has developed, but before neuronal loss and behavioural deficits. Another cohort of mice were treated from 9 w.p.i (n=9), when spongiosis is present, but the disease can still be reversed (Mallucci et al., 2003) (Figure 5.3.1). Control animals were treated with vehicle from 7 w.p.i (n=9) or 9 w.p.i (n=8), and an uninfected group of mice were inoculated with 1% NBH for comparison (n=10).

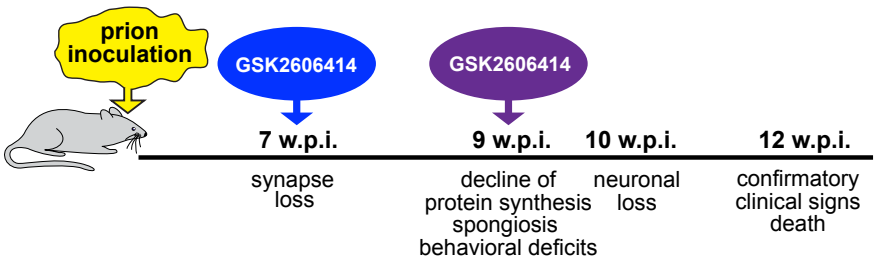

Figure 5.3.1 Experimental design*. Tg37 prion infected mice were treated twice daily with 50mg/kg GSK2606414 from 7 w.p.i (blue), or from 9 w.p.i (purple). At 7 w.p.i synapse loss has occurred, followed by spongiosis and translational failure at 9 w.p.i. Prion disease continues to progress with neuronal loss at 10 w.p.i, and death at 12w.p.i.*

5.3.2 GSK2606414 prevents clinical signs of prion disease at both treatment timepoints.

Each treatment group was monitored as the progression of prion disease occurred. Remarkably, at 12 w.p.i, when normally the animals die from prion disease, all the GSK2606414 treated animals in both groups were free from the clinical signs of prion disease, (see appendix 2 for diagnosis of clinical signs) while all the prion infected controls were clinically sick and were culled. The vehicle treated prion mice had confirmatory clinical signs of prion disease, with a mean incubation period of 82 ± 5 days (Table 5.3.2), but confirmatory prion clinical signs were absent in mice treated with GSK2606414 at both early and later stages of disease (Table 5.3.2 and Figure 5.3.2). Some treated mice showed some early indicator signs in the cohort started at 9 w.p.i, which is not surprising as these can sometimes be observed from 9 w.p.i onwards. Mice in both groups had a healthy outward appearance with improved grooming and general appearance compared to vehicle controls (Figure 5.3.2).

Although the animals were free from the clinical signs of prion disease, unfortunately survival analysis of the GSK2606414 treated animals could not be performed, as they all exhibited 20% body weight loss from the start of the treatment, which according to UK Home Office regulations meant they had to be culled. This will be discussed in greater detail in section 5.4.

	Vehicle treated mice (n = 17)	GSK2606414 treated mice: Treatment started at 7 w.p.i. (n = 20)	GSK2606414 treated mice: Treatment started at 9 w.p.i. (n = 9)
Early indicator signs			
Rigid tail	11/17	2/20*	2/9
Hind limb clasping	11/17	0	1/9
Unsustained hunched posture	9/17	2/20	2/9
Piloerection	11/17	5/20	1/9
Mild loss of co-ordination	9/17	0	1/9
Confirmatory signs			
Ataxia	0/17	0	0
Impairment of righting reflex	11/17	0	0
Dragging of limbs (front/hind)	3/17	0	0
Sustained hunched posture	2/17	0	0
Significant abnormal breathing	1/17	0	0
Scrapie incubation time			
Days ± SD	82 ± 5	N/A	N/A
Number of animals succumbing to prion disease	17/17	0/20	0/9

*not sustained

***Table 5.3.2: Clinical signs of prion disease in GSK2606414 treated or vehicle treated mice**. Prion-infected mice treated with PERK inhibitor or vehicle, were observed over their disease course and scored according to early indicator and confirmatory signs of prion disease. The presence of two early indicator signs plus one confirmatory sign, or two confirmatory signs alone were used to diagnose clinical disease. The time to confirmatory signs is the scrapie incubation time. All vehicle treated animals had confirmatory signs of terminal prion disease by 82 ± 5 days. None of the animals treated with compound at either early or later stage of prion infection developed diagnostic signs of scrapie in this time. N/A = not applicable; * = not sustained.*

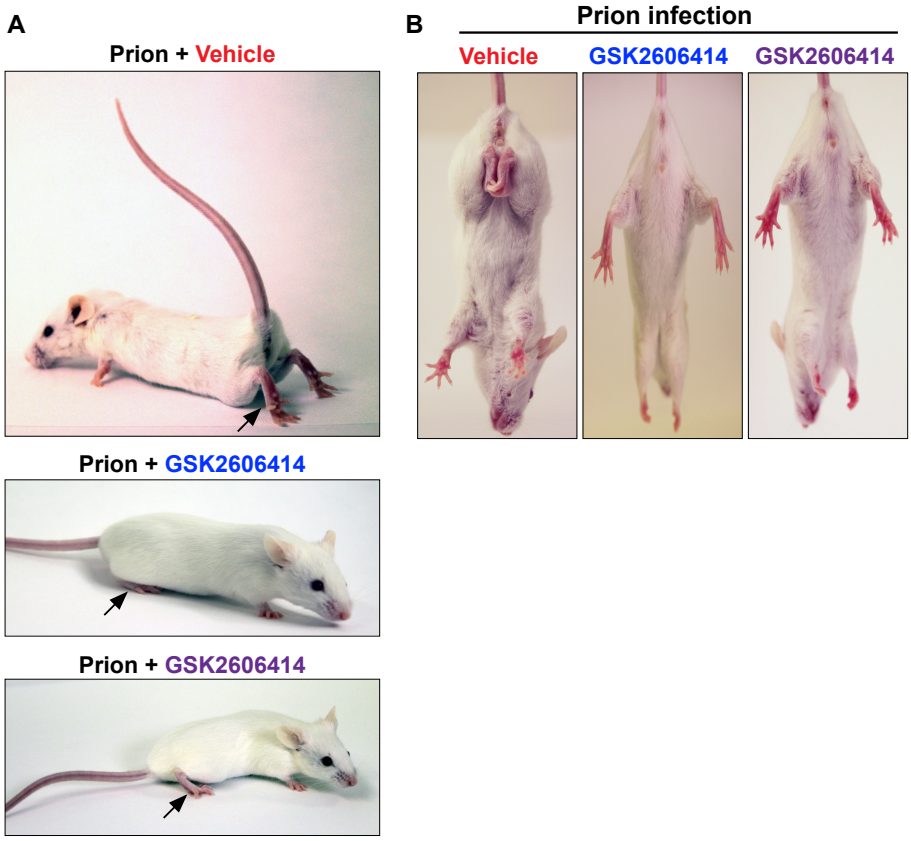

Figure 5.3.2 Clinical signs of prion disease are prevented in GSK2606414-treated mice*. Representative images of prion infected mice at 12 w.p.i after treatment with vehicle or with GSK2606414 from 7 and 9 w.p.i, respectively. A) The vehicle treated mice show the early indicator signs of hind limb paralysis (arrow) and rigid tail, while the treated animals do not. B) Vehicle treated mice exhibit marked hind limb clasping, but treated animals do not. GSK2606414-treated mice also exhibit normal grooming and posture.*

5.3.3 *GSK2606414* is neuroprotective in prion-diseased mice

The degree of spongiosis and neuronal loss was measured. Histological examination focused on the hippocampus, as this is where RML prions are first found to convert from PrP^{C} to PrP^{Sc} and cause the most pathology. The cortex, thalamus, brainstem and cerebellum were also examined. At 12 w.p.i there was substantial neuroprotection in the hippocampus of both GSK2606414 treated mice cohorts, consistent with the absence of clinical signs (Figure 5.3.3A panels c,g and d,h; B right hand panels, n = 5) compared to vehicle-treated mice, which displayed neuronal loss and spongiform degeneration (Figure 5.3.3A, panels b and f; and Figure 5.3.3 B, panels b,g,j,n). However in the later treated cohort, there was some spongiosis present in the hippocampus (figure 5.3.3A panel h). In both groups of treated animals, the neuronal ribbon of hippocampal regions CA1-4 was protected and did not degenerate as it did in vehicle-treated animals by 12 wpi (Figure 5.3.3 A compare panels c,g and d,h with b and f). This was confirmed by counting CA1 pyramidal neurons. The prion infected GSK2606414 treated mice at both time points had an equivalent number of neurons to those in non-prion infected mouse brains, while in vehicle-treated animals the neuronal counts had declined to less than 30% of control values (Figure 3.2.3C, n = 4).

Treatment with GSK2606414 was also neuroprotective throughout the brain. There was minimal spongiform degeneration throughout the brain in both treatment groups, although there was some present in the cortex and brainstem in the cohort that started treatment at 9 wpi. This is possibly because of some

spongiform pathology already being present at the time of treatment in this group (Figure 5.3.3A panels c,g and d,h; Figure 3.2.3B right hand panels; see Table in Figure 5.3.3 D). As expected, uninfected mice did not display any spongiosis, astrocytosis or reduction in pyramidal neuron count. Another hallmark of prion disease is astrocytosis, which proliferate in response to dying neurons, but die themselves as the disease progresses. There were fewer astrocytes and reduced activation in both GSK2606414 treatment groups compared to vehicle controls (Figure 5.3.3 A, panels i-l). This implies reduced neuronal damage in these mice.

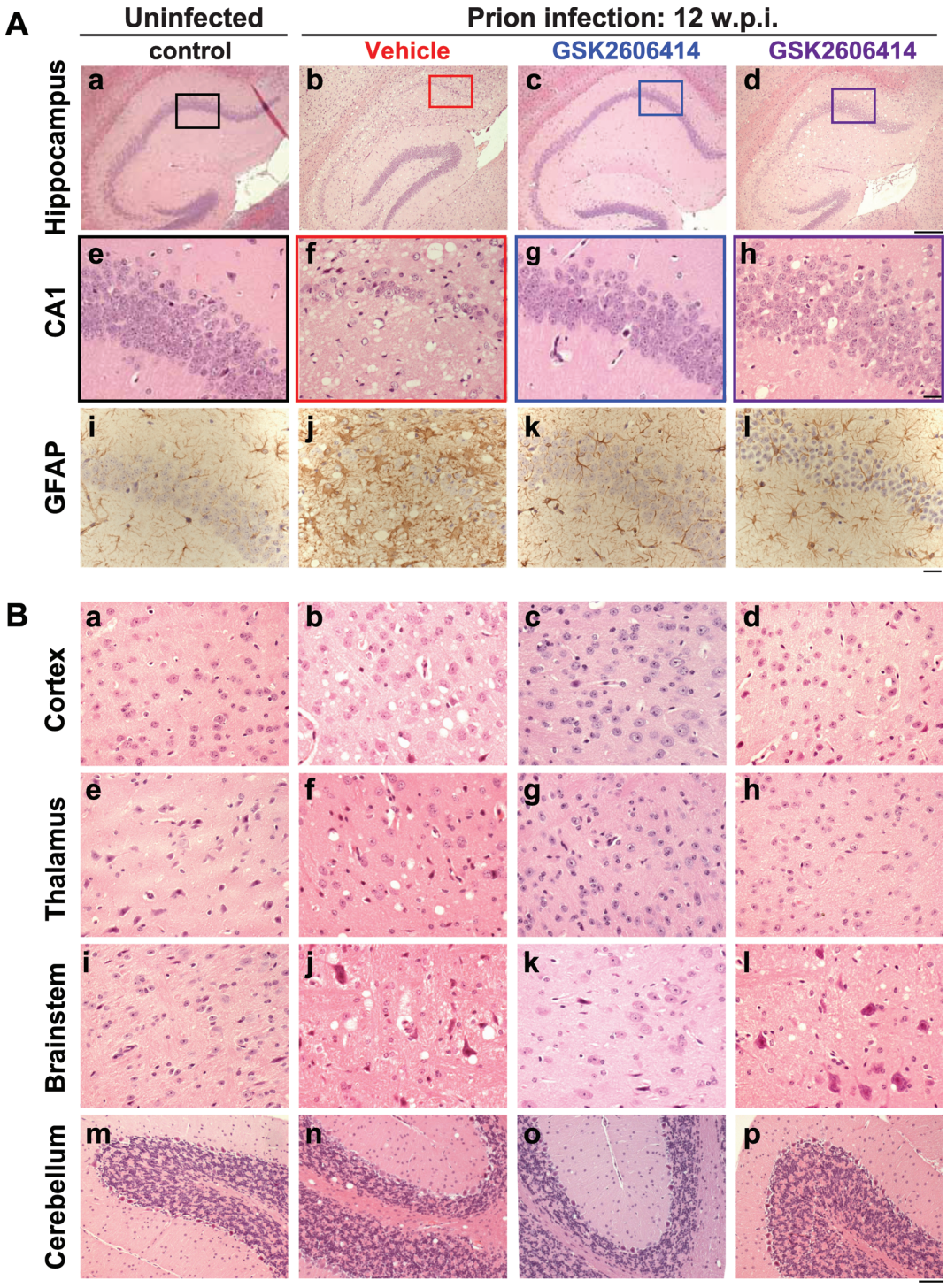
A
Uninfected
control
Prion infection: 12 w.p.i.
Vehicle
GSK2606414
GSK2606414
Hippocampus
CA1
GFAP
a
b
c
d
e
f
g
h
i
j
k
l
B
Cortex
Thalamus
Brainstem
Cerebellum
a
b
c
d
e
f
g
h
i
j
k
l
m
n
o
p
C
CA1 pyramidal neuronal count
600
400
200
0
***
D
Degree of Spongiosis
Uninfected control
Prion + Vehicle
Prion + GSK2606414
Prion + GSK2606414
Hippocampus - +++ - +
Cortex - +++ - +
Thalamus - ++ - -
Brainstem - +++ - +
Cerebellum - + - -

Figure 5.3.3 GSK2606414 is neuroprotective in prion disease. A, *panels a-h. Representative images of haematoxylin and eosin stained hippocampal sections from uninfected control mice (panels a,e) and prion-infected animals treated with vehicle (b,f) or GSK2606414 from 7 w.p.i (c,g) and from 9 w.p.i (d,h) at 12 wpi. Vehicle treated animals have marked neuronal loss in CA1-4 region of hippocampus, with shrinkage of whole hippocampus and extensive spongiosis (b,f). GSK2606414 treatment from both time points prevents neuronal loss (compare thickness of neuronal ribbon in panel f to other panels) and spongiosis, although some spongiosis is present in the later treated animals (panel h). Panels i-j: GFAP immunostaining for astrocytic activation shows that this is greatly reduced in GSK2606414 treated mice, confirming the neuronal protective effects of compound.* ***B****, Neuroprotection by treatment with GSK2606414 is marked throughout other brain regions: vehicle treated mice show spongiform change in cortex, thalamus, brainstem and cerebellum (panels b,f,j,n) which is absent in GSK2606414-treated mice from 7 w.p.i and much reduced in mice treated from 9 w.p.i.* ***C****, quantitation of CA1 pyramidal neuronal numbers shows these remained at normal levels (black bar, uninfected controls) after GSK2606414 treatment from both time points (blue and purple bars), compared to extensive neuronal loss seen in vehicle treated animals (red bar) (n = 4 for each group; p < 0.001).* ***D****, table showing semi-quantitative assessment of spongiosis in sections from all mice. – absent, + mild, ++ moderate, +++ severe. Sections from 5 mice were examined for each condition. Scale bar = 200 μm except for A, panels e-j where is = 50 μm. Control samples are from mice inoculated with normal brain homogenate (NBH).*

5.3.4 GSK2606414 reverses cognitive deficits in prion-infected mice

The GSK2606414 treated mice were assessed for behavioural changes using the burrowing and novel object recognition assays introduced in the previous chapter. Vehicle treated mice lose their preference for the novel object at 9 w.p.i, as seen by a preference ratio of 1 or lower, compared to uninfected animals that have a preference ratio for the novel object of 1.4. Treatment with GSK2606414 from 7 w.p.i prevented loss of object recognition memory in prion-infected mice when tested at 9 w.p.i, as demonstrated by a preference ratio of 1.4 (Figure 5.3.4A). Treatment from 9 w.p.i did not prevent the loss of novel object recognition when tested at 10 w.p.i. The adult onset PrP knockout mice that lose the prion protein at approximately 9 w.p.i do recover novel object preference at 10 w.p.i (Mallucci et al., 2007), so it is possible that the later treated animals may not have been treated for long enough to see the full therapeutic benefits of GSK2606414, or the treatment started too late to be effective.

Additionally, treatment with GSK2606414 prevented the decline in burrowing behavior that is seen in early prion diseased mice in the group treated from 7 w.p.i. The group that started treatment at 9 w.p.i already showed a reduction in burrowing behaviour, but this was reversed at 10 w.p.i with GSK2606414 treatment (Figure 5.3.4 B).

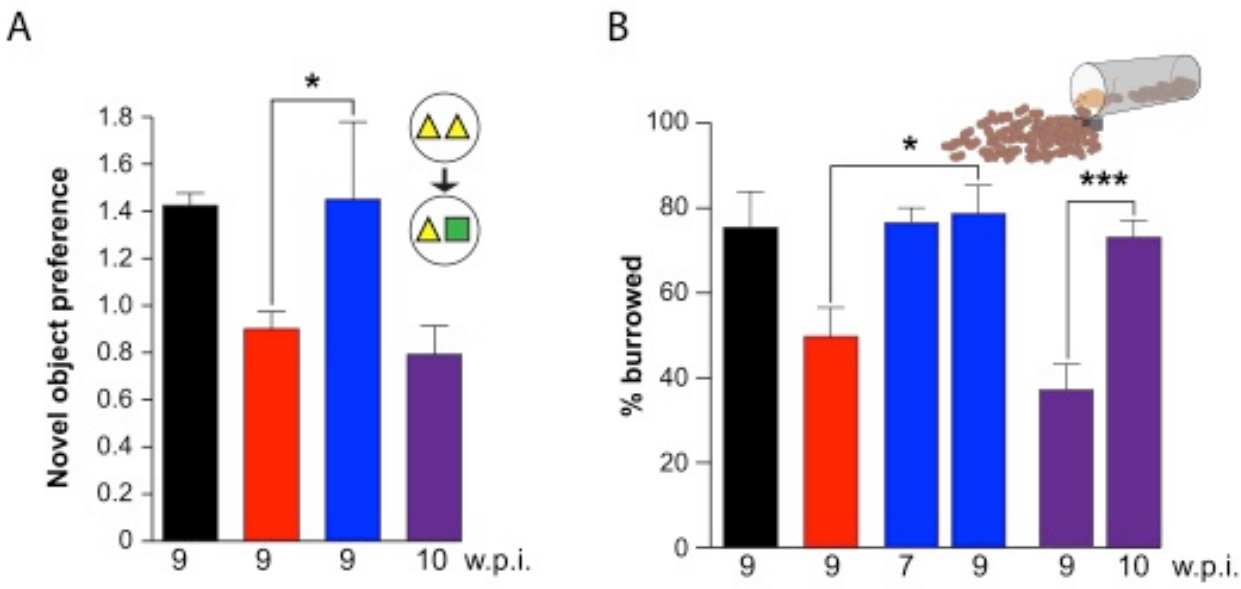

Figure 5.3.4 Recovery of behavioural defects after treatment with GSK2606414 A, *vehicle treated animals tested at 9 w.p.i (red bar) have impaired object recognition memory, but mice treated with GSK2606414 from 7 w.p.i (blue bar) have normal memory when tested at 9 w.p.i. Treatment with compound after 9 w.p.i when memory loss is already established does not reverse the deficit when tested at 10 w.p.i (purple bar, n = 9 for each) (p = 0.01).* ***B,*** *Decline in burrowing activity in prion-infected mice occurs by 9 w.p.i in vehicle-treated mice (red bar), but is prevented in mice treated with GSK2606414 from 7 w.p.i (blue bars), and reversed in mice treated from 9 w.p.i (purple bars, n = 12 for each) (* p < 0.01; *** p < 0.0001). Error bars ± SEM.*

5.3.5 GSK2606414 treatment inhibits PERK phosphorylation and prevents UPR mediated translational shutdown

If GSK2606414 is working as expected, it should be inhibiting PERK and therefore inhibiting eIF2α phosphorylation. As PERK autodimerises and autophosphorylates after activation, measuring the levels of PERK phosphorylation will determine if it is being activated or not. PERK-P levels were determined by western blotting using a phosphorylation specific antibody, using hippocampal brain tissue. The levels of PERK-P were much higher in vehicle treated animals compared to uninfected controls (Figure 5.3.5A). Treatment with GSK2606414 at both timepoints reduced the levels of PERK-P, confirming a potent inhibition of the protein. The levels of total PERK remained constant across treatment groups (Figure 5.3.5A). There were increased eIF2α-P levels in vehicle treated animals compared to uninfected controls (Figure 5.3.5B). eIF2α levels were reduced in both groups of prion infected animals receiving GSK2606414 compared to those receiving vehicle alone, consistent with inhibition of PERK phosphorylation by the compound.

Prion disease causes a sustained reduction in global protein synthesis rates due to continued UPR activation, which contributes to the disease pathogenesis (Moreno et al., 2012). Protein synthesis was determined by measuring the amount of incorporated radioactive methionine [^{35}S] into hippocampal slices. There was a reduction in [^{35}S] incorporation in the vehicle treated group, compared to uninfected controls (Figure 5.3.5C). Treatment with GSK2606414 at both timepoints led to a recovery of global protein synthesis rates (Figure

5.3.5C). Thus, as predicted in the rationale for using PERK inhibition in prion disease, inhibition of PERK phosphorylation by GSK2606414 prevented UPR-mediated translational inhibition in prion diseased mice.

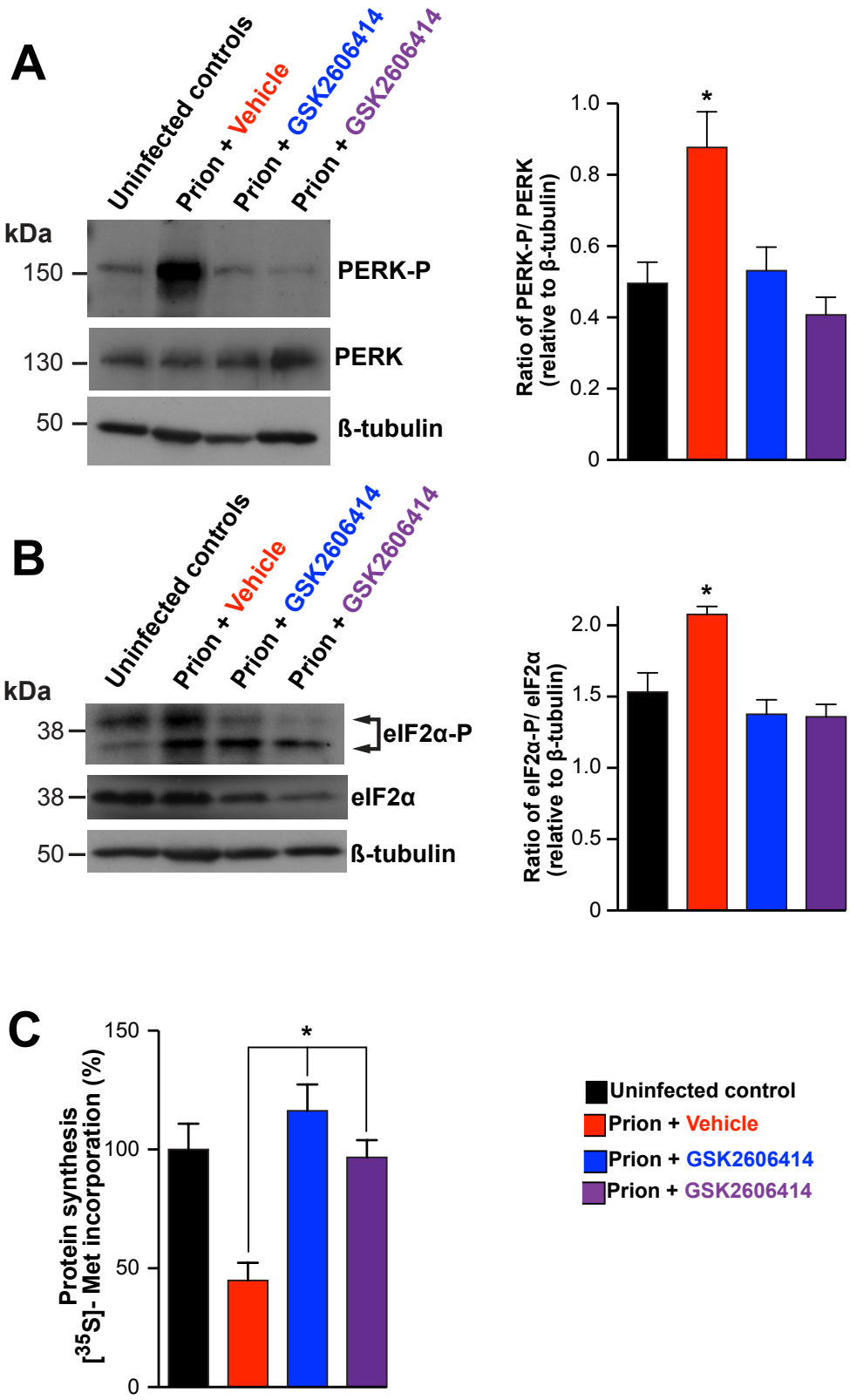
A
Uninfected controls
Prion + Vehicle
Prion + GSK2606414
Prion + GSK2606414
kDa
150
PERK-P
130
PERK
50
ß-tubulin
Ratio of PERK-P/ PERK (relative to ß-tubulin)
1.0
0.8
0.6
0.4
0.2
0
*
B
Uninfected controls
Prion + Vehicle
Prion + GSK2606414
Prion + GSK2606414
kDa
38
eIF2α-P
38
eIF2α
50
ß-tubulin
Ratio of eIF2α-P/ eIF2α (relative to ß-tubulin)
2.0
1.5
1.0
0.5
0
*
C
Protein synthesis [35S]- Met incorporation (%)
150
100
50
0
*
Uninfected control
Prion + Vehicle
Prion + GSK2606414
Prion + GSK2606414

Figure 5.3.5 GSK2606414 inhibits PERK phosphorylation, eIF2α phosphorylation and restores global synthesis rates. *Treatment of prion-infected mice with GSK2606414 from 7 w.p.i and 9 w.p.i reduced* ***A*** *PERK-P levels and* ***B*** *eIF2α-P levels at 12 w.p.i, consistent with inhibition of PERK. Representative immunoblots and bar charts quantitating relative levels of proteins in 4 independent samples are shown.* ***C****, Protein synthesis rates in hippocampal slices, determined by* ^{35}*S-methionine incorporation into protein, showed ~60% reduction in prion-infected vehicle-treated mice. In contrast, GSK2606414 treatment from both 7 and 9 w.p.i, resulted in maintenance of global translation rates at normal levels (n = 3 for each group).*

5.3.6 GSK2606414 treatment restores synthesis of vital synaptic proteins but does not effect PrP levels

As global synthesis rates were restored by GSK2606414, the levels of vital synaptic proteins were also measured to see if they recover. Pre-synaptic SNAP25 and post-synaptic PSD95 levels fall in the brain of vehicle treated animals compared to uninfected controls (Figure 5.3.6A and B, red bars). Treatment with GSK2606414 at both time points restored SNAP25 and PSD95 levels to almost uninfected levels (Figure 5.3.6A and B). As synapses are the first neuronal component to be lost during prion disease, it appears GSK2606414 treatment is beneficial from the earliest to the latest stages of prion disease. GSK2606414 treatment did not affect levels of total PrP and protease resistant PrP^{Sc} levels, which were equivalent in all prion-infected groups (Figure 5.3.6C and D). This is as expected, since PERK activation occurs downstream of prion replication and is unlikely to affect it. This also reiterates the fact that PrP^{Sc} by itself is not toxic to neurons, especially *in vivo*.

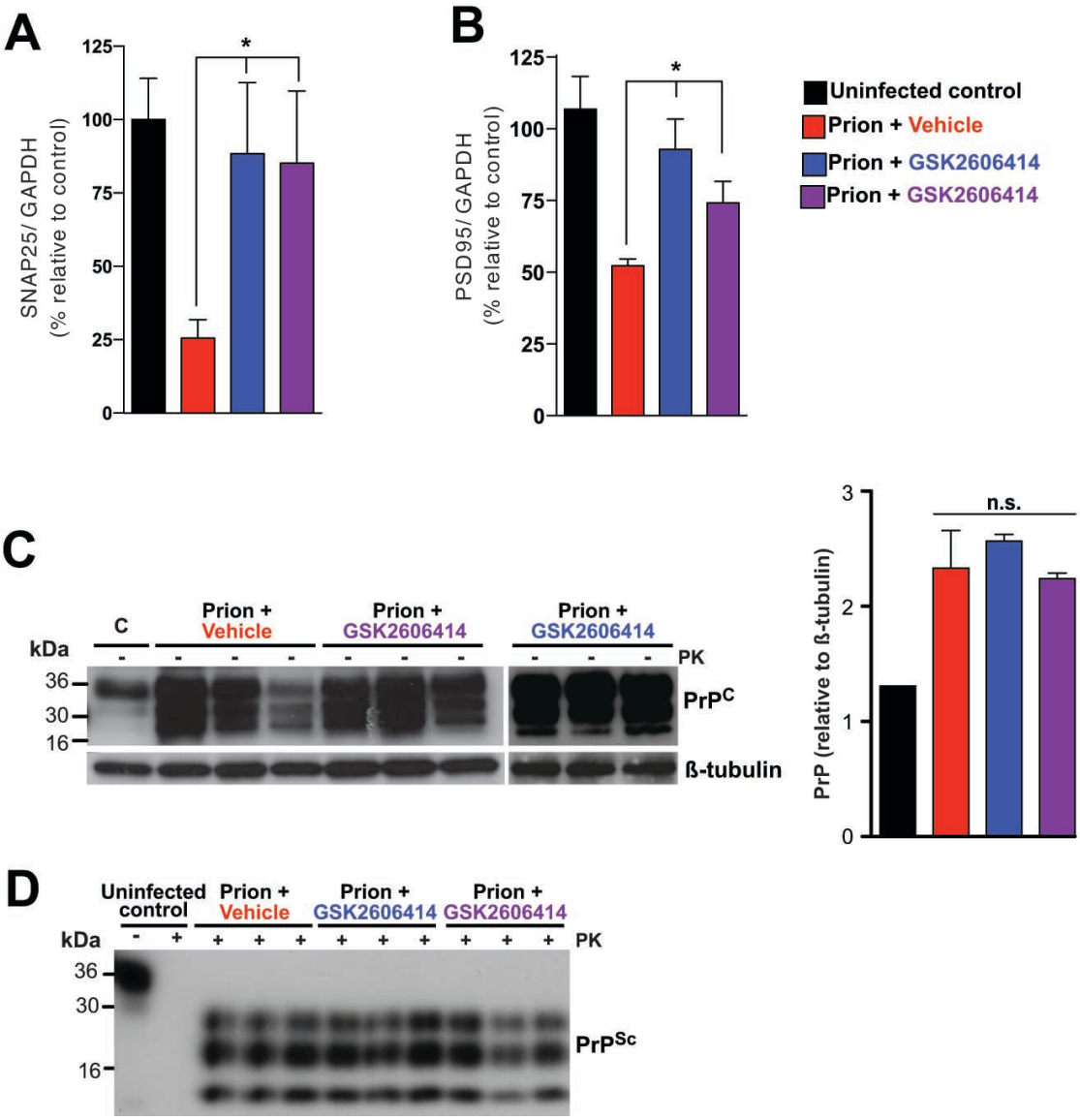

Figure 5.3.6 GSK2606414 inhibition of translational shutdown restores levels of key synaptic proteins and is independent of PrP levels. *GSK2606414 treatment at both stages of disease maintains near normal levels of* ***A,*** *pre-synaptic (SNAP25) and* ***B,*** *post-synaptic (PSD95) proteins, compared to marked reduction in levels of these seen in vehicle-treated animals (n=3)* ***C,*** *Total PrP levels at 12 w.p.i were equivalent in vehicle-treated and both early and late onset GSK2606414–treated animals, as were levels of* PrP^{Sc}*,* ***D****, detected after proteinase K (PK) digestion.*

5.3.7 GSK2606414 specifically inhibits the PERK arm of the UPR

The effects of GSK2606414 on the other arms of the UPR was tested, to give a better idea of how the neuroprotective effects of GSK2606414 are mediated. Although activation of the PERK arm of the UPR leads to a global attenuation of translation, specific RNAs can still be preferentially translated. ATF4 and CHOP are two such transcripts; ATF4 is a transcription factor that stimulates the expression of a variety of UPR effector genes, while CHOP expression ultimately leads to apoptosis (Spriggs et al., 2010). There were increased levels of ATF4 and CHOP found in vehicle treated animals (Figure 5.3.7A and B) compared to uninfected animals. GSK2606414 treatment led to a reduction in both ATF4 and CHOP at both timepoints (Figure 5.3.7A and B), consistent with inhibition of the PERK arm of the UPR. This may explain why there is less neuronal death with GSK2606414 treatment, as CHOP mediated inhibition of apoptosis is inhibited (Figure 5.3.3C).

The other branches of the UPR, the ATF6 arm and the IRE1 arm that mediates XBP1 splicing, were also examined to determine if GSK2606414 acts specifically through PERK (Figure 1.2.1). In fact, XBP-1 spicing was not observed in vehicle treated animals as with uninfected controls, which was unaffected by GSK2606414 administration (Figure 5.3.7 D). Conversion of ATF6 to its neuronal fragment was present in both uninfected and vehicle treated animals (figure 5.3.7 C). It is not clear if the ATF6 arm is being activated in both groups, or if conversion to the neuronal fragment is a normal phenomenon in the mouse

brain. Although ATF6 splicing is thought to only occur with UPR activation, this is not the first report of ATF6 splicing in control samples (Fernandez et al., 2011). Administration of GSK2606414 had no effect on conversion of ATF6 to its neuronal fragment, consistent with its described specificity for PERK.

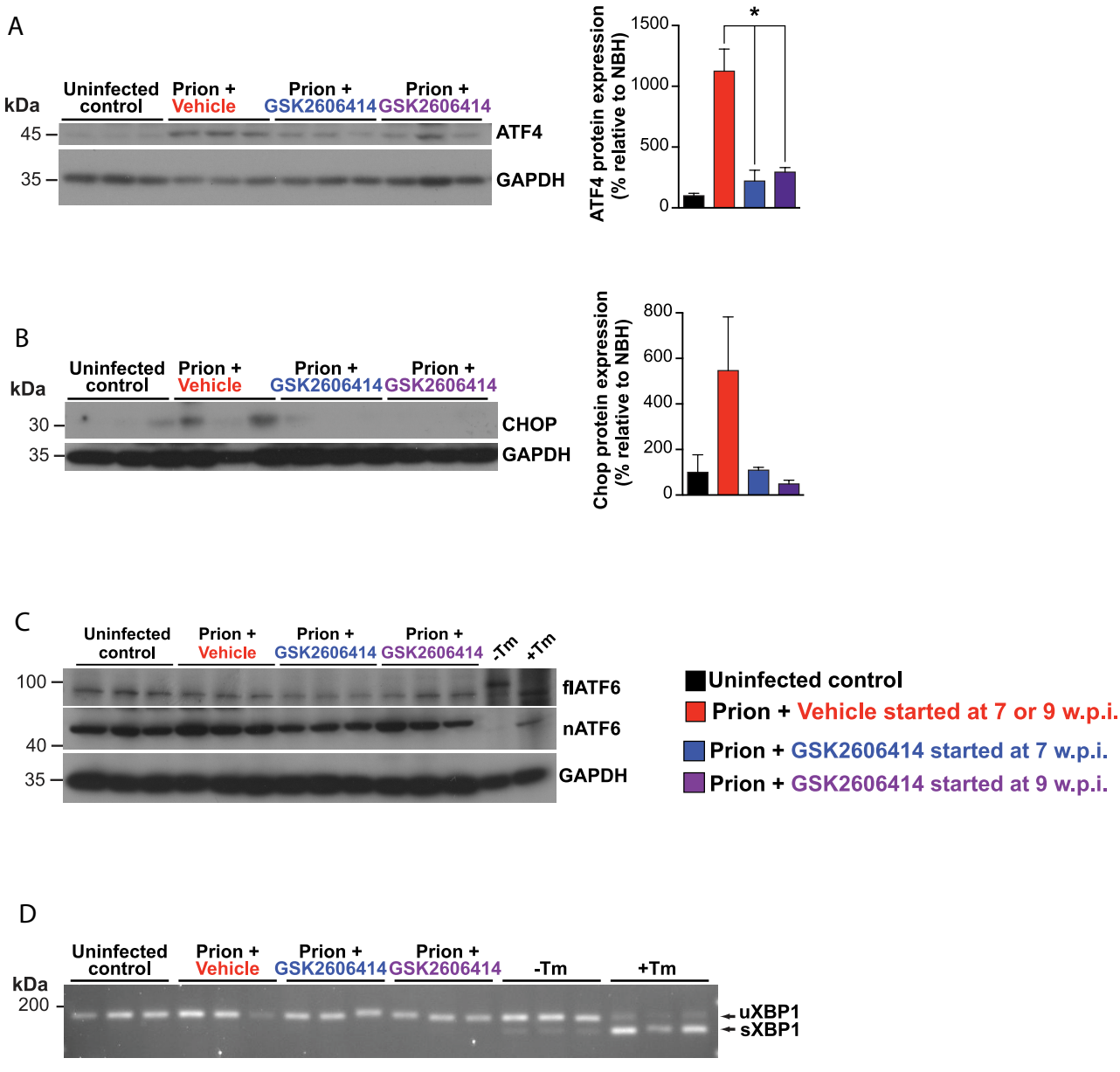
A
kDa
Uninfected control
Prion + Vehicle
Prion + GSK2606414
Prion + GSK2606414
45
35
ATF4
GAPDH
ATF4 protein expression (% relative to NBH)
1500
1000
500
0
*
B
kDa
Uninfected control
Prion + Vehicle
Prion + GSK2606414
Prion + GSK2606414
30
35
CHOP
GAPDH
Chop protein expression (% relative to NBH)
800
600
400
200
0
C
Uninfected control
Prion + Vehicle
Prion + GSK2606414
Prion + GSK2606414
-Tm
+Tm
100
40
35
flATF6
nATF6
GAPDH
Uninfected control
Prion + Vehicle started at 7 or 9 w.p.i.
Prion + GSK2606414 started at 7 w.p.i.
Prion + GSK2606414 started at 9 w.p.i.
D
kDa
Uninfected control
Prion + Vehicle
Prion + GSK2606414
Prion + GSK2606414
-Tm
+Tm
200
uXBP1
sXBP1

Figure 5.3.7 GSK2606414 does not affect the other branches of the UPR. A*. Reduced levels of ATF4 and* ***B,*** *CHOP, were found in prion-infected mice treated with GSK2606414.* ***C*** *representative western blot showing that administration of GSK2606414 does not alter cleavage of ATF6 to its nuclear fragment (nATF6), which occurs equally in all samples except HEK293 negative controls.* ***D,*** *RT-PCR of XBP1 transcripts show that there is no splicing of these in prion infection and with GSK2606414 treatment. Control lanes contain RNA from untreated N2a cells, Tm lanes contains RNA from N2a cells treated with tunicamycin (Tm) as a positive control for activation of IRE1. All data in bar charts show mean ± s.e.m.; * p <0.05 and ** denotes p <0.01. All immunoblots were performed on hippocampal lysates. Control samples are from mice inoculated with normal brain homogenate (NBH).*

5.4 Toxicity of GSK2606414

5.4.1 Effect of GSK2606414 on body weight and blood glucose levels.

As mentioned in section 5.3.2, survival studies on the mice treated with GSK2606414 were unable to be performed, as these animals had a cumulative weight loss equivalent to 20% of body mass soon after 12 w.p.i (Figure 5.4.1A). Post mortem organs weights were recorded for the brain, liver, pancreas, spleen and kidneys to determine if any toxicity was occurring in these organs. Pancreas weights were found to be greatly reduced (~50%) in GSK2606414 treated animals compared to vehicle controls, showing an acute pancreatic toxicity of the compound (Figure 5.4.1B). Elevated blood glucose levels were also found in GSK2606414 treated animals, likely due to the pancreatic toxicity. Blood levels of 10-15 mmol/l glucose in GSK2606414-treated animals were observed, compared to 8-10 mmol/l in vehicle-treated controls. Despite being raised, this is well below the diabetic blood glucose range in mice of >22 mmol/l (Sreenan et al., 1999) (Figure 5.4.1C). Both effects are likely due to systemic effects of PERK inhibition, particularly on pancreatic function. Despite the weight loss, all animals were otherwise overtly well and active, with no other systemic signs and no other indication for culling.

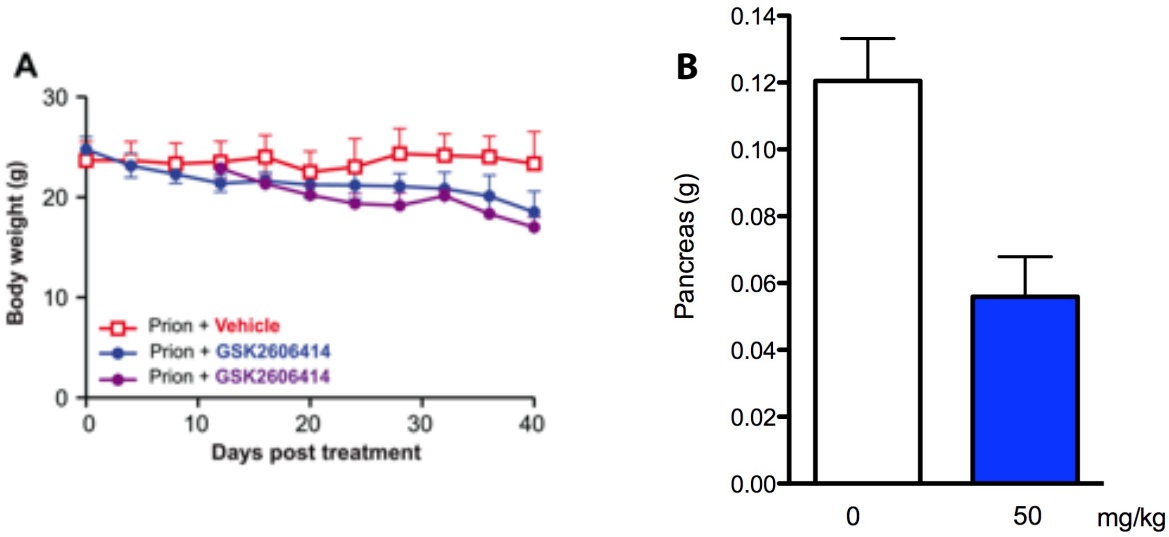
A
Body weight (g)
30
20
10
0
0
10
20
30
40
Days post treatment
Prion + Vehicle
Prion + GSK2606414
Prion + GSK2606414
B
Pancreas (g)
0.14
0.12
0.10
0.08
0.06
0.04
0.02
0.00
0
50
mg/kg

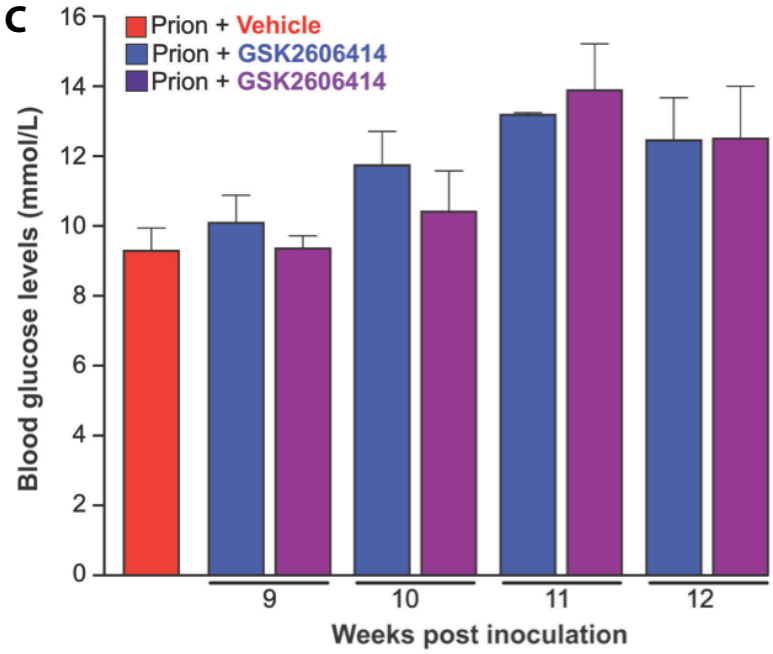
C
Prion + Vehicle
Prion + GSK2606414
Prion + GSK2606414
Blood glucose levels (mmol/L)
16
14
12
10
8
6
4
2
0
9
10
11
12
Weeks post inoculation

Figure 5.4.1 Body weights, pancreas weights and blood glucose levels of prion-infected mice treated with GSK2606414 and vehicle. *Mice were weighed daily throughout treatment with vehicle and both groups of PERK inhibitor.* ***A.*** *Prion-infected mice treated with GSK2606414 from 7 and 9 wpi lost ~20% of body weight by 12 wpi. Vehicle treated animals maintained body weight despite having terminal prion disease at 12 wpi.* ***B.*** *Pancreatic weights were greatly reduced in GSK2606414 treated animals.* ***C.*** *GSK2606414 treatment caused mild hyperglycaemia approximately 3 weeks after starting treatment at 7 w.p.i (blue bars) and 2 weeks after starting treatment at 9 wpi (purple bars). Vehicle treated mice had normal glucose levels. Error bars ± SEM.*

5.4.2 GSK2606414 causes pancreatic toxicity

As GSK2606414 treatment caused a reduction in pancreas weight, histological examination of the pancreas was performed. The pancreas is comprised of two main cell types, the endocrine islets of Langerhans that secrete a number of hormones including insulin and glucagon, and the exocrine acini cells that secret a number of digestive enzymes. Treatment with 5 or 10 mg/kg GSK2606414 caused no obvious pancreatic pathology, while treatment with 50 mg/kg GSK2606414 led to a fragmentation of the pancreas, and a reduction in total volume (Figure 5.4.2). Both acinar cells and the islets of Langerhans appeared to be equally effected, as there was no change in the ratio of these cells (the islets of Langerhans normally make up 1-2% of the total volume of the pancreas).

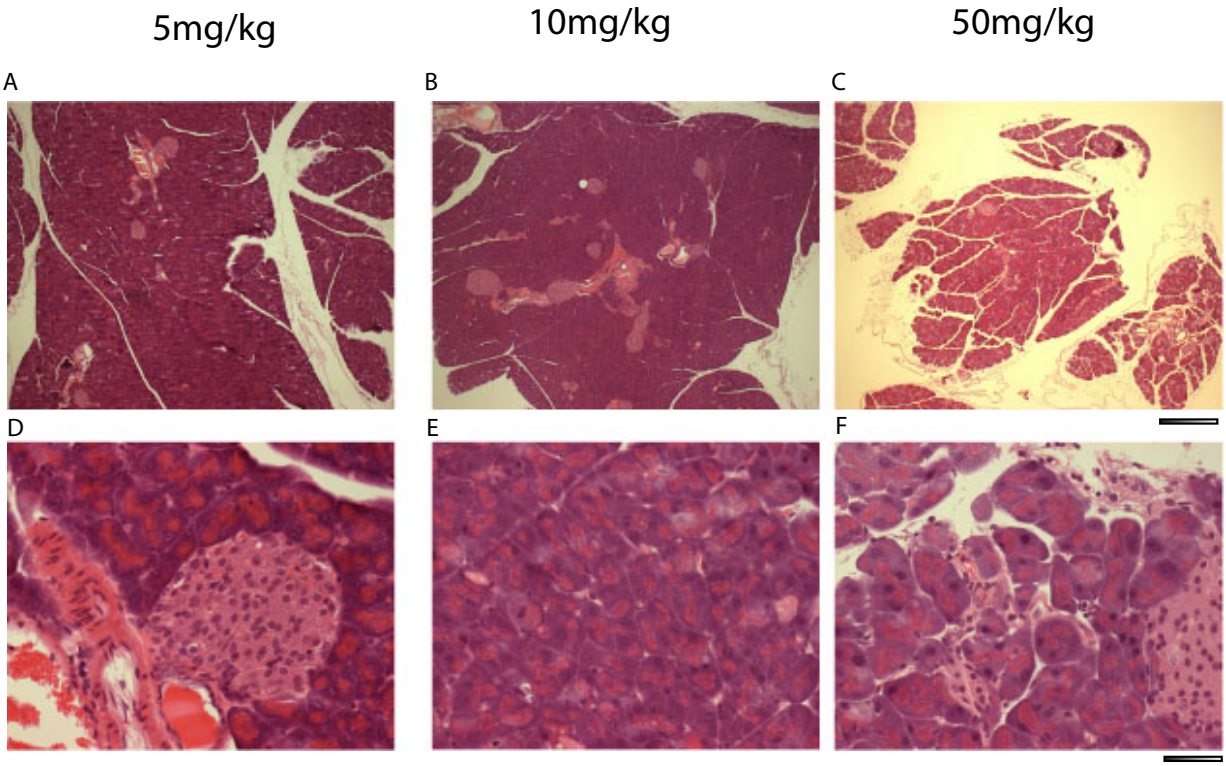

Figure 5.4.2 The effect of GSK2606414 on the pancreas. *Representative images of haematoxylin and eosin stained pancreatic slices. The islets of Langerhans appear as large, lightly stained, spherical clusters, while the acinar cells appear as smaller darker-staining, berry-like clusters. 5mg/kg,* ***A*** *and* ***D****, and 10mg/kg,* ***B*** *and* ***E****, GSK2606414 treated animals showed no obviously pathology, while 50mg/kg treated animals,* ***C*** *and* ***F****, displayed fragmentation of the pancreas, and a reduction in total volume. Scale bar = 200 μm, except for D-E where it is = 50 μm.*

5.4.3 Effective neuroprotective doses also cause pancreatic toxicity

Due to the pancreatic toxicity of treatment with 50mg/kg GSK2606414, several lower doses were tested to search for a dose that maintained neuroprotection without the associated toxicity. Treatment with 10, 22.5 or 37.5 mg/kg GSK2606414 restored protein synthesis, while treatment with 5mg/kg did not (Figure 5.4.3B). Treatment with 37.5 mg/kg was the only dose that caused a significant neuroprotection similar to treatment with 50 mg/kg (Figure 5.4.3A e-f), all the other doses tested displayed significant neuronal loss and spongiosis similar to vehicle treated animals (Figure 5.4.3A a-d). 10, 22.5 and 37.5 mg/kg treated animals all suffered a decrease in pancreatic weight and had to be culled, similar to 50 mg/kg treated animals (Figure 5.4.3C). 5mg/kg treated animals succumbed to prion disease. Pancreatic toxicity appears to start at a concentration of 10 mg/kg, while neuroprotection only occurs at a concentration of 37.5 mg/kg, meaning the toxic effects of GSK2606414 cannot be mitigated. Interestingly, although protein synthesis was restored in 10 and 22.5 mg/kg treated animals, neuroprotection was not observed, showing that restoration of protein synthesis is not the only mediator of the neuroprotection observed from the GSK2606414.

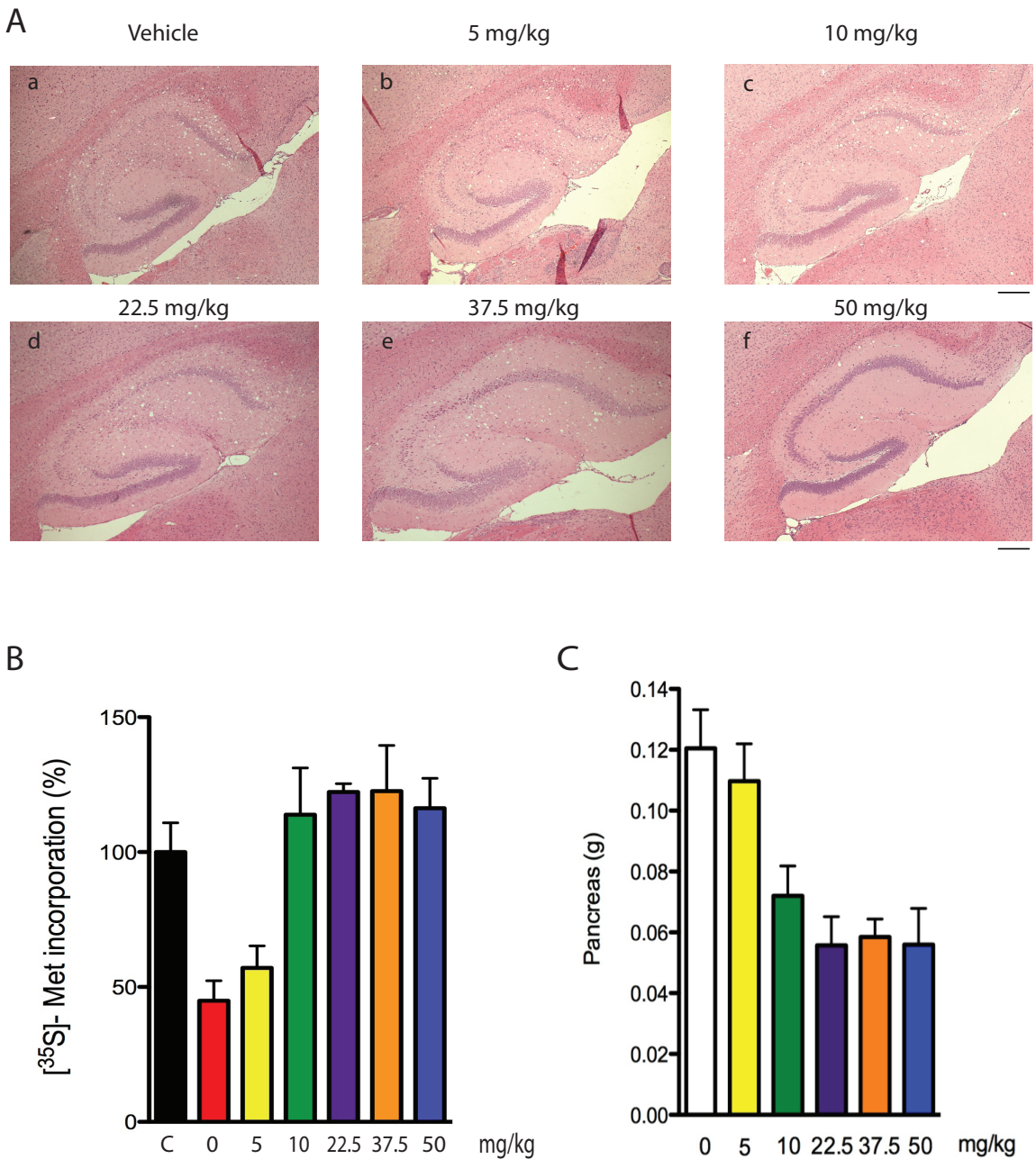

Figure 5.4.3 Lower doses of GSK2606414 do not mitigate the pancreatic toxicity. A *5, 10 and 22.5 mg/kg GSK2606414 treated animals do not exhibit neuroprotection (b-d) compared to controls (a). 37.5 (e) and 50 mg/kg (f) treated animals do exhibit neuroprotection.* ***B*** *[35S] met incorporation is restored with treatment with 10mg/kg GSK2606414 or higher.* ***C*** *Pancreatic toxicity occurs with 10mg/kg GSK2606414 treatment or higher. Scale bars = 200μM, error bars ± SEM.*

5.4.4 GSK2606414 in uninfected mice

GSK2606414 was characterised further in healthy mice, to look for any direct toxic effects. GSK2606414 treatment had no effect on neuronal numbers and hippocampal morphology, on levels of UPR proteins, global translation rates or on burrowing behaviour in uninfected control mice (Figure 5.4.4).

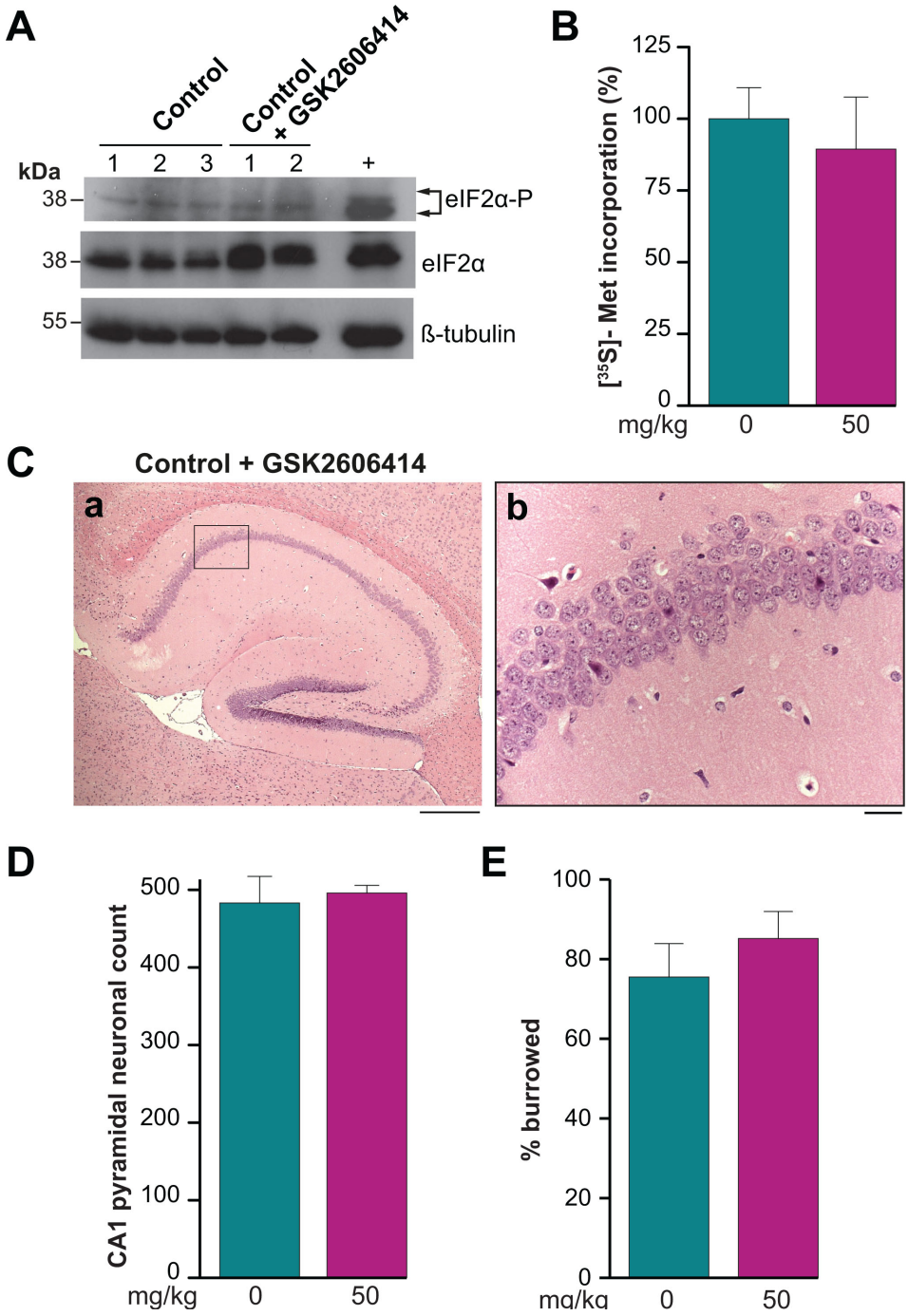

Figure 3.3.2 Biochemical, morphological and behavioral characterization of uninfected mice treated with GSK2606414. *There is no change in* ***A,*** *eIF2a-P levels,* ***B,*** *rates of global protein synthesis measured by* ^{35}*S-methionine incorporation into brain slices,* ***C*** *morphology of hippocampus (a, b),* ***D,*** *hippocampal pyramidal neuronal count and* ***E,*** *burrowing behavior in uninfected mice treated with GSK2620414A, compared to vehicle treatment. Data in bar charts represents mean ± s.e.m, n = 3. Scale bar = 200 mm, panel a; = 50 mm, panel b.*

5.5 Summary

A specific inhibitor of PERK, GSK2606414 was tested for the first time in an *in vivo* model of prion disease as a potential therapeutic. Inhibiting the UPR was previously identified as a novel therapeutic target, and genetic manipulation of this pathway was found to be extremely beneficial (Moreno et al., 2012). This led to the hypothesis that inhibiting the UPR with a specific inhibitor of PERK would also provide a therapeutic affect. GSK2606414 treatment began in prion infected mice at two time points, at a pre-symptomatic stage were synaptic dysfunction has begun, and a systematic stage were behavioural phenotypes and cellular pathology is present. GSK2606414 treatment prevented the emergence of prion disease symptoms, and demonstrated a substantial neuroprotection in the hippocampus and other brain regions. This was associated with improved behavioural phenotypes. GSK2606414 inhibited PERK *in vivo*, and restored global protein synthesis levels, leading to a recovery of essential synaptic proteins. GSK2606414 was found to specifically inhibit the PERK arm of the UPR, having no effect on the ATF6 and IRE1 arms. These promising results validate PERK inhibition as an efficacious and novel therapeutic target in the treatment of prion disease. However, PERK inhibition also caused pancreatic toxicity and an increase in blood glucose levels, leading to a reduction in body weight in treated animals. This prevented important longevity studies to be performed that would have likely had positive results, as an increase in lifespan is the ultimate goal of any successful treatment that targets neurodegenerative disease, especially in such a rapidly fatal disease such as prion disease. Lower doses of GSK2606414 did not mitigate the toxicity of the compound. Although the immediate

translational value of GSK2606414 may be limited by its pancreatic toxicity, it has at shown the value of PERK inhibition *in vivo*. Related compounds without the pancreatic toxicity are likely to be extremely efficacious in the treatment of prion disease.

Chapter 6: Discussion

6.1. Overview of the thesis

All of the major neurodegenerative diseases are characterised by the build up of disease specific misfolded proteins in the brain. Aβ aggregates in Alzheimer's disease, α-synuclein builds up in Parkinson's disease, expanded huntingtin accumulates in Huntington's disease, and PrP^{Sc} in prion disease. A great deal of research effort has focused on how these misfolded proteins can cause pathology in each of their respective diseases. Despite the differences in these disorders, common mechanisms of toxicity do exist. The UPR has emerged as one such mechanism. The UPR is a protective cellular mechanism that is induced during periods of cellular and endoplasmic reticulum stress. Misfolded proteins are one such cause of ER stress, as improperly folded proteins often lose their biological function, and can clump together to form aggregates. UPR activation aims to restore protein homeostasis, by reducing protein translation, and up-regulating chaperone proteins that assist with proper protein folding. However, sustained activation of this pathway is detrimental to cells.

UPR activation has been observed in post-mortem brain samples in CJD (Hetz et al., 2003; Yoo et al., 2002), AD (Hoozemans et al., 2009; Hoozemans et al., 2005; Unterberger et al., 2006) and PD (Hoozemans et al., 2007). The UPR was also recently established to be central to the pathogenesis of prion disease in mice (Moreno et al., 2012). Moreno and colleagues showed sustained overactivation of the UPR by continuing prion replication leads to a catastrophic reduction in

protein translation rates and synaptic protein levels that was central to the pathogenesis of the disease in prion-infected mice. Genetic modulation of this pathway that reduced eIF2α-P levels was highly neuroprotective, while preventing eIF2α dephosphorylation exacerbated the disease.

This thesis aimed to build on these findings, by searching for small molecules that can inhibit the UPR and produce neuroprotection, further validating the UPR as an important therapeutic target in prion disease. Two approaches were used to identify potential small molecule therapeutics. The first approach was to screen for modulators of the UPR in *C. elegans* using the NINDS custom collection 2 drug library. 34 hits were discovered, 5 of which were further investigated. The five drugs, dibenzoylmethane (DBZ), diallyl sulfide (DAS), estradiol valerate (EV), trazodone hydrochloride (Traz) and trifluoperazine hydrochloride (Tri) were then tested in a mouse model of prion disease. Two of the drugs, dibenzoylmethane and trazodone hydrochloride were efficacious in the treatment of prion disease, validating the use of *C. elegans* as a useful screening tool for unfolded protein disorders, and providing two potential new therapeutic compounds. The second targeted approach involved testing a newly identified inhibitor of PERK (the upstream kinase of eIF2α), GSK2606414, which we predicted to be beneficial in prion diseased mice. It was found to be extremely effective, completely preventing the development of symptoms associated with prion disease. However, its immediate therapeutic value is reduced by its pancreatic toxicity. Taken together, these results further emphasize the important role the UPR plays in prion disease, and highlights new compounds that may be of use in its treatment.

6.2 Discussion of the UPR screen in *C. elegans*

6.2.1 Developing the screen

The first aim of chapter 3 was to develop a drug screen that was to be used to search for modulators of the UPR. Initially a model of unfolded protein stress was developed. Many compounds have been used experimentally to induce UPR activation, including thapsigargin, tunicamycin, 2-deoxyglucose, dithiothreitol, brefeldin A and eeyarestatin I (Shinjo et al., 2013). Tunicamycin was chosen as it is the archetypal inducer of unfolded protein induced ER stress; it blocks the formation of N-linked glycoproteins leading to the formation of unfolded proteins (Olden et al., 1979). Other inducers of the UPR such as thapsigargin, which inhibits the sarco-endoplasmic reticulum Ca^{2+} ATPase (Thastrup et al., 1990), or eeyarestatin I, which inhibits ERAD (Fiebiger et al., 2004), induce ER stress and unfolded proteins indirectly.

Worms exposed to tunicamycin stall mainly at the L3 stage of development. A critical time for worm development is between the L3 and L4, as the worms increase greatly in size, requiring a high level of protein synthesis. There is background homeostatic UPR activation in the worm during normal development (Richardson et al., 2011), it is predicted that the UPR activation induced by tunicamycin overloads the UPR mainly at the L3 stage due to the increased demands from protein translation required at this stage. Higher concentrations of tunicamycin led to more worms stalling at the L1 and L2 stages, likely reflecting overloaded UPR activation even at these earlier

developmental stages. Tunicamycin treatment can also cause the worms to die; it is unclear if it is the effects of the unfolded proteins themselves or overactivation of the UPR that causes this. Interestingly, UPR mutant worms with an incomplete UPR were much more likely to die after tunicamycin treatment (Figure 3.2.3). This demonstrates the importance of a functioning UPR when dealing with unfolded proteins. Is inhibiting the UPR therefore an imprudent approach for the potential treatment of prion disease? There is a difference between knocking out an entire arm of the UPR compared to a more targeted approach. Inhibiting eIF2α-P formation while maintaining the downstream chaperone protein translation is likely to be the most beneficial approach. It was hoped that any drugs identified in the screen would more likely reflect a targeted inhibition of protein translational attenuation than the inhibition of entire arms of the UPR.

Screening drugs in *C. elegans* has many experimental advantages, however appropriate models for the biological question being addressed need to be chosen. It was hoped that tunicamycin treatment in the worm would model the effects of an increased unfolded protein load in an analogous fashion to the increased unfolded protein deposition in prion diseased mice. Despite the large evolutionary differences between the two organisms, the UPR is remarkably conserved between them, as it is in all Metazoans. Decreasing levels of eIF2α-P was demonstrated to be protective in prion disease (Moreno et al., 2012), if the worm model was to in any way reflect what happens in mice, it was important to demonstrate that decreasing levels of eIF2α-P in the worm improved the UPR-induced phenotype chosen to model it. Importantly, this was indeed the case, *gcn-1* worms that are reported to exhibit reduced eIF2α-P (Nukazuka et al.,

2008) were almost completely resistant to tunicamycin treatment at the doses tested (Figure 3.2.3F). These worms presumably still contained a buildup of unfolded proteins induced by tunicamycin treatment, but due to the reduced UPR translational attenuation caused by lower levels of eIF2α-P, were able to develop normally. This suggests it is overactivation of the UPR, and not the buildup of unfolded proteins, that are more toxic to the worms. This perhaps mirrors the translational attenuation that is more toxic than the high levels of misfolded PrP in prion diseased mice. Because of this, the *C. elegans* model of UPR activation was deemed to be a suitable readout for testing the drug library.

The effects of DMSO was also tested in this model, as the NINDS drug library was supplied in 100% DMSO, and would reach a final concentration of 1% in the test plates during the drug screen. DMSO has been reported to decrease the paralysis associated with Aβ aggregation in the worm (Frankowski et al., 2013) suggesting it has effects on protein homeostasis or reduces the toxic effects of unfolded proteins. This had the potential to affect the results of the drug screen, leading to false positives if DMSO was reducing UPR stress and not the drug dissolved in it. In contrast to this study, the addition of DMSO enhanced the developmental phenotype induced by tunicamycin in the worms. This caused a shift to the left in the dose response curve compared to tunicamycin treated worms in the absence of DMSO (Figure 3.2.4). This means it took less tunicamycin to produce the same effects in the presence of DMSO. It has previously been reported that DMSO can increase absorption of the large molecule icariin (Cai et al., 2011). Due to structural similarities between tunicamycin and icariin (Figure 6.2.1), it is predicted DMSO is increasing tunicamycin absorption into the worm by a similar

mechanism. DMSO treated worms were otherwise phenotypically similar to untreated worms in the presence of tunicamycin, so it is not thought DMSO had any significant effect on the results of the drug screen.

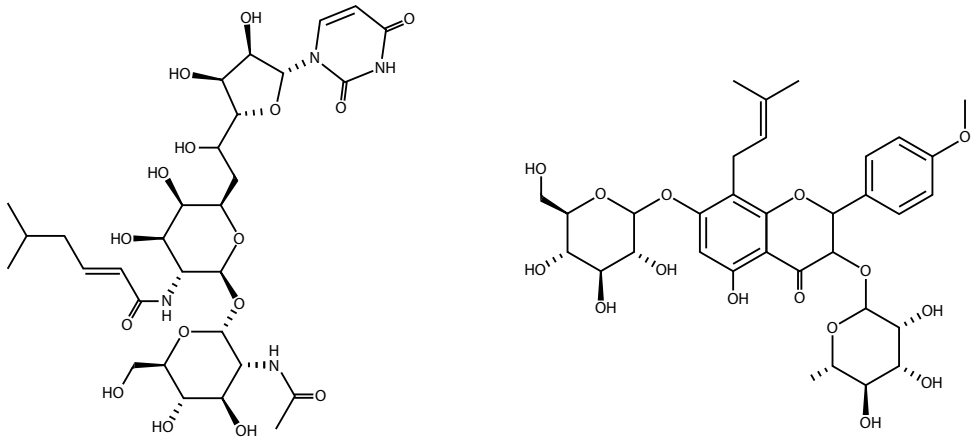

Tunicamycin Icariin

Figure 6.2.1 Comparison of the structures of tunicamycin and icariin.

6.2.2 The drug screen

Drug screens are often a balance between choosing the most biologically relevant readout, and maintaining a high enough throughput to remain useful. Measuring the proportion of worms that reach the L4 stage of development or older was chosen as the readout for the screen, as it was quick to identify test plates that exhibited improvements compared to controls. Plates that showed no improvement or decreased the viability of the worms were not counted to further speed up the screen. As not all of the test plates were counted, it is possible potential hits may have been missed, however due to the obvious differences in test plates containing drugs that caused an improvement and

controls, it is unlikely many were missed. The drugs were added to the NGM media before it set, usually at a temperature of around 60^{0}C. It is possible this caused some of the drugs to degrade. 75% of the NINDS library contains approved drugs, so it is assumed they exhibit a certain amount of stability to be useful in a clinical setting, so the number of false negatives caused by this is likely to be low.

It was decided to display the results as the fold increase in the proportion of worms reaching L4 or older. This is because control plates tested on different days often varied in the percentage of worms reaching L4 by 10-15%, so expressing the data this way allowed easy comparison of results from different test days. *C. elegans* are sensitive to the levels of moisture on the NGM plates they grow on. If plates dry out the worms can sometimes desiccate and die. Every effort was made to ensure the plates remained moist, but due to the experiment running for three days, the plates lost variable amounts of moisture due to the atmospheric conditions at the time. This explains some of the variability on test days. However, test plates that showed no improvements and control plates tested on the same day displayed the same proportions of developmental stages independent of the levels of moisture of the plates. This allowed direct comparison between test days when expressed as a fold increase.

Overall the drug screen was successful, with 34 compounds identified as possible UPR modulators. None of the compounds had previously been reported to have an effect on the UPR. One drawback of the screen is that it provides no indication of how the drugs produced their beneficial effects. It was possible the

compounds reduce eIF2α-P levels, stimulate translation by other mechanisms, reduce UPR activation more generally, reduce ER stress by reducing reactive oxygen species or via other methods, promote proper protein folding or work by way of completely different, unidentified mechanisms. Using *hsp-4::GFP* worms introduced in section 3.4.1 for the screen, and screening for levels of GFP expression instead of the proportion of worms that reach the L4 stage of development, would have narrowed down the results to drugs that reduce ER stress. However, this would also have greatly increased the time taken to perform the screen, due to the time consuming preparation and viewing of slides under a confocal microscope.

When performing a drug screen, or indeed any experiment, there is a potential for false positive results. In this screen, this would occur when a drug appears to be rescuing the developmental phenotype, when in fact the drug may be influencing the experiment by another mechanism, or the recovery is solely due to chance. Some of the drugs identified in the screen may be influencing the uptake of tunicamycin, which would likely lessen the developmental phenotype. Tunicamycin enters cells via the transporter MFSD2A (Reiling et al., 2011), it is possible that the hits are inhibiting the action of this transporter and not reducing levels of ER stress. The drugs could also be influencing the rate of tunicamycin metabolism, accelerating its breakdown. One of the hits, DBZ, has been shown to induce the expression of hepatic detoxification enzymes (Dinkova-Kostova and Talalay, 1999), perhaps explaining the rescue of the developmental phenotype. However, DBZ was demonstrated to provide neuroprotection and increased lifespan when tested in the mouse model of prion

disease (chapter 4), so is unlikely to be acting solely through this mechanism. Although OP50 is used as the bacterial food source for *C. elegans*, it is believed to be slightly pathogenic to the worms, as feeding with other food sources increases lifespan in wild type animals (Garsin et al., 2001). This may explain why a high number of antibiotics where identified in the screen. If the antibiotics tested in the screen were killing the OP50, this may remove a source of stress from the worms, helping to improve their developmental phenotype. Some of the hits did appear to reduce the size and thickness of the OP50 lawn, and were therefore not chosen for further analysis. It is also possible the drugs were causing the OP50 to increase metabolism of the tunicamycin, providing another method of false positive generation. Out of the five drugs tested for further analysis, none were revealed to be false positives (Figure 3.3.3) after the acquisition of further quantities of compound. It is not known if the other 29 hits were false positives due to the complete supply of each drug being used in the initial screen.

6.2.3 Exploring the drugs to be tested

hsp-4::GFP worms were used to test the mechanism of action of the drugs selected for further study. This experiment did not reveal their exact action, as *hsp-4::GFP* worms are markers of general ER stress, not necessarily UPR activation. Nevertheless all five of the drugs tested reduced ER stress in this model, narrowing down their mechanism of action. However, proper quantification of GFP levels was not performed. An attempt was made to quantify GFP expression levels across the treatment groups by calculating the relative area of GFP expression (μm^3) from Z-stack 3-D images. Due to the drugs

recovering the developmental phenotype of tunicamycin treatment, the worms were at a later developmental stages and hence a larger size in the treatment groups, leading to an increased area of GFP expression despite having a more diffuse and weaker signal compared to tunicamycin only treated worms, affecting the analysis. To avoid this, the experiment could be repeated in adult worms that would be comparable sizes to each other. The adult worms would be transferred to plates containing high levels of tunicamycin (10μg/ml) and the drug to be tested, or tunicamycin plates only, and left for 4 hours to induce a rapid UPR activation, before being examined under a confocal microscope. If insufficient amounts of drug are absorbed in this time to reduce ER stress, they could be grown on plates containing drug only before being transferred to the high concentration tunicamycin plates.

The drugs were also tested to see which arm of the UPR the act on, if any (Figure 3.4.2). The recovery observed with drug treatment was independent of the presence of fully functioning PEK-1, IRE-1 and ATF-6 suggesting the drugs do not work via manipulation of the UPR. It was not surprising the drugs do not act through IRE-1 or ATF-6, as they are transcription factors that induce chaperone expression without affecting global translation levels. PEK-1 controls protein translation and is the arm of the UPR shown to mediate prion neurotoxicity (Moreno et al., 2012), if the recovery was dependent on PEK-1, it would nicely explain how the drugs cause recovery in the worms. It is possible the UPR screen performed in the worms was in fact a screen for the reduction in ER stress more than the reduction in UPR activation. Another possibility is that compounds that inhibit ER stress are more common than inhibitors of the UPR, and due to only

1040 drugs being screened, no inhibitors of the UPR were contained in the NINDS library, or that simply out of all the hits there was a range of mechanisms of action, but the five drugs that were selected were all reducers of ER stress but not UPR activation by chance.

6.3 Discussion of testing potential UPR inhibitors in prion infected mice

The five drugs selected, DBZ, DAS, EV, Traz and Tri were tested in prion diseased mice as potential therapeutics. DBZ, DAS and Traz were neuroprotective (Figure 4.2.2), and also improved performance in behavioural tests (Figure 4.2.3). DBZ, DAS, Traz and Tri all increased global protein synthesis rates (Figure 4.2.4), however this increase was not dependent on reduction of eIF2α-P levels (Figure 4.2.5), and the increase in protein synthesis had little effect on the levels of synaptic proteins (Figure 4.2.6). Traz and DBZ treated mice also exhibited increased lifespan compared to controls. It is concluded that DBZ and Traz exhibit efficacy in the treatment of prion disease in mice. DAS treatment showed some benefits, such as partial neuroprotection and benefits to burrowing activity, but overall is not effective enough for use as a potential therapeutic. Treatment with EV or Tri was not effective in prion disease due to no changes in neuroprotection or lifespan.

The main remaining question is how these drugs are causing their beneficial effects. The restoration of protein synthesis is predicated to be beneficial, and indeed contributed to the dramatic improvements observed with GSK2606414 treatment. However, Tri treatment restored protein synthesis levels but had no

effect on the outcomes measured, such as behavioural assays and neuroprotection in the hippocampus. It appears restoration of protein synthesis by itself is not enough to explain the neuroprotection exhibited by these drugs. Interestingly, treatment with GSK2606414 at doses of 10 mg/kg, and 22.5 mg/kg restored protein synthesis but was not neuroprotective, but treatment with 37.5 mg/kg or 50 mg/kg GSK2606414 also restored protein synthesis, but was highly neuroprotective (Figure 5.4.3). [^{35}S] methionine labeling experiments do not identify specific proteins that are being synthesized. It is possible that although translation is restored with Tri and lower concentrations of GSK2606414, the specific subset of proteins induced are not as protective as the subset of neuroprotective proteins induced after DBZ, Traz or higher doses of GSK2606414. So Tri and low dose GSK2606414 treatment might induce more general protein synthesis first, and Traz, DBZ and high dose GSK2606414 treatment may cause a stronger induction of protein translation that includes neuroprotective proteins. A more targeted analysis of specific proteins by western blotting, or measuring mRNA changes by polysomal profiling or mRNA arrays would provide better insight into what proteins are being produced after treatment with the various drugs. It is also possible that [^{35}S] methionine experiments are not sensitive enough to give accurate comparative readings of protein translation rates between treatment groups. Although the data is expressed as the percentage rate of [^{35}S] incorporation into the slices compared to uninfected controls, perhaps the experiment in reality only gives a binary readout of improvement in protein synthesis rates. It would be expected that GSK2606414 treatment would increase protein synthesis in a dose dependent manner, with higher doses causing larger improvements than lower doses.

However all the doses tested above 10 mg/kg caused the same restoration in synthesis rates to approximately 100% of controls (Figure. 5.4.3B). DBZ, DAS, Traz and Tri treatment also caused the same amount of recovery in protein synthesis rates (Figure 4.2.4), to approximately 100% of controls. Experimental limitations may be hiding true differences between the rates of protein synthesis between the treatment groups, explaining why the apparent recovery of protein synthesis is protective in some groups but not others.

DBZ and Traz treated mice showed improvements in novel object recognition tests compared to controls, likely reflecting the neuroprotection exhibited by these two compounds (Figure 4.2.3). DAS treatment did not improve novel object performance, despite improving burrowing rates. This suggests that the novel object recognition assay is more sensitive than the burrowing assay, as overall DAS treatment was not efficacious. Future experiments might find the novel object recognition assay a better predictor of treatment outcome.

6.3.1 Potential mechanisms of neuroprotection

Another question that remains is how the drugs are restoring protein synthesis rates without reducing eIF2α-P. It is possible that they are acting downstream of eIF2α-P, preventing it from attenuating translation. eIF2 (which is comprised of α, β and γ subunits) is an essential component of the ternary complex that mediates the initiation of translation by allowing the ribosome to attach the first methionine to a strand of mRNA. eIF2 binds GTP and the initiator methionine-transfer RNA (tRNA) to form the ternary complex, which associates with the 40S

ribosomal subunit forming the 43S pre-initiation complex. This scans the 5′UTR of mRNAs to find the initiating AUG codon. Upon phosphorylation of its α-subunit, eIF2 can bind to eIF2B (Hinnebusch and Lorsch, 2012). This prevents the ternary complex from being formed, and hence prevents the initiation of translation, causing a reduction in protein synthesis (Krishnamoorthy et al., 2001). The drugs could possibly be acting by inhibiting the binding of eIF2α-P to eIF2B, allowing the ternary complex to still be formed in the presence of eIF2α-P. eIF2B is the guanine nucleotide exchange factor for the ternary complex and converts the inactive eIF2-GDP to the active eIF2-GTP. The drugs could also allow eIF2B to convert GDP to GTP even in the presence of eIF2α-P. This mechanism has been reported to occur after activation of toll-like receptor 4, which activates eIF2B catalytic activity through dephosphorylation of the eIF2B ε-subunit (Woo et al., 2012). Due to the differing molecular structures of the drugs tested (Figure 3.3.2), it is unlikely that all, if any of DBZ, DAS, Traz or Tri work by this mechanism.

The other major controller of protein synthesis is the mammalian target of rapamycin (mTOR) pathway. mTOR regulates protein synthesis through the phosphorylation and inactivation of a repressor of mRNA translation, eukaryotic initiation factor 4E-binding protein (4E-BP1), and through the phosphorylation and activation of S6 kinase (S6K1), reviewed in (Hay and Sonenberg, 2004). mTOR activation stimulates translation, so it is possible the drugs are acting on the mTOR pathway.

Examining the drugs individually may shed light on their neuroprotective effects. DBZ is a minor constituent of liquorice that has been found to have antineoplastic effects, with efficacy against prostate and mammary tumors (Huang et al., 1998; Khor et al., 2009). Carcinogen detoxification has been proposed as a possible mechanism of action since DBZ has been reported to potently induce phase 2 hepatic detoxification enzymes (Dinkova-Kostova and Talalay, 1999). DBZ has also been reported to induce the Nrf2 survival pathway (Thimmulappa et al., 2008), which is activated downstream of UPR activation (He et al., 2001). This potentially explains the neuroprotective effect of DBZ treatment. DBZ derivatives have been shown to induce protection from necrotic cell death (Hegedus et al., 2013) and protect dopaminergic neurons against both oxidative stress and endoplasmic reticulum stress (Takano et al., 2007). It is unclear if DBZ shares these effects with its derivatives.

Traz is an antidepressant in the serotonin antagonist and reuptake inhibitor class, which also has anxiolytic and hypnotic effects. Traz has been shown to reduce the Behavioral and Psychological Symptoms of Dementia (BPSD) in AD (Lopez-Pousa et al., 2008) and frontotemporal dementia (Lebert et al., 2004), but no studies have looked at the progression of neurodegeneration with Traz treatment. Although its pharmacological actions in humans are not fully understood, trazodone is thought to have more than one mechanism of therapeutic action, making it a multifunctional drug (Stahl, 2009). Traz is the first antidepressant with a dual mechanism of action involving inhibition of the serotonin transporter (SERT) and antagonism of the serotonin type 2 (5-HT_2) receptor (Stahl, 2009). It produces its antidepressant effect by blocking SERT,

and increasing serotonin concentrations in the brain. Trazodone exerts antagonistic properties against α1- and α2-adrenergic receptors and histamine H1 receptors, with minimal anticholinergic effects (Stahl, 2009). The sleep inducing effects of Traz are caused by its ability to inhibit H1 receptors, which control wakefulness (Monti et al., 1986). Antidepressants have been linked to neurogenesis in rats (Malberg et al., 2000), and also to BDNF production (Shimizu et al., 2003), which may explain the neuroprotective effects of Traz.

Diallyl sulfide (DAS) is an organosulfur compound derived from garlic that is an inhibitor of chemically induced carcinogenesis (Yang et al., 2001), and also has antibacterial properties (Tsao and Yin, 2001). It has also been reported to reduce apoptosis in a rat stroke model (Lin et al., 2012). An anti-apoptotic effect of DAS treatment would explain the neuroprotection observed in Figure 4.2.2, but how DAS inhibits apoptosis has not been deduced.

Tri is a typical antipsychotic that has antidopaminergic effects, and has been shown to increase the degradation of long lived proteins by increasing autophagy (Zhang et al., 2007), leading to the suggestion that it could be a possible treatment for ER stress disorders (Kim et al., 2008). Tri has also been shown to reduce the buildup of PrP^{Sc} *in vitro* (Kocisko et al., 2003). Tri appeared to be reducing PrP^{Sc} deposition *in vivo* (Figure 4.2.7.2), however this did not provide neuroprotection, which is not surprising due to PrP^{Sc} not being the toxic species in prion disease (Mallucci et al., 2007).

Estradiol valerate (EV) is a synthetic ester of the naturally occurring sex hormone estradiol, which acts as a pro-drug, being cleaved in the body into estradiol and valeric acid. EV is used for hormone replacement therapy, and estradiol has been shown to be neuroprotective following ischemic stroke, reviewed in (Brann et al., 2012). Observational studies of hormone replacement therapy had shown that estradiol appears to be neuroprotective in AD (Kawas et al., 1997). Randomised control trials have also observed beneficial effects with estradiol treatment (Dumas et al., 2008; Joffe et al., 2006). However, there seems to be a critical period for intervention, as only early initiation of hormone therapy appears to provide cognitive benefits, particularly to verbal memory and other functions mediated by the hippocampus (Maki, 2006). It is possible that as EV treatment started at 7 w.p.i, when prion disease has already progressed, the critical period for intervention was missed, explaining the negative results seen after EV treatment.

6.4 Discussion of the effects of GSK2606414 treatment

In chapter 5, a specific inhibitor of PERK was tested in prion disease. GSK2606414 inhibited PERK phosphorylation as predicted, which led to a decrease in eIF2α-P levels (Figure 5.3.5). This in turn restored global protein synthesis rates (Figure 5.3.5), which led to an increase in synaptic protein levels (Figure 5.3.6). This correlated with improved performance in both burrowing and novel object recognition behavioural assays (Figure 5.3.4). The specific restoration of protein synthesis by GSK2606414 is believed to mediate its beneficial effects, which include dramatic neuroprotection (Figure 5.3.3) and the

absence of clinical signs of prion disease (Figure 5.3.2). The pharmacological inhibition of PERK throughout the brain demonstrated here has advantages over focal modulation of the pathway in previous work (Moreno et al., 2012). GSK2606414 was so effective that treatment started at 9 w.p.i, well into the clinical phase of disease, was also protective. These later treated mice had early prion behavioral changes and early spongiform pathology, but still showed recovery from behavioral deficits, no progression in spongiform degeneration, and protection from neuronal loss (Figure 5.3.2 and 5.3.3).

However, despite neuroprotection in the brain and absence of clinical prion disease, GSK2606414 treated mice suffered weight loss and mild hyperglycemia, very likely due to systemic effects of the compound. PERK is ubiquitously expressed, with high expression levels in the pancreas (Shi et al., 1998). Under physiological conditions, PERK is partially constitutively activated in the pancreas, accounting for much of the eIF2α-P observed in the pancreas (Harding et al., 2001). $PERK^{-/-}$ mice have been developed, which develop normally prenatally (Harding et al., 2001). However, $PERK^{-/-}$ mice exhibit early post-natal lethality, hyperglycemia arising from inadequate insulin levels due to pancreatic islet cell death, and exocrine pancreatic insufficiency (Harding et al., 2001). Hemizygous $PERK^{+/-}$ mice have a much milder phenotype. They exhibit impaired glucose tolerance, but weight and longevity are normal (Harding et al., 2001). In a different PERK knockout mouse model, $PERK^{-/-}$ mice were morphologically and functionally normal at birth, but the islets of Langerhans progressively degenerated, resulting in loss of insulin-secreting beta cells and development of diabetes mellitus. The exocrine pancreas exhibited a reduction in the synthesis of

several major digestive enzymes, and succumbed to massive apoptosis after the fourth postnatal week (Zhang et al., 2002). The effects on glucose metabolism observed due to GSK2606414 treatment were relatively mild, similar to those in $PERK^{+/-}$ mice, and did not approach mouse diabetic concentrations of >22 mmol/l of glucose (Sreenan et al., 1999). However, this was enough to cause weight loss and due to UK Home Office regulations on animal welfare regarding body mass, the animals had to be culled. Given the increase in survival seen even with focal inhibition of UPR-mediated translational shutdown (Moreno et al., 2012), it is predicted that GSK2606414 treatment in the brain would have a dramatic beneficial effect on longevity in prion-infected mice if the toxic side effects could be mitigated. Management of diabetes is routine in a clinical setting, and given the scarcity of treatments for prion disease, any disadvantage from pancreatic toxicity would need to be weighed against the potential benefit of neuroprotection in a rapidly fatal neurodegenerative disease.

6.5 Is the UPR a valid target in neurodegenerative disease?

The data presented in this thesis strongly supports the emerging role of the UPR as being central to the pathogenesis of neurodegenerative diseases, at least in prion disease. Overactivation of the UPR is associated with a number of neurodegenerative diseases in post mortem human brains as well as a number of animal and cell based models. Manipulation of the UPR via genetic methods has also demonstrated that UPR activation can directly contribute to neurodegeneration. This raises the tantalizing prospect of a general treatment for neurodegeneration, independent of any disease-specific mechanisms.

Although its systemic effects on the pancreas may limit the immediate translational value of GSK2606414, the results presented provide strong evidence that inhibition of the UPR is neuroprotective.

Targeting the UPR may well prove beneficial in several of these disorders, especially by inhibiting the formation of eIF2α-P. However, there is conflicting evidence as to whether inhibiting or activating eIF2α-P, and consequently protein translation, is the prudent approach to take when modulating the UPR. Salubrinal inhibits the dephosphorylation of eIF2α-P, and has been shown to be protective in cells exposed to ER stress (Boyce et al., 2005). Phosphorylated eIF2α was shown to be protective in cells exposed to tunicamycin by preventing oxidative stress that can lead to apoptosis (Han et al., 2013), and eIF2α-P can also induce ATF4 and consequently the Nrf2 cell survival pathway (Lee et al., 2003).

How can the conundrum of the conflicting reports on the beneficial or detrimental effects of phosphorylated eIF2α be reconciled? UPR activation is undoubtedly an advantageous response to ER stress and unfolded proteins. The answer may lie in the nature of the ER stress, and more importantly, in its duration. Attenuation of protein synthesis is commonly protective in *in vitro* models, where ER stress is acute, and strongly induced. In animal models, especially those that model the unfolded proteins found in neurodegenerative disease, ER stress gradually builds up until it is chronically induced. Here the UPR is constitutively active, and the translational repression that is beneficial during acute insults becomes detrimental, as essential proteins aren't produced.

It is likely that a certain amount of fine-tuning will be needed to observe the largest therapeutic benefit if the UPR is to become a valuable drug target. It is likely that such approaches will ultimately form part of a combined approach to inhibiting translation, including manipulation of the initiation step of translation via eIF4E/4E-BP (cap-dependent translation) (Merrick, 2004), in addition to the UPR mediated effects on the initiation step of protein synthesis. Indeed, inhibition of cap-dependent translation through mTOR inhibition has been shown to be protective in neurodegeneration, see Bove et al., for review (Bove et al., 2011). Ultimately, the ideal method is to achieve a balance between restoring global protein synthesis with manipulation of target specific translation for maximal protection of neuronal function, while protecting from the pathological effects of dysregulation of protein synthesis.

6.6 Current treatments targeting the UPR

Other treatments targeting the UPR in neurodegenerative disease have recently begun to emerge. Sidrauski et al., screened for inhibitors of PERK signaling, and identified ISRIB, a small molecule that potently reverses the effects of eIF2α phosphorylation (Sidrauski et al., 2013). Although ISRIB decreased the viability of cells exposed to ER stress, ISRIB-treated mice display significant enhancement in spatial and fear-associated learning, making it a promising potential therapeutic. Interestingly, ISRIB did not change the levels of eIF2α-P, despite allowing the increased protein synthesis required for memory formation. This mirrors the increase in protein synthesis independent of eIF2α-P observed with DBZ, DAS, Traz and Tri treatment presented in this thesis. In agreement with the

action of ISRIB, mice heterozygous for a mutation that prevents eIF2α phosphorylation display enhanced memory (Jiang et al., 2010). Ma et al., deleted the PERK and GCN2 genes in a mouse model of AD, causing a reduction in the amount of phosphorylated eIF2α (Ma et al., 2013). This reduced deficits in synaptic plasticity and memory exhibited by these mice, providing evidence of a benefit in another neurodegenerative disease model by reducing eIF2α-P. Phenyl acyl acids have been demonstrated to protect against tunicamycin induced cell death in neuronal SH-SY5H cells by acting as chemical chaperones (Zamarbide et al., 2013). This suggests that phenyl acyl acids might be useful adjunct therapies in combination with compounds such as GSK2606414 or ISRIB that restore protein synthesis.

2.7 Future work

The results presented in this thesis strongly support the concept that PERK inhibition is a target for drug discovery in the treatment of prion disorders. The manipulation of a generic cellular pathway involved in protein homeostasis that is neuroprotective, but independent of specific disease causing proteins, has broad relevance. Investigating UPR inhibition in other disorders that exhibit increased eIF2α-P, such as AD (Hoozemans et al., 2009; Hoozemans et al., 2005; Unterberger et al., 2006), PD (Hoozemans et al., 2007), amyotrophic lateral sclerosis (Atkin et al., 2008) and a mouse model of tauopathy (Abisambra et al., 2013) is an important next step. GSK2606414, DBZ and Traz treatment have the potential to be beneficial in all of these diseases, testing these compounds in other mouse models of neurodegeneration is the next planned step. Further the

better characterization of the mechanism of action of DBZ and Traz is also planned, along with testing other hits from the drug screen in prion diseased mice, which may uncover other compounds with potential therapeutic value.

It may also be possible to ameliorate the toxic side effects of GSK2606414. If the action of the compound on the pancreas can be prevented, while maintaining it's effects in the brain, it would possibly prevent the associated weight loss and allow proper lifespan analysis to be performed. This could be achieved by antagonizing the action of the drug peripherally by preventing GSK2606414 binding to PERK, or activating PERK in direct opposition to GSK2606414, with a compound that doesn't cross the blood-brain barrier. Pancreatic supplementation with pancreatic enzymes and/or insulin may help to counteract the effects of decreased pancreas weight in GSK2606414 treated mice.

This thesis has studied mice with rapidly evolving prion neurodegeneration. The ultimate goal of searching for new therapeutics is for translation into human patients. Before this occurs, further development of this approach is essential, particularly as this would involve treatment for years or even decades in many cases. Drugs acting predominantly in neurons and devoid of systemic side-effects are needed, and fine-tuning of both the inhibition of translational repression and it's timing for maximal therapeutic benefit, should be explored.

Appendix 1: Results of the drug screen

ID	Molecular Name	Score	fold increase
02300348	1- (2-METHOXYPHENYL)PIERAZINE HYDROCHLORIDE	0	
01502219	1-BENZYLOXYCARBONYLAMINOPHENETHYL CHLOROMETHYL KETONE	0	
02300329	1-METHYLXANTHINE	0	
01503641	1-PHENYLBIGUANIDE HYDROCHLORIDE	0	
01502116	1,2-DIMETHYLHYDRAZINE HYDROCHLORIDE	0	
02300063	1,3-DIPROPYL-8-CYCLOPENTYLXANTHINE [DPCPX]	0	
01500989	18alpha-GLYCYRRHETINIC ACID	0	
01500156	1R-CAMPHOR	-1	
02300253	1R,2S-PHENYLPROPYLAMINE	0	
01501009	1R,9S-HYDRASTINE	0	
01500484	1S,2R-PHENYLPROPANOLAMINE HYDROCHLORIDE	0	
01503647	2- (2,6-DIMETHOXYPHENOXYETHYL)AMINOMETHYL-1,4-BENZODIOXANE HYDROCHLORIDE (WB 4101)	0	
01504225	2-MERCAPTOBENZOTHIAZOLE	0	
01503973	2-THIOURACIL	3	3.36
01504232	2,3-DIHYDROXY-6,7-DICHLOROQUINOXALINE	0	
01600716	2,6-DI-t-BUTYL-4-METHYLPHENOL	0	
01501125	3-AMINOPROPANESULPHONIC ACID	0	
01505298	3-ISOBUTYL-1-METHYLXANTHINE (IBMX)	0	
01503635	3-METHYL-1-PHENYL-2-PYRAZOLIN-5-ONE (MCI-186)	0	
01504182	3-METHYLXANTHINE	0	
01505331	3,3'-DIINDOLYLMETHANE	0	
01503631	3,5-DINITROCATECHOL (OR-486)	0	
01502074	4-NAPHTHALIMIDOBUTYRIC ACID	0	
01505328	4'-DEMETHYLEPIPODOPHYLLOTOXIN	0	
01501126	5-AMINOPENTANOIC ACID HYDROCHLORIDE	0	
01502057	5-CHLOROINDOLE-2-CARBOXYLIC ACID	0	
01501189	5-FLUORO-5'-DEOXYURIDINE	0	
01502092	5-FLUOROINDOLE-2-CARBOXYLIC ACID	0	
01502153	5-NITRO-2-PHENYLPROPYLAMINOBENZOIC ACID [NPPB]	0	
01500114	6-AMINOCAPROIC ACID	-2	0.72
01505315	6-AMINONICOTINAMIDE	0	
01502070	6,7-DICHLORO-3-HYDROXY-2-QUINOXALINECARBOXYLIC ACID	0	
01503254	6alpha-METHYLPREDNISOLONE ACETATE	0	
01502059	7-CHLOROKYNURENIC ACID	0	

01505342	7-NITROINDAZOLE	0	
02300193	8-CYCLOPENTYLTHEOPHYLLINE	0	
02300104	9-AMINO-1,2,3,4-TETRAHYDROACRIDINE HYDROCHLORIDE	0	
01502236	ABRINE (L)	0	
01500665	ACEBUTOLOL HYDROCHLORIDE	0	
01500101	ACETAMINOPHEN	0	1.29
01501170	ACETAMINOSALOL	0	
01501173	ACETANILIDE	0	
01500102	ACETAZOLAMIDE	2	2.29
01500103	ACETOHYDROXAMIC ACID	0	1.16
00300610	ACETOSYRINGONE	-1	
01500695	ACETYL TYROSINE ETHYL ESTER	0	
01502001	ACETYL-L-LEUCINE	0	
01502089	ACETYLCARNITINE	1	1.93
01500104	ACETYLCHOLINE	0	
01500105	ACETYLCYSTEINE	0	0.87
01500715	ACETYLGLUCOSAMINE	0	
01500703	ACETYLGLUTAMIC ACID	-1	
01500702	ACETYLTRYPTOPHAN	0	
01500699	ACETYLTRYPTOPHANAMIDE	0	
01503045	ACEXAMIC ACID	0	
01502002	ACIVICIN	0	
01500655	ACONITINE	0	
01500618	ACRIFLAVINIUM HYDROCHLORIDE	3	6.17
01504218	ACRISORCIN	-2	
01503603	ACYCLOVIR	0	
01500107	ADENOSINE	1	2.01
01503073	ADIPHENINE HYDROCHLORIDE	-2	
01500274	ADRENALINE BITARTRATE	-1	
01500901	AESCULIN	0	
01503982	AGMATINE SULFATE	0	
01500656	AJMALINE	0	
00200022	AKLAVINE HYDROCHLORIDE	0	
01503014	AKLOMIDE	0	
01504136	ALAPROCLATE	0	
01503074	ALEXIDINE HYDROCHLORIDE	1	1.03
01505263	ALFLUZOCIN	0	
01500801	ALLANTOIN	0	
01500108	ALLOPURINOL	0	
01500802	ALLOXAN	0	
01505204	ALMOTRIPTAN	0	
01502095	alpha-CYANO-3-HYDROXYCINNAMIC ACID	0	
00310040	alpha-TOCHOPHERYL ACETATE	0	
01500804	ALTHIAZIDE	0	
01503065	ALTRETAMINE	0	
01500109	ALVERINE CITRATE	2	2.70
01500110	AMANTADINE HYDROCHLORIDE	0	
01503080	AMBROXOL HYDROCHLORIDE	0	
01503816	AMCINONIDE	0	

01500111	AMIKACIN SULFATE	1	1.68
01500112	AMILORIDE HYDROCHLORIDE	1	1.76
01500810	AMINACRINE	0	
01502130	AMINOCYCLOPROPANECARBOXYLIC ACID	0	
01500115	AMINOGLUTETHIMIDE	2	2.37
01503069	AMINOHIPPURIC ACID	0	
01503041	AMINOHYDROXYBUTYRIC ACID	0	
01504184	AMINOLEVULINIC ACID HYDROCHLORIDE	0	
01500621	AMINOPHENAZONE	0	
01500679	AMINOPTERIN	0	
01501130	AMINOPYRIDINE	0	
01500116	AMINOSALICYLATE SODIUM	0	
01503017	AMINOTHIAZOLE	0	
02300165	AMIODARONE HYDROCHLORIDE	0	
01503083	AMIPRILOSE	-3	
01505299	AMITRAZ	1	1.62
01500117	AMITRIPTYLINE HYDROCHLORIDE	2	2.51
01505202	AMLODIPINE BESYLATE	0	
01500119	AMODIAQUINE DIHYDROCHLORIDE	0	
02300161	AMOXAPINE	0	
01500120	AMOXICILLIN	1	1.52
01500122	AMPHOTERICIN B	0	0.91
01500123	AMPICILLIN SODIUM	0	
01500124	AMPROLIUM	0	0.92
01502244	AMYGDALIN	-1	
01503675	ANDROSTERONE SODIUM SULFATE	0	
01502198	ANISINDIONE	0	
00300047	ANISODAMINE	0	
01503906	ANISOMYCIN	0	
01500126	ANTAZOLINE PHOSPHATE	0	
01500127	ANTHRALIN	2	3.13
01502103	ANTHRAQUINONE	0	
01500128	ANTIPYRINE	0	
00200846	APIGENIN	0	
01500129	APOMORPHINE HYDROCHLORIDE	2	2.22
01505249	APRAMYCIN	0	
01500680	ARECOLINE HYDROBROMIDE	0	
01503042	ARTEMISININ	-1	
01505306	ASPARTAME	0	
01500130	ASPIRIN	0	
02300094	ASTEMIZOLE	0	
01501127	ATENOLOL	0	
01503722	ATORVASTATIN CALCIUM	3	3.85
01504210	ATOVAQUONE	0	
01502117	ATRACTYLOSIDE POTASSIUM	0	
01500131	ATROPINE	0	
01504190	AVOBENZONE	0	
01505234	AVOCADYNE	0	
01505235	AVOCADYNONE ACETATE	0	
01502111	AZACITIDINE	0	

01503802	AZADIRACHTIN	3	7.75
01505332	AZAPERONE	0	
01502113	AZASERINE	0	
01500133	AZATHIOPRINE	2	2.32
01500648	AZELAIC ACID	0	
01505340	AZELASTINE HYDROCHLORIDE	0	
01503679	AZITHROMYCIN	0	
01503101	AZLOCILLIN SODIUM	0	
01501172	AZOBENZENE	0	
01503102	BACAMPICILLIN HYDROCHLORIDE	0	
01500134	BACITRACIN	-1	
01500135	BACLOFEN	-1	
01504002	BAICALEIN	0	
01505200	BENAZEPRIL HYDROCHLORIDE	0	
01503104	BENDROFUMETHIAZIDE	0	
01500669	BENFLUOREX HYDROCHLORIDE	0	
01500137	BENSERAZIDE HYDROCHLORIDE	0	1.23
01503610	BENZALKONIUM CHLORIDE	0	
01505272	BENZANTHRONE	1	
01500138	BENZETHONIUM CHLORIDE	1	1.55
01500139	BENZOCAINE	2	2.23
01500141	BENZTHIAZIDE	2	2.58
01500142	BENZTROPINE	-1	
01503006	BENZYL ISOTHIOCYANATE	1	1.59
01500465	BENZYL PENICILLIN POTASSIUM	1	1.13
01503106	BEPRIDIL HYDROCHLORIDE	0	1.22
01501019	BERBAMINE HYDROCHLORIDE	0	
01500811	BERBERINE CHLORIDE	0	
00300546	BERGAPTEN	0	
01500143	beta-CAROTENE	-2	0.22
01504739	beta-PELTATIN	0	
01503234	BETA-PROPIOLACTONE	-2	
01500144	BETAMETHASONE	-1	
01504244	BETAMIPRON	0	
01500146	BETHANECHOL CHLORIDE	-1	
01504081	BETULINIC ACID	0	
01502046	BEZAFIBRATE	0	
01505309	BIFONAZOLE	2	3.49
01503009	BIOTIN	0	
01500147	BISACODYL	0	0.79
01500148	BITHIONOL	1	1.93
01504206	BOVINOCIDIN (3-nitropropionic acid)	0	
01502018	BRETYLIUM TOSYLATE	0	
01503107	BROMHEXINE HYDROCHLORIDE	0	
01503108	BROMOPRIDE	0	
01503985	BROMPHENIRAMINE MALEATE	0	
01500623	BROXYQUINOLINE	3	5.14
01503043	BUCLADESINE	0	
01500813	BUDESONIDE	0	
01502004	BUMETANIDE	0	

01503818	BUPIVACAINE HYDROCHLORIDE	-2	
01504174	BUPROPION	0	
01500152	BUSULFAN	-1	
01503914	BUTACAINE	0	
01500767	BUTAMBEN	0	
01503947	CACODYLIC ACID	0	
01500155	CAFFEINE	-1	
01500763	CALCEIN	0	
01502232	CAMPTOTHECIN	0	
01504261	CANDESARTAN CILEXTIL	0	
01500828	CANRENOIC ACID, POTASSIUM SALT	0	
01505248	CANRENONE	0	
01500157	CAPREOMYCIN SULFATE	-1	
01505276	CAPSANTHIN	0	
01500682	CAPTOPRIL	0	
01500158	CARBACHOL	-2	0.63
01505294	CARBADOX	0	
01500159	CARBAMAZEPINE	-1	
01500160	CARBENICILLIN DISODIUM	2	2.03
01502005	CARBENOXOLONE SODIUM	0	
01501129	CARBETAPENTANE CITRATE	0	
01505323	CARBIMAZOLE	0	
01500161	CARBINOXAMINE MALEATE	2	2.15
01502106	CARBOPLATIN	0	
01500162	CARISOPRODOL	0	
01505317	CARMOFUR	0	
01503110	CARMUSTINE	-1	
01500624	CARNITINE HYDROCHLORIDE	0	
01502006	CARPROFEN	0	
01504257	CARVEDILOL TARTRATE	0	
01500771	CEFACLOR	0	
01500163	CEFADROXIL	0	
01502041	CEFAMANDOLE NAFATE	0	
01500164	CEFAZOLIN SODIUM	0	
01505208	CEFDINIR	1	1.84
01505360	CEFDITORIN PIVOXIL	0	
01502040	CEFMETAZOLE SODIUM	0	
01502042	CEFOPERAZONE SODIUM	0	
01500165	CEFOTAXIME SODIUM	0	1.39
01502031	CEFOXITIN SODIUM	0	
01505207	CEFTIBUTEN	1	1.01
01503111	CEFTRIAXONE SODIUM	-2	0.00
01502033	CEFUROXIME SODIUM	0	
00201664	CELASTROL	0	
01503678	CELECOXIB	0	
01502028	CEPHALEXIN	0	
01502050	CEPHALORIDINE	0	
01500166	CEPHALOTHIN SODIUM	-1	
01500167	CEPHAPIRIN SODIUM	-3	
01505322	CEPHARANTHINE	0	

01500168	CEPHRADINE	0	
01503200	CETRIMONIUM BROMIDE	0	
01500169	CETYLPYRIDINIUM CHLORIDE	0	1.46
01503815	CEVADINE	0	
01600654	CHAULMOSULFONE	0	
01500174	CHLORAMPHENICOL	2	2.64
01500173	CHLORAMPHENICOL HEMISUCCINATE	2	3.25
01504212	CHLORANIL	1	
01505327	CHLORMADINONE ACETATE	0	
02300062	CHLORMEZANONE	0	
01503341	CHLOROACETOXYQUINOLINE	0	
01500178	CHLOROCRESOL	2	3.00
01504211	CHLOROGUANIDE HYDROCHLORIDE	3	4.96
01505308	CHLOROPHYLLIDE Cu COMPLEX Na SALT	0	
01500179	CHLOROQUINE DIPHOSPHATE	-1	
01500180	CHLOROTHIAZIDE	0	
01500181	CHLOROTRIANISENE	1	1.59
01503202	CHLOROXINE	0	
01500182	CHLOROXYLENOL	0	
01500183	CHLORPHENIRAMINE (S) MALEATE	0	0.64
01500184	CHLORPROMAZINE	-2	
01500185	CHLORPROPAMIDE	0	
01500186	CHLORTETRACYCLINE HYDROCHLORIDE	2	3.55
01500187	CHLORTHALIDONE	0	1.06
01500188	CHLORZOXAZONE	-1	
01504800	CHRYSANTHEMIC ACID	0	
01500709	CHRYSIN	0	
01500189	CICLOPIROX OLAMINE	-1	
01505230	CILOSTAZOL	0	
01500684	CIMETIDINE	0	
01500294	CINEOLE	0	
01503204	CINNARAZINE	0	
01500190	CINOXACIN	-1	0.58
01503614	CIPROFLOXACIN	-3	
01502107	CISPLATIN	0	
01505244	CITICOLINE	0	
01503205	CITIOLONE	0	
00210186	CITRININ	0	
01500707	CITROPTEN	0	
01504231	CLARITHROMYCIN	0	
01503991	CLEBOPRIDE MALEATE	3	2.55
01500191	CLEMASTINE	0	0.77
01500192	CLIDINIUM BROMIDE	2	2.32
01500193	CLINDAMYCIN HYDROCHLORIDE	0	0.96
01503918	CLOBETASOL PROPIONATE	0	
01500195	CLOFIBRIC ACID	1	2.07
01503206	CLOFOCTOL	-2	0.58
01500196	CLOMIPHENE CITRATE	-1	0.58
02300061	CLOMIPRAMINE HYDROCHLORIDE	0	
01500198	CLONIDINE HYDROCHLORIDE	-1	

01503920	CLOPERASTINE HYDROCHLORIDE	0	
01503710	CLOPIDOGREL SULFATE	-2	
01505319	CLOPIDOL	0	
01500200	CLOTRIMAZOLE	0	
01500201	CLOXACILLIN SODIUM	-2	
01500202	CLOXYQUIN	-1	
01500685	CLOZAPINE	0	
01800067	COLCHICEINE	0	
01500205	COLCHICINE	0	1.48
01503804	COLFORSIN	0	
01500206	COLISTIMETHATE SODIUM	1	1.69
01503994	CONVALLATOXIN	0	
01500861	CORALYNE CHLORIDE	0	
01500207	CORTISONE ACETATE	1	1.92
01500208	COTININE	0	0.90
01600300	CREATININE	0	
01500209	CRESOL	0	0.84
01500210	CROMOLYN SODIUM	0	
01505271	CROTAMITON	0	
01504228	CRUSTECDYSONE	0	
01505345	CURCUMIN	0	
01500211	CYCLIZINE	0	
01503207	CYCLOBENZAPRINE HYDROCHLORIDE	0	
01502085	CYCLOCREATINE	0	
01502112	CYCLOHEXIMIDE	0	
01502128	CYCLOLEUCINE	0	
01500212	CYCLOPENTOLATE HYDROCHLORIDE	1	
01500213	CYCLOPHOSPHAMIDE HYDRATE	1	
01500215	CYCLOSERINE	0	
01502202	CYCLOSPORINE	0	
01503921	CYPROTERONE	0	
01503821	CYSTAMINE DIHYDROCHLORIDE	0	
01500217	CYTARABINE	1	
01504027	CYTISINE	0	
01503391	D-PHENYLALANINE	0	
01502182	d[-Arg-2]KYOTORPHAN ACETATE	-3	
01500220	DANAZOL	0	
01500222	DAPSONE	0	
01500224	DEFEROXAMINE MESYLATE	-1	
00201138	DEGUELIN(-)	0	
01504205	DELTALINE	0	
01500226	DEMECLOCYCLINE HYDROCHLORIDE	1	
01503127	DEQUALINIUM CHLORIDE	-1	
01505222	DERACOXIB	0	
01500227	DESIPRAMINE HYDROCHLORIDE	1	
02300192	DESMETHYLDIHYDROCAPSAICIN	0	
00300029	DESOXYCORTICOSTERONE ACETATE	0	
01500230	DEXAMETHASONE	0	
01500231	DEXAMETHASONE ACETATE	-1	
01500232	DEXAMETHASONE SODIUM PHOSPHATE	0	

01500514	DEXPROPRANOLOL HYDROCHLORIDE	0	
01500233	DEXTROMETHORPHAN HYDROBROMIDE	0	
01505293	DIALLYL SULFIDE	3	3.49
02300206	DIAZOXIDE	0	
01500235	DIBENZOTHIOPHENE	0	
01505311	DIBENZOYLMETHANE	3	4.47
01500236	DIBUCAINE HYDROCHLORIDE	-1	
01500237	DICLOFENAC SODIUM	0	
01500238	DICLOXACILLIN SODIUM	3	5.75
01500239	DICUMAROL	1	
01500241	DIENESTROL	0	
01500242	DIETHYLCARBAMAZINE CITRATE	0	
01500244	DIETHYLSTILBESTROL	0	
01601020	DIETHYLTOLUAMIDE	0	
01500245	DIFLUNISAL	0	
01500246	DIGITOXIN	0	
01500247	DIGOXIN	-1	
01504104	DIHYDROJASMONIC ACID	-2	
01504910	DIHYDROJASMONIC ACID, METHYL ESTER	0	
01500249	DIHYDROSTREPTOMYCIN SULFATE	0	
02300214	DILTIAZEM HYDROCHLORIDE	0	
01500251	DIMENHYDRINATE	-1	
01500253	DIMETHADIONE	0	
01503036	DINITOLMIDE	0	1.04
01500255	DIOXYBENZONE	0	
01500256	DIPHENHYDRAMINE HYDROCHLORIDE	1	
01500258	DIPHENYLPYRALINE HYDROCHLORIDE	0	
01504209	DIPLOSALSALATE	0	
01500259	DIPYRIDAMOLE	0	
01503298	DIPYRONE	0	
01504144	DIRITHROMYCIN	0	
01500261	DISOPYRAMIDE PHOSPHATE	0	
01500262	DISULFIRAM	-1	
01500263	DOPAMINE HYDROCHLORIDE	0	
01500264	DOXEPIN HYDROCHLORIDE	0	
01500266	DOXYCYCLINE HYDROCHLORIDE	0	
01500267	DOXYLAMINE SUCCINATE	0	
01501002	DROPERIDOL	0	
01501004	DROPROPIZINE	0	
01500268	DYCLONINE HYDROCHLORIDE	0	
01500269	DYPHYLLINE	1	
01501188	EBSELEN	0	
01501185	ECONAZOLE NITRATE	0	
02300219	EDROPHONIUM CHLORIDE	0	
01505337	ELAIDYLPHOSPHOCHOLINE	0	
01502245	ELLAGIC ACID	0	
01500272	EMETINE	0	
01504060	EMODIC ACID	3	3.94
01501214	ENALAPRIL MALEATE	1	2.08
01503215	ENOXACIN	1	1.51

01500273	EPHEDRINE (1R,2S) HYDROCHLORIDE	0	
01500276	ERGOCALCIFEROL	0	
01500277	ERGONOVINE MALEATE	1	
01501176	ERYTHROMYCIN ESTOLATE	0	
01500753	ESERINE	0	
01500282	ESTRADIOL	1	2.08
01501184	ESTRADIOL ACETATE	0	
01500283	ESTRADIOL CYPIONATE	2	3.00
01501180	ESTRADIOL DIACETATE	0	
01501183	ESTRADIOL METHYL ETHER	0	
01501179	ESTRADIOL PROPIONATE	0	
01500284	ESTRADIOL VALERATE	3	6.10
01501192	ESTRADIOL-3-SULFATE, SODIUM SALT	0	
01500285	ESTRIOL	3	8.50
01501191	ESTRIOL BENZYL ETHER	0	
01501178	ESTRIOL METHYL ETHER	0	
01500286	ESTRONE	0	
01501181	ESTRONE ACETATE	0	
01503676	ESTRONE HEMISUCCINATE	0	
01503412	ETANIDAZOLE	0	
01500288	ETHAMBUTOL HYDROCHLORIDE	0	
01501000	ETHAVERINE HYDROCHLORIDE	0	
01500291	ETHINYL ESTRADIOL	1	
01500292	ETHIONAMIDE	0	
01503221	ETHISTERONE	0	
01500293	ETHOPROPAZINE HYDROCHLORIDE	0	
01502196	ETHOSUXIMIDE	-2	
02300078	ETHYL 1-BENZYL-3-HYDROXY- 2-OXO[5H]PYRROLE-4-CARBOXYLATE	0	
01504088	ETHYLNOREPINEPHRINE HYDROCHLORIDE	0	
01501005	ETODOLAC	0	
01500295	EUCATROPINE HYDROCHLORIDE	0	
01500296	EUGENOL	0	
01503403	EXALAMIDE	-1	
01505203	EZETIMIBE	0	
01505201	FAMCICLOVIR	0	
01501003	FAMOTIDINE	0	
01501016	FENBENDAZOLE	0	
01501008	FENBUFEN	0	
01504223	FENBUTYRAMIDE	0	
01501026	FENDILINE HYDROCHLORIDE	0	
01501010	FENOFIBRATE	0	
01501011	FENOPROFEN	0	
01501007	FENOTEROL HYDROBROMIDE	0	
01501021	FENSPIRIDE HYDROCHLORIDE	0	
01503222	FIPEXIDE HYDROCHLORIDE	0	
01503059	FLOXURIDINE	1	2.66
01500299	FLUDROCORTISONE ACETATE	0	
01501015	FLUFENAMIC ACID	0	
01500992	FLUMEQUINE	0	

01500300	FLUMETHAZONE PIVALATE	0	
01500993	FLUNARIZINE HYDROCHLORIDE	-2	
01501187	FLUNISOLIDE	0	
01500303	FLUOCINONIDE	3	6.86
01500304	FLUOROMETHOLONE	0	
01500305	FLUOROURACIL	0	
01504173	FLUOXETINE	0	
01500994	FLUPHENAZINE HYDROCHLORIDE	0	
01501175	FLURANDRENOLIDE	0	
01500308	FLURBIPROFEN	-1	
01500995	FLUTAMIDE	0	1.14
01502020	FOLIC ACID	0	
01504116	FORMESTANE	0	
01502019	FOSCARNET SODIUM	0	
01502039	FOSFOMYCIN	0	
01502012	FOSFOSAL	0	
01500309	FURAZOLIDONE	-2	
01501195	FUREGRELATE SODIUM	0	
01500310	FUROSEMIDE	0	
01500311	FUSIDIC ACID	0	
01503648	GABOXADOL HYDROCHLORIDE	0	
01501202	GALANTHAMINE HYDROBROMIDE	0	
01500312	GALLAMINE TRIETHIODIDE	1	1.25
00200007	GAMBOGIC ACID	0	
01500678	gamma-AMINOBUTYRIC ACID	0	
01504272	GATIFLOXACIN	1	1.51
00100032	GEDUNIN	0	
01500313	GEMFIBROZIL	0	
01505802	GEMIFLOXACIN MESYLATE	0	
01505302	GENETICIN	0	
01500314	GENTAMICIN SULFATE	3	5.38
01500315	GENTIAN VIOLET	1	
01505247	GINKGOLIC ACID	0	
01500996	GLAFENINE	0	
01504145	GLICLAZIDE	0	
01503092	GLUCONOLACTONE	0	
01500316	GLUCOSAMINE HYDROCHLORIDE	0	
01502248	GLUTATHIONE	0	
02300229	GLYBURIDE	0	
01502212	GLYCYLLEUCYLPHENYLALANINE	0	
01504019	GOSSYPOL	1	
00200046	GRISEOFULVIN	0	
01500321	GUAIFENESIN	0	
01500322	GUANABENZ ACETATE	0	
01500323	GUANETHIDINE SULFATE	-1	
01500761	GUANIDINE CARBONATE	0	
01502126	GUVACINE HYDROCHLORIDE	0	
01500324	HALAZONE	0	
01503237	HALCINONIDE	0	
01500325	HALOPERIDOL	1	

01500864	HARMALINE	0	
01500865	HARMALOL HYDROCHLORIDE	0	
01500867	HARMINE	0	
01502237	HARMOL HYDROCHLORIDE	0	
01500760	HECOGENIN	0	
01500327	HETACILLIN POTASSIUM	3	5.15
01500328	HEXACHLOROPHENE	1	
01503297	HEXAMETHONIUM BROMIDE	0	
01500632	HEXESTROL	0	
01500633	HEXETIDINE	0	
01500330	HEXYLRESORCINOL	0	
01500331	HISTAMINE DIHYDROCHLORIDE	0	
01500332	HOMATROPINE BROMIDE	0	
01500333	HOMATROPINE METHYLBROMIDE	0	
01505255	HUPERZINE A	1	1.53
01503239	HYCANTHONE	0	
01500334	HYDRALAZINE HYDROCHLORIDE	-1	
01500335	HYDROCHLOROTHIAZIDE	1	
00300024	HYDROCORTISONE	0	
01500338	HYDROCORTISONE ACETATE	1	
01503273	HYDROCORTISONE BUTYRATE	0	
01500339	HYDROCORTISONE HEMISUCCINATE	0	
01500341	HYDROFLUMETHIAZIDE	0	
01500657	HYDROQUINIDINE	0	
01504237	HYDROQUINONE	0	
01503978	HYDROXYCHLOROQUINE SULFATE	0	
01500343	HYDROXYPROGESTERONE CAPROATE	1	
02300100	HYDROXYTACRINE MALEATE	0	
01500344	HYDROXYUREA	0	
01500345	HYDROXYZINE PAMOATE	-1	
01500346	HYOSCYAMINE	0	
01500347	IBUPROFEN	0	
01505257	ICARIIN	0	
01505251	IMIDACLOPRID	0	
01500348	IMIPRAMINE HYDROCHLORIDE	0	
01500349	INDAPAMIDE	0	
01502082	INDOLE-2-CARBOXYLIC ACID	0	
01505320	INDOLE-3-CARBINOL	0	
01500350	INDOMETHACIN	0	
01500351	INDOPROFEN	0	
01500772	IODIPAMIDE	0	
01500353	IODOQUINOL	0	
01503923	IOPANIC ACID	0	
01500354	IPRATROPIUM BROMIDE	0	
01500634	IPRONIAZID SULFATE	0	
01504259	IRBESARTAN	0	
02300204	ISOBUTYLMETHYLXANTHINE	0	
01504200	ISOLIQUIRITIGENIN	0	
01500355	ISONIAZID	0	
01500356	ISOPROPAMIDE IODIDE	0	

01500357	ISOPROTERENOL HYDROCHLORIDE	0	
00300534	ISORESERPINE	0	
01500358	ISOSORBIDE DINITRATE	1	1.40
01503242	ISOXICAM	1	1.22
01500359	ISOXSUPRINE HYDROCHLORIDE	0	
00300038	JUGLONE	0	
02300228	KAINIC ACID	0	
01500360	KANAMYCIN SULFATE	0	
01500362	KETOCONAZOLE	0	
01501215	KETOPROFEN	0	
01503925	KETOROLAC TROMETHAMINE	0	
01500668	KETOTIFEN FUMARATE	0	
01500764	KINETIN	0	
01800166	KOJIC ACID	0	
01500688	KYNURENIC ACID	0	
01502207	L-LEUCYL-L-ALANINE	0	
01505339	L-PHENYLALANINOL	0	
01503243	LABETALOL HYDROCHLORIDE	0	
01500363	LACTULOSE	0	
01503926	LANSOPRAZOLE	-1	
01501204	LAPACHOL	0	
01503244	LASALOCID SODIUM	1	1.62
01503927	LEFUNOMIDE	-2	
01502178	LEUCINE ENKEPHALIN	0	
01500364	LEUCOVORIN CALCIUM	0	
01503245	LEVAMISOLE HYDROCHLORIDE	-2	
02300205	LEVODOPA	0	
01504260	LEVOFLOXACIN	1	1.60
01500365	LEVONORDEFRIN	0	
01500689	LIDOCAINE HYDROCHLORIDE	0	
01500368	LINCOMYCIN HYDROCHLORIDE	1	1.27
01502047	LIOTHYRONINE SODIUM	0	
01501217	LISINOPRIL	0	
01500758	LOBELINE HYDROCHLORIDE	0	
01502037	LOMEFLOXACIN HYDROCHLORIDE	0	
02300241	LOPERAMIDE HYDROCHLORIDE	0	
01503712	LORATADINE	0	
01504268	LOSARTAN	1	1.46
01503977	LOVASTATIN	0	
02300242	LOXAPINE SUCCINATE	0	
01504021	LUPININE	0	
01502186	LYSYL-TYROSYL-LYSINE ACETATE	0	
01502214	LYSYLPHENYLALANYLTYROSINE	-2	
01505250	MADECASSIC ACID	0	
01500372	MAFENIDE HYDROCHLORIDE	0	
01500373	MAPROTILINE HYDROCHLORIDE	-2	
01501110	MEBENDAZOLE	0	
01501117	MEBEVERINE HYDROCHLORIDE	0	
01501116	MEBHYDROLIN NAPHTHALENESULFONATE	0	

01500374	MECAMYLAMINE HYDROCHLORIDE	0	
01500375	MECHLORETHAMINE	0	
01500376	MECLIZINE HYDROCHLORIDE	0	
01501118	MECLOCYCLINE SULFOSALICYLATE	0	
01500377	MECLOFENAMATE SODIUM	0	
01500379	MEDROXYPROGESTERONE ACETATE	1	1.18
01500380	MEDRYSONE	-2	
01501103	MEFENAMIC ACID	0	
01501108	MEFEXAMIDE	0	
01503070	MEFLOQUINE	0	
01500381	MEGESTROL ACETATE	0	
01500690	MELATONIN	0	
01504150	MELOXICAM	3	2.10
01501121	MEMANTINE HYDROCHLORIDE	0	
01502254	MENADIONE	0	
01503134	MENTHOL(-)	0	
01500383	MEPENZOLATE BROMIDE	0	
01501140	MEPHENESIN	0	
01503250	MEPHENTERMINE SULFATE	0	
01504148	MEPIVACAINE HYDROCHLORIDE	0	
01500637	MERBROMIN	0	
01504226	MERCAPTAMINE HYDROCHLORIDE	0	
01500387	MERCAPTOPURINE	0	
01502014	MESNA	0	
01502034	METAMPICILLIN SODIUM	0	
01500390	METAPROTERENOL	0	
01503251	METARAMINOL BITARTRATE	0	
01504229	METAXALONE	0	
00300565	METERGOLINE	0	
01500391	METHACHOLINE CHLORIDE	0	
01501104	METHACYCLINE HYDROCHLORIDE	0	
01503229	METHAPYRILENE HYDROCHLORIDE	-2	
01503252	METHAZOLAMIDE	0	
01500394	METHENAMINE	0	
01500395	METHICILLIN SODIUM	0	
01500396	METHIMAZOLE	0	
01502177	METHIONYL-LEUCYLPHENYLALANINE ACETATE	1	2.19
01503637	METHIOTHEPIN MALEATE	-2	
01500397	METHOCARBAMOL	0	
01500398	METHOTREXATE	0	
01500399	METHOXAMINE HYDROCHLORIDE	0	
01500400	METHOXSALEN	0	
01503970	METHOXYAMINE HYDROCHLORIDE	-2	
01500401	METHSCOPOLAMINE BROMIDE	0	
01503253	METHYLBENZETHONIUM CHLORIDE	0	
01500403	METHYLDOPA	0	
01500404	METHYLERGONOVINE MALEATE	0	
01500406	METHYLPREDNISOLONE	0	
01500408	METHYLTHIOURACIL	0	

01500410	METOCLOPRAMIDE HYDROCHLORIDE	0	
02300325	METOLAZONE	0	
01500411	METOPROLOL TARTRATE	0	
01500412	METRONIDAZOLE	0	
02300296	MEXAMINE	0	
01500413	MICONAZOLE NITRATE	0	
01503257	MIDODRINE HYDROCHLORIDE	0	
01504273	MIGLITOL	0	
01505329	MILTEFOSINE	0	
01500869	MIMOSINE	0	
01501120	MINAPRINE HYDROCHLORIDE	0	
01500415	MINOXIDIL	1	
01503278	MITOXANTHRONE HYDROCHLORIDE	0	
01503416	MIZORIBINE	0	
01505361	MODAFINIL	0	
01500673	MOLSIDOMINE	0	
01502258	MONENSIN SODIUM (monensin A is shown)	0	
01502252	MONOCROTALINE	0	
01503931	MORANTEL CITRATE	0	
01502259	MORIN	1	1.33
01500418	MOXALACTAM DISODIUM	1	1.71
01504303	MOXIFLOXACIN HYDROCHLORIDE	1	2.21
01500674	MYCOPHENOLIC ACID	0	
01502155	N (g)-NITRO-L-ARGININE	0	
01503633	N- (3-TRIFLUOROMETHYLPHENYL)PIPERAZINE HYDROCHLORIDE (TFMPP)	-1	
01502083	N- (9-FLUORENYLMETHOXYCARBONYL)-L-LEUCINE	0	
01504213	N-ACETYLASPARTIC ACID	-1	
02300147	N-ACETYLNEURAMIC ACID	0	
01500704	N-ACETYLPROLINE	0	
01503627	N-AMINOHEXYL-5-CHLORO-1-NAPTHALENESULFONAMIDE HYDROCHLORIDE	0	
01505815	N-CHLOROETHYL-N-ETHYL-2'-METHYLBENZYLAMINE HYDROCHLORIDE	0	
01502173	N-FORMYLMETHIONYL-LEUCYLPHENYLALANINE	0	
01502175	N-FORMYLMETHIONYLPHENYLALANINE	0	
01502217	N-HISTIDYL-2-AMINONAPHTHALENE (betaNA)	0	
02300137	N-HYDROXYMETHYLNICOTINAMIDE	0	
01504215	N,N-HEXAMETHYLENEAMILORIDE	0	
01503650	NABUMETONE	0	
01503260	NADOLOL	0	
01500420	NAFCILLIN SODIUM	-2	
01503419	NAFRONYL OXALATE	-3	
01501115	NALBUPHINE HYDROCHLORIDE	0	
01500756	NALIDIXIC ACID	0	
01500422	NALOXONE HYDROCHLORIDE	0	
01503262	NALTREXONE HYDROCHLORIDE	0	

01500424	NAPHAZOLINE HYDROCHLORIDE	0	
01500425	NAPROXEN(+)	0	
01503801	NAPROXOL	0	
01502035	NARASIN	0	
01500746	NARINGENIN	0	
01500765	NARINGIN	0	
01504258	NATEGLINIDE	0	
01501137	NEFOPAM	0	
01500750	NEOHESPERIDIN DIHYDROCHALCONE	0	
01500427	NEOMYCIN SULFATE	0	
01500428	NEOSTIGMINE BROMIDE	1	1.24
01501132	NEROL	0	
01502194	Ng-METHYL-L-ARGININE ACETATE	0	
01500430	NIACIN	-1	
01501135	NICARDIPINE HYDROCHLORIDE	0	
01501133	NICERGOLINE	0	
02300259	NICOTINE DITARTRATE	0	
01503038	NICOTINYL TARTRATE	0	
01500431	NIFEDIPINE	-1	
01503230	NIFENAZONE	0	
01503913	NIGERICIN SODIUM	0	
01504152	NILUTAMIDE	0	
01503231	NIMESULIDE	1	1.35
01503600	NIMODIPINE	0	
01504151	NIMUSTINE	-1	
02300345	NIPECOTIC ACID	0	
01503609	NITRENDIPINE	2	2.07
01500433	NITROFURANTOIN	1	1.91
01500434	NITROFURAZONE	0	
01500435	NITROMIDE	0	
01503267	NOMIFENSINE MALEATE	0	
01504153	NORCANTHARIDIN	-2	
01500436	NOREPINEPHRINE	0	
01500438	NORETHINDRONE ACETATE	0	
01500439	NORETHYNODREL	0	
01500440	NORFLOXACIN	1	
01500441	NORGESTREL	0	
01500871	NORHARMAN	0	
01500442	NORTRIPTYLINE	1	1.59
01500443	NOSCAPINE HYDROCHLORIDE	0	
01500444	NOVOBIOCIN SODIUM	0	
01500445	NYLIDRIN HYDROCHLORIDE	0	
01500446	NYSTATIN	0	
01500639	OCTOPAMINE HYDROCHLORIDE	0	
01502044	OFLOXACIN	0	
01500675	OLEANDOMYCIN PHOSPHATE	0	
01505205	OLMESARTAN MEDOXOMIL	0	
01504300	ORLISTAT	0	
01500447	ORPHENADRINE CITRATE	1	1.37
01500676	OUABAIN	0	

01500448	OXACILLIN SODIUM	0	
01505267	OXAPROZIN	0	
01504243	OXCARBAZEPINE	0	
01505296	OXFENDAZOLE	0	
01505330	OXICONAZOLE NITRATE	0	
01500450	OXIDOPAMINE HYDROCHLORIDE	0	
01503626	OXOTREMORINE SESQUIFUMARATE	1	
01500451	OXYBENZONE	1	1.33
01500453	OXYMETAZOLINE HYDROCHLORIDE	0	
01500455	OXYPHENBUTAZONE	0	
01503932	OXYPHENCYCLIMINE HYDROCHLORIDE	0	
01500456	OXYQUINOLINE HEMISULFATE	0	
01500457	OXYTETRACYCLINE	0	
01502162	p-CHLOROPHENYLALANINE	0	
01503908	PACLITAXEL	-2	
01601021	PAEONOL	0	
01505252	PALMATINE	0	
01500872	PALMATINE CHLORIDE	0	
01500459	PAPAVERINE HYDROCHLORIDE	0	
01500460	PARACHLOROPHENOL	0	
01503223	PARAROSANILINE PAMOATE	0	
02300170	PARAXANTHINE	0	
01503228	PAROMOMYCIN SULFATE	1	2.25
01503904	PATULIN	0	
01505305	PEFLOXACINE MESYLATE	1	1.50
01500464	PENICILLAMINE	1	1.23
01500467	PENICILLIN V POTASSIUM	0	
01500641	PENTAMIDINE ISETHIONATE	0	
02300347	PENTETRAZOL	0	
01503933	PENTOLINIUM TARTRATE	0	
01503611	PENTOXIFYLLINE	-3	
01505810	PEONIFLORIN	0	
01503227	PERHEXILINE MALEATE	0	
01503936	PERICIAZINE	0	
01502101	PERILLIC ACID (-)	0	
01505297	PERILLYL ALCOHOL	0	
01505212	PERINDOPRIL ERBUMINE	0	
01503934	PERPHENAZINE	0	
01501113	PERUVOSIDE	0	
01500642	PHENACETIN	0	
01500473	PHENAZOPYRIDINE HYDROCHLORIDE	1	1.58
01500476	PHENELZINE SULFATE	0	
01502209	PHENETHYL CAFFEATE (CAPE)	0	
01500477	PHENINDIONE	0	
01500478	PHENIRAMINE MALEATE	0	
01504098	PHENOTHRIN	3	7.83
02300176	PHENOXYBENZAMINE HYDROCHLORIDE	0	
01502221	PHENYLALANYLTYROSINE	0	
01504221	PHENYLBUTYRATE SODIUM	0	
01500483	PHENYLEPHRINE HYDROCHLORIDE	0	

01500644	PHENYLMERCURIC ACETATE	0	
01500485	PHENYTOIN SODIUM	0	
00300547	PHLORIDZIN	0	
01504070	PHYSCION	0	
01500486	PHYSOSTIGMINE SALICYLATE	0	
01504410	PICROPODOPHYLLOTOXIN	0	
01501107	PICROTOXININ	0	
01500487	PILOCARPINE NITRATE	0	
01501134	PIMOZIDE	0	
00300013	PIMPINELLIN	0	
02300270	PINACIDIL	0	
01500488	PINDOLOL	0	
01504154	PINOCEMBRIN	-1	
01504401	PIOGLITAZONE HYDROCHLORIDE	0	
01500489	PIPERACILLIN SODIUM	0	
01500490	PIPERAZINE	3	4.13
01502197	PIPERIDOLATE HYDROCHLORIDE	0	
01500873	PIPERINE	0	
01502195	PIRACETAM	0	
01501138	PIRENZEPINE HYDROCHLORIDE	0	
01502045	PIROMIDIC ACID	0	
01500491	PIROXICAM	0	
02300332	PODOFILOX	0	
00201580	POMIFERIN	0	
01500113	POTASSIUM p-AMINOBENZOATE	0	0.93
01502043	PRALIDOXIME MESYLATE	0	
01501139	PRAMOXINE HYDROCHLORIDE	0	
01505803	PRAVASTATIN SODIUM	0	
01500494	PRAZIQUANTEL	0	
01500496	PREDNISOLONE	0	
01500497	PREDNISOLONE ACETATE	0	
01500499	PREDNISONE	0	
01505816	PREGABALIN	0	
01500645	PREGNENOLONE	0	
01503077	PRIDINOL METHANESULFONATE	0	
01503270	PRILOCAINE HYDROCHLORIDE	0	
01500500	PRIMAQUINE DIPHOSPHATE	0	
01500501	PRIMIDONE	0	
01504181	PRISTIMERIN	3	3.17
01502084	PROADIFEN HYDROCHLORIDE	0	
01500502	PROBENECID	0	
01501109	PROBUCOL	0	
01500503	PROCAINAMIDE HYDROCHLORIDE	0	
01500505	PROCHLORPERAZINE EDISYLATE	0	
01500507	PROCYCLIDINE HYDROCHLORIDE	0	
01500508	PROGESTERONE	0	
01501119	PROGLUMIDE	0	
01500509	PROMAZINE HYDROCHLORIDE	0	
01500510	PROMETHAZINE HYDROCHLORIDE	0	
01503628	PRONETALOL HYDROCHLORIDE	0	

01503935	PROPAFENONE HYDROCHLORIDE	3	5.02
01500511	PROPANTHELINE BROMIDE	0	
01505270	PROPRANOLOL HYDROCHLORIDE (+/-)	0	
01500515	PROPYLTHIOURACIL	0	
01505316	PROTHIONAMIDE	0	
01501111	PROTOPORPHYRIN IX	0	
01500938	PROTOVERATRINE B	0	
01500516	PSEUDOEPHEDRINE HYDROCHLORIDE	2	2.82
01501105	PUROMYCIN HYDROCHLORIDE	0	
01505300	PURPURIN	1	
01500517	PYRANTEL PAMOATE	0	
01500518	PYRAZINAMIDE	0	
01503240	PYRIDOSTIGMINE BROMIDE	0	
01500519	PYRILAMINE MALEATE	0	
01500520	PYRIMETHAMINE	0	
01500260	PYRITHIONE ZINC	-3	
01503085	PYRITHYLDIONE	0	
01500521	PYRVINIUM PAMOATE	0	
00310028	QUASSIN	0	
01500672	QUERCETIN	0	
01500752	QUERCITRIN	0	
01500522	QUINACRINE HYDROCHLORIDE	0	
01500759	QUINALIZARIN	0	
01503076	QUINAPRIL HYDROCHLORIDE	0	
01500523	QUINIDINE GLUCONATE	0	
01500524	QUININE SULFATE	0	
01502102	QUINOLINIC ACID	0	
01500525	RACEPHEDRINE HYDROCHLORIDE	0	
01503822	RAMIFENAZONE	0	
01501151	RANITIDINE	0	
01503639	RAUWOLSCINE HYDROCHLORIDE	-2	
01500527	RESORCINOL	0	
01503500	RESORCINOL MONOACETATE	0	
01502223	RESVERATROL	0	
01501203	RETINOL	0	
01503051	RETINYL ACETATE	0	
01503604	RETINYL PALMITATE	0	
01502243	RHAPONTIN	0	
01505347	RIBOFLAVIN	0	
01500529	RIFAMPIN	0	
01505321	RIFAXIMIN	-1	
01505348	RILUZOLE	0	
01501149	RITODRINE HYDROCHLORIDE	0	
01504235	ROFECOXIB	0	
01501154	RONIDAZOLE	0	
01504263	ROSIGLITAZONE	0	
01502094	ROSMARINIC ACID	0	
01500762	ROSOLIC ACID	0	
01505213	ROSUVASTATIN	0	
00200013	ROTENONE	0	

01500530	ROXARSONE	3	3.31
01503276	ROXITHROMYCIN	0	
00201606	RUTILANTINONE	0	
01502216	S-(1,2-DICARBOXYETHYL)GLUTATHIONE	1	1.99
01502215	S-METHYL-L-THIOCITRULLINE ACETATE	0	
01501171	SACCHARIN	1	1.91
01503620	SAFROLE	0	
01502255	SALICIN	-1	
01500531	SALICYL ALCOHOL	0	
01500532	SALICYLAMIDE	-2	
01503602	SALINOMYCIN, SODIUM	-1	
01504025	SALSOLINE	1	
01505314	SARAFLOXACIN HYDROCHLORIDE	0	
01500534	SCOPOLAMINE HYDROBROMIDE	0	
01505304	SECNIDAZOLE	-1	
01505334	SECURININE	0	
01503720	SELAMECTIN	-3	
01503422	SEMUSTINE	0	
01504078	SENNOSIDE A	0	
01505262	SERTRALINE HYDROCHLORIDE	0	
01505210	SIBUTRAMINE HYDROCHLORIDE	0	
01504099	SILDENAFIL	0	
01505256	SILIBININ	1	
01505253	SINOMENINE	0	
01500536	SISOMICIN SULFATE	0	
01502060	SNAP (S-NITROSO-N-ACETYLPENICILLAMINE)	0	
01503902	SODIUM beta-NICOTINAMIDE ADENINE DINUCLEOTIDE PHOSPHATE	1	
01500225	SODIUM DEHYDROCHOLATE	0	
01502193	SPAGLUMIC ACID	0	
01505241	SPARTEINE HYDROIODIDE	0	
00300548	SPARTEINE SULFATE	0	
01500538	SPECTINOMYCIN HYDROCHLORIDE	0	
01503940	SPERMIDINE TRIHYDROCHLORIDE	0	
01501152	SPIPERONE	0	
01503423	SPIRAMYCIN	1	
01500539	SPIRONOLACTONE	0	
01500541	STREPTOMYCIN SULFATE	0	
01500543	STREPTOZOSIN	3	3.39
01500651	STRYCHNINE	0	
01501148	SULCONAZOLE NITRATE	1	1.74
01500544	SULFABENZAMIDE	0	
01500545	SULFACETAMIDE	3	4.36
01501142	SULFACHLORPYRIDAZINE	0	
01500546	SULFADIAZINE	0	
01501144	SULFADIMETHOXINE	0	
01501146	SULFAGUANIDINE	0	
01500547	SULFAMERAZINE	0	
01501155	SULFAMETER	0	
01500548	SULFAMETHAZINE	0	

01500549	SULFAMETHIZOLE	0	
01500550	SULFAMETHOXAZOLE	0	
01501156	SULFAMETHOXYPYRIDAZINE	0	
01500646	SULFANILAMIDE	0	
01501143	SULFAPHENAZOLE	0	
01500551	SULFAPYRIDINE	0	
01500552	SULFASALAZINE	0	
01500553	SULFATHIAZOLE	2	2.66
01500554	SULFINPYRAZONE	0	
01500555	SULFISOXAZOLE	1	1.52
01500556	SULINDAC	3	4.97
01501153	SULOCTIDIL	0	
01501150	SULPIRIDE	1	1.75
01501161	SUPROFEN	0	
01500779	SUPROFEN METHYL ESTER	0	
01501157	SUXIBUZONE	0	
01500557	TAMOXIFEN CITRATE	0	
01504105	TANNIC ACID	3	4.21
01502213	TARGININE HYDROCHLORIDE	0	
01505215	TEGASEROD MALEATE	0	
01504187	TELENZEPINE HYDROCHLORIDE	0	
01505265	TELITHROMYCIN	0	
01504094	TENIPOSIDE	0	
01503142	TENOXICAM	0	
01500558	TERBUTALINE HEMISULFATE	0	
01500564	TETRACAINE HYDROCHLORIDE	0	
01504101	TETRACHLOROISOPHTHALONITRILE	3	2.83
01500566	TETRACYCLINE HYDROCHLORIDE	0	
01504178	TETRAHYDROPALMATINE	0	
01500567	TETRAHYDROZOLINE HYDROCHLORIDE	0	
01504185	TETRANDRINE	2	2.05
01502208	Tfa-VAL-TYR-VAL-OH	0	
01500649	THEOBROMINE	0	
01500568	THEOPHYLLINE	0	
01500570	THIABENDAZOLE	0	
01503136	THIAMPHENICOL	0	
01500572	THIMEROSAL	0	
01503941	THIOCTIC ACID	0	
01500573	THIOGUANINE	0	
01500575	THIORIDAZINE HYDROCHLORIDE	0	
01503324	THIOTEPA	0	
01500576	THIOTHIXENE	0	
01500774	THYROXINE	0	
01503086	TIAPRIDE HYDROCHLORIDE	0	
01500578	TIMOLOL MALEATE	0	
01502127	TINIDAZOLE	0	
01503094	TIOXOLONE	0	
01501174	TODRALAZINE HYDROCHLORIDE	0	
01501201	TOLAZAMIDE	0	
01500580	TOLAZOLINE HYDROCHLORIDE	-2	

01500581	TOLBUTAMIDE	0	
01501198	TOLFENAMIC ACID	0	
01500582	TOLMETIN SODIUM	0	
01500583	TOLNAFTATE	3	6.28
01504079	TOMATINE	0	
01505801	TOPIRAMATE	0	
01505211	TORSEMIDE	0	
01505264	TRANDOLAPRIL	0	
01502026	TRANEXAMIC ACID	0	
01505333	TRANILAST	0	
01500584	TRANYLCYPROMINE SULFATE	0	
01503121	TRAZODONE HYDROCHLORIDE	3	4.20
01502016	TRETINON	0	
01500585	TRIACETIN	0	
01505307	TRIADIMEFON	0	
01500586	TRIAMCINOLONE	0	
01500587	TRIAMCINOLONE ACETONIDE	0	
01500588	TRIAMCINOLONE DIACETATE	0	
01500589	TRIAMTERENE	0	
01500590	TRICHLORMETHIAZIDE	0	
01500591	TRIFLUOPERAZINE HYDROCHLORIDE	3	3.87
01500592	TRIHEXYPHENIDYL HYDROCHLORIDE	2	2.73
01504135	TRIMEDLURE	0	
01500593	TRIMEPRAZINE TARTRATE	0	
01500594	TRIMETHOBENZAMIDE HYDROCHLORIDE	0	
01500595	TRIMETHOPRIM	0	
01503117	TRIMIPRAMINE MALEATE	-3	
01500596	TRIOXSALEN	0	
01500598	TRIPROLIDINE HYDROCHLORIDE	0	
01500270	TRISODIUM ETHYLENEDIAMINE TETRACETATE	0	
01502203	TROLEANDOMYCIN	0	
01500599	TROPICAMIDE	0	
01505245	TROXERUTIN	-1	
01503922	TRYPTAMINE	0	
01500600	TRYPTOPHAN	2	2.32
01500601	TUAMINOHEPTANE SULFATE	1	1.38
01503954	TULOBUTEROL	0	
01505312	TYLOSIN TARTRATE	0	
01500603	TYROTHRICIN	0	
01503304	URETHANE	0	
01500605	URSODIOL	0	
00300147	USNIC ACID	0	
01504302	VALDECOXIB	0	
01505336	VALERYL SALYCILATE	0	
01500606	VALPROATE SODIUM	0	
01505209	VALSARTAN	0	
01502210	VALYLTRYPTOPHAN	-1	0.68
01500607	VANCOMYCIN HYDROCHLORIDE	0	
01504171	VENLAFAXINE	3	3.85

02300307	VERAPAMIL HYDROCHLORIDE	0	
01503662	VERATRIDINE	1	
00310300	VERATRINE SULFATE	0	
02300309	VESAMICOL HYDROCHLORIDE	0	
01500609	VIDARABINE	0	
01502239	VINBURNINE	0	
01500647	VINCAMINE	0	
01503115	VINPOCETINE	0	
00300146	VULPINIC ACID	-2	
01500754	XANTHURENIC ACID	0	
01501200	XYLAZINE	0	
01500614	XYLOMETAZOLINE HYDROCHLORIDE	0	
01500663	YOHIMBINE HYDROCHLORIDE	0	
01501199	ZAPRINAST	0	
01502109	ZIDOVUDINE [AZT]	0	
01505281	ZOLMITRIPTAN	1	1.76
01500615	ZOMEPIRAC SODIUM	0	
01504216	ZOXAZOLAMINE	0	

Appendix 2 –Prion symptom sheets

Note that scrapie cannot be diagnosed on even all of the early signs below, without the presence of at least one confirmatory sign.

2 early indicator signs plus 1 confirmatory sign or 2 confirmatory signs are observed contact lab

Date:	Mouse ID	Mouse ID	Mouse ID	Mouse ID	Mouse ID	Mouse ID	Mouse ID
Early indicators of prion disease							
Piloerection							
Sustained erect ears							
Intermittent generalised tremor							
Erect penis							
Clasping hind legs when lifted by tail							
Rigid tail							
Unsustained hunched posture							
Mild loss of co-ordination							
Confirmatory signs of prion disease							
Ataxia							
Impairment of righting reflex							
Dragging of hind limbs							
Sustained hunched posture							
Significant abnormal breathing							
Severe signs *(rare: less than 5% of animals)*							
Profound ataxia							
Complete lack of response to stimulation							
Unable to drink – looks dehydrated							
Unable to eat							
Extensive periods of prostration							
Non-specific signs							
Head shake							
Head tilt							
Agitation							
Aggression							
Unusual gait							
Apparent weight loss							
Eyes become dull							
Pale extremities							
An altered breathing rate							

Appendix 3 – H&E staining protocol

HAEMATOXYLIN AND EOSIN (H&E) STAINING SCHEDULE MRC TOXICOLOGY UNIT

Slide staining machine – Shandon Varistain 24-4 using the following schedule :

Container (minutes)	Reagent	Time
1	Xylene	2
2	Xylene	3
3	IMS	1
4	IMS	1
5	70 % IMS	1
6	Water	1
7	Haematoxylin	15
8	Water	1
9	1% Acid Alcohol	0.25
10	Water	6
11	Water	1
12	Water	2
13	1% Aqueous Eosin	3
14	Water	2
15	70% IMS	1
16	IMS	1
17	IMS	1
18	IMS	1
19	IMS	1
20	Xylene	2
21	Xylene	5

Results : Nuclei—*blue-black* , Cytoplasm—*varying shades of pink,* Muscle fibres—*deeply pinky red,*
Red blood cells—*orange/red,* Fibrin—*deep pink*

Xylene SLR (specified reagent for general laboratory work) (Fisher X/0200/PB17),IMS : - Industrial Methylated Spirit Grade 99 (obtained from stores),Hydrochloric acid HCl (Fisher H/1000/PB17),Harris Haematoxylin (Sigma HHS32-1L),Eosin Y (Sigma E4382)

Jennifer M. Edwards December 1985

Appendix 4 – Papers bound in

M Halliday, G.R. Mallucci, Targeting the unfolded protein response in neurodegeneration: A new approach to therapy, Neuropharmacology (2014), Jan;76 Pt A:169-74

J. A. Moreno, M. Halliday, C. Molloy, H. Radford, N. Verity, J. M. Axten, C. A. Ortori, A. E. Willis, P. M. Fischer, D. A. Barrett, G. R. Mallucci, Oral treatment targeting the unfolded protein response prevents neurodegeneration and clinical disease in prion-infected mice. Sci Transl (2013) Med 5, 206ra137

The published articles (pp. 192-207), detailed on the previous page, have been removed from the electronic version of this thesis due to copyright restrictions.

The unabridged version can be consulted at the University of Leicester Library.

References

Abisambra, J.F., Jinwal, U.K., Blair, L.J., O'Leary, J.C., 3rd, Li, Q., Brady, S., Wang, L., Guidi, C.E., Zhang, B., Nordhues, B.A., *et al.* (2013). Tau accumulation activates the unfolded protein response by impairing endoplasmic reticulum-associated degradation. J Neurosci *33*, 9498-9507.

Acosta-Alvear, D., Zhou, Y., Blais, A., Tsikitis, M., Lents, N.H., Arias, C., Lennon, C.J., Kluger, Y., and Dynlacht, B.D. (2007). XBP1 controls diverse cell type- and condition-specific transcriptional regulatory networks. Mol Cell *27*, 53-66.

Alper, T., Cramp, W.A., Haig, D.A., and Clarke, M.C. (1967). Does the agent of scrapie replicate without nucleic acid? Nature *214*, 764-766.

Alper, T., Haig, D.A., and Clarke, M.C. (1966). The exceptionally small size of the scrapie agent. Biochem Biophys Res Commun *22*, 278-284.

Andre, R., and Tabrizi, S.J. (2012). Misfolded PrP and a novel mechanism of proteasome inhibition. Prion *6*, 32-36.

Atkin, J.D., Farg, M.A., Walker, A.K., McLean, C., Tomas, D., and Horne, M.K. (2008). Endoplasmic reticulum stress and induction of the unfolded protein response in human sporadic amyotrophic lateral sclerosis. Neurobiol Dis *30*, 400-407.

Atkins, C., Liu, Q., Minthorn, E., Zhang, S.Y., Figueroa, D.J., Moss, K., Stanley, T.B., Sanders, B., Goetz, A., Gaul, N., *et al.* (2013). Characterization of a novel PERK kinase inhibitor with antitumor and antiangiogenic activity. Cancer Res *73*, 1993-2002.

Axten, J.M., Medina, J.R., Feng, Y., Shu, A., Romeril, S.P., Grant, S.W., Li, W.H., Heerding, D.A., Minthorn, E., Mencken, T., *et al.* (2012). Discovery of 7-methyl-5-(1-{[3-(trifluoromethyl)phenyl]acetyl}-2,3-dihydro-1H-indol-5-yl)-7H-p yrrolo[2,3-d]pyrimidin-4-amine (GSK2606414), a potent and selective first-in-class inhibitor of protein kinase R (PKR)-like endoplasmic reticulum kinase (PERK). J Med Chem *55*, 7193-7207.

Bellucci, A., Navarria, L., Zaltieri, M., Falarti, E., Bodei, S., Sigala, S., Battistin, L., Spillantini, M., Missale, C., and Spano, P. (2011). Induction of the unfolded protein response by alpha-synuclein in experimental models of Parkinson's disease. J Neurochem *116*, 588-605.

Bizat, N., Peyrin, J.M., Haik, S., Cochois, V., Beaudry, P., Laplanche, J.L., and Neri, C. (2010). Neuron dysfunction is induced by prion protein with an insertional mutation via a Fyn kinase and reversed by sirtuin activation in Caenorhabditis elegans. J Neurosci *30*, 5394-5403.

Blais, J.D., Filipenko, V., Bi, M., Harding, H.P., Ron, D., Koumenis, C., Wouters, B.G., and Bell, J.C. (2004). Activating transcription factor 4 is translationally regulated by hypoxic stress. Mol Cell Biol *24*, 7469-7482.

Bolton, D.C., and Bendheim, P.E. (1991). Purification of scrapie agents: how far have we come? Curr Top Microbiol Immunol *172*, 39-55.

Bounhar, Y., Zhang, Y., Goodyer, C.G., and LeBlanc, A. (2001). Prion protein protects human neurons against Bax-mediated apoptosis. J Biol Chem *276*, 39145-39149.

Bove, J., Martinez-Vicente, M., and Vila, M. (2011). Fighting neurodegeneration with rapamycin: mechanistic insights. Nat Rev Neurosci *12*, 437-452.

Boyce, M., Bryant, K.F., Jousse, C., Long, K., Harding, H.P., Scheuner, D., Kaufman, R.J., Ma, D., Coen, D.M., Ron, D.*, et al.* (2005). A selective inhibitor of eIF2alpha dephosphorylation protects cells from ER stress. Science *307*, 935-939.

Brandner, S., Isenmann, S., Raeber, A., Fischer, M., Sailer, A., Kobayashi, Y., Marino, S., Weissmann, C., and Aguzzi, A. (1996). Normal host prion protein necessary for scrapie-induced neurotoxicity. Nature *379*, 339-343.

Brann, D., Raz, L., Wang, R., Vadlamudi, R., and Zhang, Q. (2012). Oestrogen signalling and neuroprotection in cerebral ischaemia. Journal of neuroendocrinology *24*, 34-47.

Bravo, R., Parra, V., Gatica, D., Rodriguez, A.E., Torrealba, N., Paredes, F., Wang, Z.V., Zorzano, A., Hill, J.A., Jaimovich, E.*, et al.* (2013). Endoplasmic reticulum and the unfolded protein response: dynamics and metabolic integration. Int Rev Cell Mol Biol *301*, 215-290.

Bremer, J., Baumann, F., Tiberi, C., Wessig, C., Fischer, H., Schwarz, P., Steele, A.D., Toyka, K.V., Nave, K.A., Weis, J.*, et al.* (2010). Axonal prion protein is required for peripheral myelin maintenance. Nat Neurosci *13*, 310-318.

Brenner, S. (1974). The genetics of Caenorhabditis elegans. Genetics *77*, 71-94.

Brown, D.R. (1999). Prion protein expression aids cellular uptake and veratridine-induced release of copper. J Neurosci Res *58*, 717-725.

Brown, D.R., Nicholas, R.S., and Canevari, L. (2002). Lack of prion protein expression results in a neuronal phenotype sensitive to stress. J Neurosci Res *67*, 211-224.

Brown, D.R., Schulz-Schaeffer, W.J., Schmidt, B., and Kretzschmar, H.A. (1997). Prion protein-deficient cells show altered response to oxidative stress due to decreased SOD-1 activity. Exp Neurol *146*, 104-112.

Bueler, H., Aguzzi, A., Sailer, A., Greiner, R.A., Autenried, P., Aguet, M., and Weissmann, C. (1993). Mice devoid of PrP are resistant to scrapie. Cell *73*, 1339-1347.

Bueler, H., Fischer, M., Lang, Y., Bluethmann, H., Lipp, H.P., DeArmond, S.J., Prusiner, S.B., Aguet, M., and Weissmann, C. (1992). Normal development and

behaviour of mice lacking the neuronal cell-surface PrP protein. Nature *356*, 577-582.

Cai, W.J., Huang, J.H., Zhang, S.Q., Wu, B., Kapahi, P., Zhang, X.M., and Shen, Z.Y. (2011). Icariin and its derivative icariside II extend healthspan via insulin/IGF-1 pathway in C. elegans. PLoS One *6*, e28835.

Calfon, M., Zeng, H., Urano, F., Till, J.H., Hubbard, S.R., Harding, H.P., Clark, S.G., and Ron, D. (2002). IRE1 couples endoplasmic reticulum load to secretory capacity by processing the XBP-1 mRNA. Nature *415*, 92-96.

Carr, J.A., Parashar, A., Gibson, R., Robertson, A.P., Martin, R.J., and Pandey, S. (2011). A microfluidic platform for high-sensitivity, real-time drug screening on C. elegans and parasitic nematodes. Lab Chip *11*, 2385-2396.

Chang, R.C., Wong, A.K., Ng, H.K., and Hugon, J. (2002). Phosphorylation of eukaryotic initiation factor-2alpha (eIF2alpha) is associated with neuronal degeneration in Alzheimer's disease. Neuroreport *13*, 2429-2432.

Chesebro, B., Race, R., Wehrly, K., Nishio, J., Bloom, M., Lechner, D., Bergstrom, S., Robbins, K., Mayer, L., Keith, J.M*., et al.* (1985). Identification of scrapie prion protein-specific mRNA in scrapie-infected and uninfected brain. Nature *315*, 331-333.

Chesebro, B., Trifilo, M., Race, R., Meade-White, K., Teng, C., LaCasse, R., Raymond, L., Favara, C., Baron, G., Priola, S*., et al.* (2005). Anchorless prion protein results in infectious amyloid disease without clinical scrapie. Science *308*, 1435-1439.

Clemens, M.J. (2004). Targets and mechanisms for the regulation of translation in malignant transformation. Oncogene *23*, 3180-3188.

Cohen, P. (2002). Protein kinases--the major drug targets of the twenty-first century? Nat Rev Drug Discov *1*, 309-315.

Collinge, J., Brown, J., Hardy, J., Mullan, M., Rossor, M.N., Baker, H., Crow, T.J., Lofthouse, R., Poulter, M., Ridley, R*., et al.* (1992). Inherited prion disease with 144 base pair gene insertion. 2. Clinical and pathological features. Brain *115 (Pt 3)*, 687-710.

Collinge, J., and Palmer, M.S. (1994). Molecular genetics of human prion diseases. Philos Trans R Soc Lond B Biol Sci *343*, 371-378.

Collinge, J., Sidle, K.C., Meads, J., Ironside, J., and Hill, A.F. (1996). Molecular analysis of prion strain variation and the aetiology of 'new variant' CJD. Nature *383*, 685-690.

Collinge, J., Whittington, M.A., Sidle, K.C., Smith, C.J., Palmer, M.S., Clarke, A.R., and Jefferys, J.G. (1994). Prion protein is necessary for normal synaptic function. Nature *370*, 295-297.

Cookson, M.R. (2009). alpha-Synuclein and neuronal cell death. Mol Neurodegener *4*, 9.

Cuillé, J., and Chelle, P.-L. (1936). La maladie dite "tremblante" du mouton est-elle inoculable? Compte Rend Acad Sci *203*.

Deacon, R.M., Croucher, A., and Rawlins, J.N. (2002). Hippocampal cytotoxic lesion effects on species-typical behaviours in mice. Behav Brain Res *132*, 203-213.

Deacon, R.M., Penny, C., and Rawlins, J.N. (2003). Effects of medial prefrontal cortex cytotoxic lesions in mice. Behav Brain Res *139*, 139-155.

Deng, J., Harding, H.P., Raught, B., Gingras, A.C., Berlanga, J.J., Scheuner, D., Kaufman, R.J., Ron, D., and Sonenberg, N. (2002). Activation of GCN2 in UV-irradiated cells inhibits translation. Curr Biol *12*, 1279-1286.

DiMasi, J.A., Hansen, R.W., and Grabowski, H.G. (2003). The price of innovation: new estimates of drug development costs. J Health Econ *22*, 151-185.

Dinkova-Kostova, A.T., and Talalay, P. (1999). Relation of structure of curcumin analogs to their potencies as inducers of Phase 2 detoxification enzymes. Carcinogenesis *20*, 911-914.

Doh-ura, K., Ishikawa, K., Murakami-Kubo, I., Sasaki, K., Mohri, S., Race, R., and Iwaki, T. (2004). Treatment of transmissible spongiform encephalopathy by intraventricular drug infusion in animal models. J Virol *78*, 4999-5006.

Drisaldi, B., Coomaraswamy, J., Mastrangelo, P., Strome, B., Yang, J., Watts, J.C., Chishti, M.A., Marvi, M., Windl, O., Ahrens, R., *et al.* (2004). Genetic mapping of activity determinants within cellular prion proteins: N-terminal modules in PrPC offset pro-apoptotic activity of the Doppel helix B/B' region. J Biol Chem *279*, 55443-55454.

Dumas, J., Hancur-Bucci, C., Naylor, M., Sites, C., and Newhouse, P. (2008). Estradiol interacts with the cholinergic system to affect verbal memory in postmenopausal women: evidence for the critical period hypothesis. Hormones and behavior *53*, 159-169.

Fiebiger, E., Hirsch, C., Vyas, J.M., Gordon, E., Ploegh, H.L., and Tortorella, D. (2004). Dissection of the dislocation pathway for type I membrane proteins with a new small molecule inhibitor, eeyarestatin. Mol Biol Cell *15*, 1635-1646.

Frankowski, H., Alavez, S., Spilman, P., Mark, K.A., Nelson, J.D., Mollahan, P., Rao, R.V., Chen, S.F., Lithgow, G.J., and Ellerby, H.M. (2013). Dimethyl sulfoxide and dimethyl formamide increase lifespan of C. elegans in liquid. Mechanisms of ageing and development *134*, 69-78.

Gajdusek, D.C., Gibbs, C.J., and Alpers, M. (1966). Experimental transmission of a Kuru-like syndrome to chimpanzees. Nature *209*, 794-796.

Gajdusek, D.C., and Zigas, V. (1957). Degenerative disease of the central nervous system in New Guinea; the endemic occurrence of kuru in the native population. N Engl J Med *257*, 974-978.

Gambetti, P., Kong, Q., Zou, W., Parchi, P., and Chen, S.G. (2003). Sporadic and familial CJD: classification and characterisation. Br Med Bull *66*, 213-239.

Garsin, D.A., Sifri, C.D., Mylonakis, E., Qin, X., Singh, K.V., Murray, B.E., Calderwood, S.B., and Ausubel, F.M. (2001). A simple model host for identifying Gram-positive virulence factors. Proc Natl Acad Sci U S A *98*, 10892-10897.

Gibbs, C.J., Jr., Joy, A., Heffner, R., Franko, M., Miyazaki, M., Asher, D.M., Parisi, J.E., Brown, P.W., and Gajdusek, D.C. (1985). Clinical and pathological features and laboratory confirmation of Creutzfeldt-Jakob disease in a recipient of pituitary-derived human growth hormone. N Engl J Med *313*, 734-738.

Gill, M.S., Olsen, A., Sampayo, J.N., and Lithgow, G.J. (2003). An automated high-throughput assay for survival of the nematode Caenorhabditis elegans. Free radical biology & medicine *35*, 558-565.

Gohel, C., Grigoriev, V., Escaig-Haye, F., Lasmezas, C.I., Deslys, J.P., Langeveld, J., Akaaboune, M., Hantai, D., and Fournier, J.G. (1999). Ultrastructural localization of cellular prion protein (PrPc) at the neuromuscular junction. J Neurosci Res *55*, 261-267.

Gordon, W.S. (1946). Advances in veterinary research. Vet Rec *58*, 516-525.

Gosai, S.J., Kwak, J.H., Luke, C.J., Long, O.S., King, D.E., Kovatch, K.J., Johnston, P.A., Shun, T.Y., Lazo, J.S., Perlmutter, D.H.*, et al.* (2010). Automated high-content live animal drug screening using C. elegans expressing the aggregation prone serpin alpha1-antitrypsin Z. PLoS One *5*, e15460.

Griffith, J.S. (1967). Self-replication and scrapie. Nature *215*, 1043-1044.

Hadlow, W.J. (1959). Scrapie and kuru. Lancet *ii*, 289-290.

Halliday, M., and Mallucci, G.R. (2014). Targeting the unfolded protein response in neurodegeneration: A new approach to therapy. Neuropharmacology *76 Pt A*, 169-174.

Hamos, J.E., Oblas, B., Pulaski-Salo, D., Welch, W.J., Bole, D.G., and Drachman, D.A. (1991). Expression of heat shock proteins in Alzheimer's disease. Neurology *41*, 345-350.

Han, A.P., Yu, C., Lu, L., Fujiwara, Y., Browne, C., Chin, G., Fleming, M., Leboulch, P., Orkin, S.H., and Chen, J.J. (2001). Heme-regulated eIF2alpha kinase (HRI) is required for translational regulation and survival of erythroid precursors in iron deficiency. EMBO J *20*, 6909-6918.

Han, J., Back, S.H., Hur, J., Lin, Y.H., Gildersleeve, R., Shan, J., Yuan, C.L., Krokowski, D., Wang, S., Hatzoglou, M.*, et al.* (2013). ER-stress-induced transcriptional

regulation increases protein synthesis leading to cell death. Nat Cell Biol *15*, 481-490.

Harding, H.P., Zeng, H., Zhang, Y., Jungries, R., Chung, P., Plesken, H., Sabatini, D.D., and Ron, D. (2001). Diabetes mellitus and exocrine pancreatic dysfunction in perk-/- mice reveals a role for translational control in secretory cell survival. Mol Cell *7*, 1153-1163.

Harding, H.P., Zhang, Y., and Ron, D. (1999). Protein translation and folding are coupled by an endoplasmic-reticulum-resident kinase. Nature *397*, 271-274.

Hardy, J., and Selkoe, D.J. (2002). The amyloid hypothesis of Alzheimer's disease: progress and problems on the road to therapeutics. Science *297*, 353-356.

Hatters, D.M. (2008). Protein misfolding inside cells: the case of huntingtin and Huntington's disease. IUBMB Life *60*, 724-728.

Hay, N., and Sonenberg, N. (2004). Upstream and downstream of mTOR. Genes & development *18*, 1926-1945.

Haze, K., Yoshida, H., Yanagi, H., Yura, T., and Mori, K. (1999). Mammalian transcription factor ATF6 is synthesized as a transmembrane protein and activated by proteolysis in response to endoplasmic reticulum stress. Mol Biol Cell *10*, 3787-3799.

He, C.H., Gong, P., Hu, B., Stewart, D., Choi, M.E., Choi, A.M., and Alam, J. (2001). Identification of activating transcription factor 4 (ATF4) as an Nrf2-interacting protein. Implication for heme oxygenase-1 gene regulation. J Biol Chem *276*, 20858-20865.

Hegedus, C., Lakatos, P., Kiss-Szikszai, A., Patonay, T., Gergely, S., Gregus, A., Bai, P., Hasko, G., Szabo, E., and Virag, L. (2013). Cytoprotective dibenzoylmethane derivatives protect cells from oxidative stress-induced necrotic cell death. Pharmacol Res *72*, 25-34.

Hetz, C., Russelakis-Carneiro, M., Maundrell, K., Castilla, J., and Soto, C. (2003). Caspase-12 and endoplasmic reticulum stress mediate neurotoxicity of pathological prion protein. EMBO J *22*, 5435-5445.

Hill, A.F., and Collinge, J. (2003). Subclinical prion infection. Trends Microbiol *11*, 578-584.

Hill, A.F., Desbruslais, M., Joiner, S., Sidle, K.C., Gowland, I., Collinge, J., Doey, L.J., and Lantos, P. (1997). The same prion strain causes vCJD and BSE. Nature *389*, 448-450, 526.

Hinnebusch, A.G., and Lorsch, J.R. (2012). The mechanism of eukaryotic translation initiation: new insights and challenges. Cold Spring Harbor perspectives in biology *4*.

Hoozemans, J.J., van Haastert, E.S., Eikelenboom, P., de Vos, R.A., Rozemuller, J.M., and Scheper, W. (2007). Activation of the unfolded protein response in Parkinson's disease. Biochem Biophys Res Commun *354*, 707-711.

Hoozemans, J.J., van Haastert, E.S., Nijholt, D.A., Rozemuller, A.J., Eikelenboom, P., and Scheper, W. (2009). The unfolded protein response is activated in pretangle neurons in Alzheimer's disease hippocampus. Am J Pathol *174*, 1241-1251.

Hoozemans, J.J., Veerhuis, R., Van Haastert, E.S., Rozemuller, J.M., Baas, F., Eikelenboom, P., and Scheper, W. (2005). The unfolded protein response is activated in Alzheimer's disease. Acta Neuropathol *110*, 165-172.

Hope, J., Ritchie, L., Farquhar, C., Somerville, R., and Hunter, N. (1989). Bovine spongiform encephalopathy: a scrapie-like disease of British cattle. Prog Clin Biol Res *317*, 659-667.

Huang, M.T., Lou, Y.R., Xie, J.G., Ma, W., Lu, Y.P., Yen, P., Zhu, B.T., Newmark, H., and Ho, C.T. (1998). Effect of dietary curcumin and dibenzoylmethane on formation of 7,12-dimethylbenz[a]anthracene-induced mammary tumors and lymphomas/leukemias in Sencar mice. Carcinogenesis *19*, 1697-1700.

Imai, Y., Soda, M., and Takahashi, R. (2000). Parkin suppresses unfolded protein stress-induced cell death through its E3 ubiquitin-protein ligase activity. J Biol Chem *275*, 35661-35664.

Iwawaki, T., Hosoda, A., Okuda, T., Kamigori, Y., Nomura-Furuwatari, C., Kimata, Y., Tsuru, A., and Kohno, K. (2001). Translational control by the ER transmembrane kinase/ribonuclease IRE1 under ER stress. Nat Cell Biol *3*, 158-164.

Jackson, G.S., Murray, I., Hosszu, L.L., Gibbs, N., Waltho, J.P., Clarke, A.R., and Collinge, J. (2001). Location and properties of metal-binding sites on the human prion protein. Proc Natl Acad Sci U S A *98*, 8531-8535.

Jiang, Z., Belforte, J.E., Lu, Y., Yabe, Y., Pickel, J., Smith, C.B., Je, H.S., Lu, B., and Nakazawa, K. (2010). eIF2alpha Phosphorylation-dependent translation in CA1 pyramidal cells impairs hippocampal memory consolidation without affecting general translation. J Neurosci *30*, 2582-2594.

Joffe, H., Hall, J.E., Gruber, S., Sarmiento, I.A., Cohen, L.S., Yurgelun-Todd, D., and Martin, K.A. (2006). Estrogen therapy selectively enhances prefrontal cognitive processes: a randomized, double-blind, placebo-controlled study with functional magnetic resonance imaging in perimenopausal and recently postmenopausal women. Menopause *13*, 411-422.

Jucker, M. (2010). The benefits and limitations of animal models for translational research in neurodegenerative diseases. Nat Med *16*, 1210-1214.

Kanaani, J., Prusiner, S.B., Diacovo, J., Baekkeskov, S., and Legname, G. (2005). Recombinant prion protein induces rapid polarization and development of

synapses in embryonic rat hippocampal neurons in vitro. J Neurochem *95*, 1373-1386.

Katayama, T., Imaizumi, K., Manabe, T., Hitomi, J., Kudo, T., and Tohyama, M. (2004). Induction of neuronal death by ER stress in Alzheimer's disease. J Chem Neuroanat *28*, 67-78.

Kawas, C., Resnick, S., Morrison, A., Brookmeyer, R., Corrada, M., Zonderman, A., Bacal, C., Lingle, D.D., and Metter, E. (1997). A prospective study of estrogen replacement therapy and the risk of developing Alzheimer's disease: the Baltimore Longitudinal Study of Aging. Neurology *48*, 1517-1521.

Kayed, R., Head, E., Thompson, J.L., McIntire, T.M., Milton, S.C., Cotman, C.W., and Glabe, C.G. (2003). Common structure of soluble amyloid oligomers implies common mechanism of pathogenesis. Science *300*, 486-489.

Khor, T.O., Yu, S., Barve, A., Hao, X., Hong, J.L., Lin, W., Foster, B., Huang, M.T., Newmark, H.L., and Kong, A.N. (2009). Dietary feeding of dibenzoylmethane inhibits prostate cancer in transgenic adenocarcinoma of the mouse prostate model. Cancer Res *69*, 7096-7102.

Kim, I., Xu, W., and Reed, J.C. (2008). Cell death and endoplasmic reticulum stress: disease relevance and therapeutic opportunities. Nat Rev Drug Discov *7*, 1013-1030.

Kirkwood, J.K., and Cunningham, A.A. (1994). Epidemiological observations on spongiform encephalopathies in captive wild animals in the British Isles. Vet Rec *135*, 296-303.

Kirkwood, J.K., Wells, G.A., Wilesmith, J.W., Cunningham, A.A., and Jackson, S.I. (1990). Spongiform encephalopathy in an arabian oryx (Oryx leucoryx) and a greater kudu (Tragelaphus strepsiceros). Vet Rec *127*, 418-420.

Klohn, P.C., Farmer, M., Linehan, J.M., O'Malley, C., Fernandez de Marco, M., Taylor, W., Farrow, M., Khalili-Shirazi, A., Brandner, S., and Collinge, J. (2012). PrP antibodies do not trigger mouse hippocampal neuron apoptosis. Science *335*, 52.

Kocisko, D.A., Baron, G.S., Rubenstein, R., Chen, J., Kuizon, S., and Caughey, B. (2003). New inhibitors of scrapie-associated prion protein formation in a library of 2000 drugs and natural products. J Virol *77*, 10288-10294.

Kocisko, D.A., Vaillant, A., Lee, K.S., Arnold, K.M., Bertholet, N., Race, R.E., Olsen, E.A., Juteau, J.M., and Caughey, B. (2006). Potent antiscrapie activities of degenerate phosphorothioate oligonucleotides. Antimicrob Agents Chemother *50*, 1034-1044.

Krishnamoorthy, T., Pavitt, G.D., Zhang, F., Dever, T.E., and Hinnebusch, A.G. (2001). Tight binding of the phosphorylated alpha subunit of initiation factor 2 (eIF2alpha) to the regulatory subunits of guanine nucleotide exchange factor eIF2B is required for inhibition of translation initiation. Mol Cell Biol *21*, 5018-5030.

Kwok, T.C., Ricker, N., Fraser, R., Chan, A.W., Burns, A., Stanley, E.F., McCourt, P., Cutler, S.R., and Roy, P.J. (2006). A small-molecule screen in C. elegans yields a new calcium channel antagonist. Nature *441*, 91-95.

Lai, E., Teodoro, T., and Volchuk, A. (2007). Endoplasmic reticulum stress: signaling the unfolded protein response. Physiology (Bethesda) *22*, 193-201.

Lebert, F., Stekke, W., Hasenbroekx, C., and Pasquier, F. (2004). Frontotemporal dementia: a randomised, controlled trial with trazodone. Dement Geriatr Cogn Disord *17*, 355-359.

Lee, J.M., Calkins, M.J., Chan, K., Kan, Y.W., and Johnson, J.A. (2003). Identification of the NF-E2-related factor-2-dependent genes conferring protection against oxidative stress in primary cortical astrocytes using oligonucleotide microarray analysis. J Biol Chem *278*, 12029-12038.

Lehmann, S., Milhavet, O., and Mange, A. (1999). Trafficking of the cellular isoform of the prion protein. Biomedicine & pharmacotherapy = Biomedecine & pharmacotherapie *53*, 39-46.

Leung, C.K., Wang, Y., Malany, S., Deonarine, A., Nguyen, K., Vasile, S., and Choe, K.P. (2013). An ultra high-throughput, whole-animal screen for small molecule modulators of a specific genetic pathway in Caenorhabditis elegans. PLoS One *8*, e62166.

Lin, M.T., and Beal, M.F. (2006). Mitochondrial dysfunction and oxidative stress in neurodegenerative diseases. Nature *443*, 787-795.

Lin, X., Yu, S., Chen, Y., Wu, J., Zhao, J., and Zhao, Y. (2012). Neuroprotective effects of diallyl sulfide against transient focal cerebral ischemia via anti-apoptosis in rats. Neurological research *34*, 32-37.

Lo, R.Y., Shyu, W.C., Lin, S.Z., Wang, H.J., Chen, S.S., and Li, H. (2007). New molecular insights into cellular survival and stress responses: neuroprotective role of cellular prion protein (PrPC). Mol Neurobiol *35*, 236-244.

Lopez-Pousa, S., Garre-Olmo, J., Vilalta-Franch, J., Turon-Estrada, A., and Pericot-Nierga, I. (2008). Trazodone for Alzheimer's disease: a naturalistic follow-up study. Archives of gerontology and geriatrics *47*, 207-215.

Ma, J., and Lindquist, S. (1999). De novo generation of a PrPSc-like conformation in living cells. Nat Cell Biol *1*, 358-361.

Ma, J., and Lindquist, S. (2001). Wild-type PrP and a mutant associated with prion disease are subject to retrograde transport and proteasome degradation. Proc Natl Acad Sci U S A *98*, 14955-14960.

Ma, J., and Lindquist, S. (2002). Conversion of PrP to a self-perpetuating PrPSc-like conformation in the cytosol. Science *298*, 1785-1788.

Ma, J., Wollmann, R., and Lindquist, S. (2002). Neurotoxicity and neurodegeneration when PrP accumulates in the cytosol. Science *298*, 1781-1785.

Ma, T., Trinh, M.A., Wexler, A.J., Bourbon, C., Gatti, E., Pierre, P., Cavener, D.R., and Klann, E. (2013). Suppression of eIF2alpha kinases alleviates Alzheimer's disease-related plasticity and memory deficits. Nat Neurosci *16*, 1299-1305.

Ma, Y., and Hendershot, L.M. (2003). Delineation of a negative feedback regulatory loop that controls protein translation during endoplasmic reticulum stress. J Biol Chem *278*, 34864-34873.

Ma, Y., and Hendershot, L.M. (2004). The role of the unfolded protein response in tumour development: friend or foe? Nature reviews Cancer *4*, 966-977.

Maki, P.M. (2006). Hormone therapy and cognitive function: is there a critical period for benefit? Neuroscience *138*, 1027-1030.

Malberg, J.E., Eisch, A.J., Nestler, E.J., and Duman, R.S. (2000). Chronic antidepressant treatment increases neurogenesis in adult rat hippocampus. J Neurosci *20*, 9104-9110.

Mallucci, G., and Collinge, J. (2005). Rational targeting for prion therapeutics. Nat Rev Neurosci *6*, 23-34.

Mallucci, G., Dickinson, A., Linehan, J., Klohn, P.C., Brandner, S., and Collinge, J. (2003). Depleting neuronal PrP in prion infection prevents disease and reverses spongiosis. Science *302*, 871-874.

Mallucci, G.R., Campbell, T.A., Dickinson, A., Beck, J., Holt, M., Plant, G., de Pauw, K.W., Hakin, R.N., Clarke, C.E., Howell, S.*, et al.* (1999). Inherited prion disease with an alanine to valine mutation at codon 117 in the prion protein gene. Brain *122 (Pt 10)*, 1823-1837.

Mallucci, G.R., Ratte, S., Asante, E.A., Linehan, J., Gowland, I., Jefferys, J.G., and Collinge, J. (2002). Post-natal knockout of prion protein alters hippocampal CA1 properties, but does not result in neurodegeneration. EMBO J *21*, 202-210.

Mallucci, G.R., White, M.D., Farmer, M., Dickinson, A., Khatun, H., Powell, A.D., Brandner, S., Jefferys, J.G., and Collinge, J. (2007). Targeting cellular prion protein reverses early cognitive deficits and neurophysiological dysfunction in prion-infected mice. Neuron *53*, 325-335.

Manson, J., West, J.D., Thomson, V., McBride, P., Kaufman, M.H., and Hope, J. (1992). The prion protein gene: a role in mouse embryogenesis? Development *115*, 117-122.

Manson, J.C., Clarke, A.R., Hooper, M.L., Aitchison, L., McConnell, I., and Hope, J. (1994a). 129/Ola mice carrying a null mutation in PrP that abolishes mRNA production are developmentally normal. Mol Neurobiol *8*, 121-127.

Manson, J.C., Clarke, A.R., McBride, P.A., McConnell, I., and Hope, J. (1994b). PrP gene dosage determines the timing but not the final intensity or distribution of lesions in scrapie pathology. Neurodegeneration *3*, 331-340.

McKinley, M.P., Bolton, D.C., and Prusiner, S.B. (1983). A protease-resistant protein is a structural component of the scrapie prion. Cell *35*, 57-62.

Merrick, W.C. (2004). Cap-dependent and cap-independent translation in eukaryotic systems. Gene *332*, 1-11.

Meusser, B., Hirsch, C., Jarosch, E., and Sommer, T. (2005). ERAD: the long road to destruction. Nat Cell Biol *7*, 766-772.

Michelitsch, M.D., and Weissman, J.S. (2000). A census of glutamine/asparagine-rich regions: implications for their conserved function and the prediction of novel prions. Proc Natl Acad Sci U S A *97*, 11910-11915.

Monti, J.M., Pellejero, T., and Jantos, H. (1986). Effects of H1- and H2-histamine receptor agonists and antagonists on sleep and wakefulness in the rat. Journal of neural transmission *66*, 1-11.

Moore, R.C., Lee, I.Y., Silverman, G.L., Harrison, P.M., Strome, R., Heinrich, C., Karunaratne, A., Pasternak, S.H., Chishti, M.A., Liang, Y.*, et al.* (1999). Ataxia in prion protein (PrP)-deficient mice is associated with upregulation of the novel PrP-like protein doppel. J Mol Biol *292*, 797-817.

Moreno, J.A., Halliday, M., Molloy, C., Radford, H., Verity, N., Axten, J.M., Ortori, C.A., Willis, A.E., Fischer, P.M., Barrett, D.A.*, et al.* (2013). Oral treatment targeting the unfolded protein response prevents neurodegeneration and clinical disease in prion-infected mice. Sci Transl Med *5*, 206ra138.

Moreno, J.A., Radford, H., Peretti, D., Steinert, J.R., Verity, N., Martin, M.G., Halliday, M., Morgan, J., Dinsdale, D., Ortori, C.A.*, et al.* (2012). Sustained translational repression by eIF2alpha-P mediates prion neurodegeneration. Nature *485*, 507-511.

Nakagawa, T., Zhu, H., Morishima, N., Li, E., Xu, J., Yankner, B.A., and Yuan, J. (2000). Caspase-12 mediates endoplasmic-reticulum-specific apoptosis and cytotoxicity by amyloid-beta. Nature *403*, 98-103.

Nijholt, D.A., de Graaf, T.R., van Haastert, E.S., Oliveira, A.O., Berkers, C.R., Zwart, R., Ovaa, H., Baas, F., Hoozemans, J.J., and Scheper, W. (2011). Endoplasmic reticulum stress activates autophagy but not the proteasome in neuronal cells: implications for Alzheimer's disease. Cell Death Differ *18*, 1071-1081.

Nijholt, D.A., van Haastert, E.S., Rozemuller, A.J., Scheper, W., and Hoozemans, J.J. (2012). The unfolded protein response is associated with early tau pathology in the hippocampus of tauopathies. J Pathol *226*, 693-702.

Novoa, I., Zeng, H., Harding, H.P., and Ron, D. (2001). Feedback inhibition of the unfolded protein response by GADD34-mediated dephosphorylation of eIF2alpha. J Cell Biol *153*, 1011-1022.

Nukazuka, A., Fujisawa, H., Inada, T., Oda, Y., and Takagi, S. (2008). Semaphorin controls epidermal morphogenesis by stimulating mRNA translation via eIF2alpha in Caenorhabditis elegans. Genes & development *22*, 1025-1036.

Nussbaum-Krammer, C.I., Park, K.W., Li, L., Melki, R., and Morimoto, R.I. (2013). Spreading of a prion domain from cell-to-cell by vesicular transport in Caenorhabditis elegans. PLoS Genet *9*, e1003351.

O'Connor, T., Sadleir, K.R., Maus, E., Velliquette, R.A., Zhao, J., Cole, S.L., Eimer, W.A., Hitt, B., Bembinster, L.A., Lammich, S.*, et al.* (2008). Phosphorylation of the translation initiation factor eIF2alpha increases BACE1 levels and promotes amyloidogenesis. Neuron *60*, 988-1009.

Olden, K., Pratt, R.M., Jaworski, C., and Yamada, K.M. (1979). Evidence for role of glycoprotein carbohydrates in membrane transport: specific inhibition by tunicamycin. Proc Natl Acad Sci U S A *76*, 791-795.

Park, K.W., and Li, L. (2008). Cytoplasmic expression of mouse prion protein causes severe toxicity in Caenorhabditis elegans. Biochem Biophys Res Commun *372*, 697-702.

Pauwels, K., Gijsbers, R., Toelen, J., Schambach, A., Willard-Gallo, K., Verheust, C., Debyser, Z., and Herman, P. (2009). State-of-the-art lentiviral vectors for research use: risk assessment and biosafety recommendations. Curr Gene Ther *9*, 459-474.

Prusiner, S.B. (1982). Novel proteinaceous infectious particles cause scrapie. Science *216*, 136-144.

Prusiner, S.B. (1989). Scrapie prions. Annu Rev Microbiol *43*, 345-374.

Qin, K., Zhao, L., Tang, Y., Bhatta, S., Simard, J.M., and Zhao, R.Y. (2006). Doppel-induced apoptosis and counteraction by cellular prion protein in neuroblastoma and astrocytes. Neuroscience *141*, 1375-1388.

Re, L., Rossini, F., Re, F., Bordicchia, M., Mercanti, A., Fernandez, O.S., and Barocci, S. (2006). Prion protein potentiates acetylcholine release at the neuromuscular junction. Pharmacol Res *53*, 62-68.

Reiling, J.H., Clish, C.B., Carette, J.E., Varadarajan, M., Brummelkamp, T.R., and Sabatini, D.M. (2011). A haploid genetic screen identifies the major facilitator domain containing 2A (MFSD2A) transporter as a key mediator in the response to tunicamycin. Proc Natl Acad Sci U S A *108*, 11756-11765.

Resende, R., Ferreiro, E., Pereira, C., and Oliveira, C.R. (2008). ER stress is involved in Abeta-induced GSK-3beta activation and tau phosphorylation. J Neurosci Res *86*, 2091-2099.

Richardson, C.E., Kinkel, S., and Kim, D.H. (2011). Physiological IRE-1-XBP-1 and PEK-1 signaling in Caenorhabditis elegans larval development and immunity. PLoS Genet *7*, e1002391.

Riesner, D., Kellings, K., Post, K., Wille, H., Serban, H., Groth, D., Baldwin, M.A., and Prusiner, S.B. (1996). Disruption of prion rods generates 10-nm spherical particles having high alpha-helical content and lacking scrapie infectivity. J Virol *70*, 1714-1722.

Ron, D., and Walter, P. (2007). Signal integration in the endoplasmic reticulum unfolded protein response. Nat Rev Mol Cell Biol *8*, 519-529.

Rubinsztein, D.C. (2006). The roles of intracellular protein-degradation pathways in neurodegeneration. Nature *443*, 780-786.

Sakagami, Y., Kudo, T., Tanimukai, H., Kanayama, D., Omi, T., Horiguchi, K., Okochi, M., Imaizumi, K., and Takeda, M. (2013). Involvement of endoplasmic reticulum stress in tauopathy. Biochem Biophys Res Commun *430*, 500-504.

Shen, X., Ellis, R.E., Lee, K., Liu, C.Y., Yang, K., Solomon, A., Yoshida, H., Morimoto, R., Kurnit, D.M., Mori, K.*, et al.* (2001). Complementary signaling pathways regulate the unfolded protein response and are required for C. elegans development. Cell *107*, 893-903.

Shen, X., Ellis, R.E., Sakaki, K., and Kaufman, R.J. (2005). Genetic interactions due to constitutive and inducible gene regulation mediated by the unfolded protein response in C. elegans. PLoS Genet *1*, e37.

Shi, Y., Vattem, K.M., Sood, R., An, J., Liang, J., Stramm, L., and Wek, R.C. (1998). Identification and characterization of pancreatic eukaryotic initiation factor 2 alpha-subunit kinase, PEK, involved in translational control. Mol Cell Biol *18*, 7499-7509.

Shim, J., Umemura, T., Nothstein, E., and Rongo, C. (2004). The unfolded protein response regulates glutamate receptor export from the endoplasmic reticulum. Mol Biol Cell *15*, 4818-4828.

Shimizu, E., Hashimoto, K., Okamura, N., Koike, K., Komatsu, N., Kumakiri, C., Nakazato, M., Watanabe, H., Shinoda, N., Okada, S.*, et al.* (2003). Alterations of serum levels of brain-derived neurotrophic factor (BDNF) in depressed patients with or without antidepressants. Biological psychiatry *54*, 70-75.

Shinjo, S., Mizotani, Y., Tashiro, E., and Imoto, M. (2013). Comparative analysis of the expression patterns of UPR-target genes caused by UPR-inducing compounds. Bioscience, biotechnology, and biochemistry *77*, 729-735.

Sidrauski, C., Acosta-Alvear, D., Khoutorsky, A., Vedantham, P., Hearn, B.R., Li, H., Gamache, K., Gallagher, C.M., Ang, K.K., Wilson, C.*, et al.* (2013). Pharmacological brake-release of mRNA translation enhances cognitive memory. eLife *2*, e00498.

Silveira, J.R., Raymond, G.J., Hughson, A.G., Race, R.E., Sim, V.L., Hayes, S.F., and Caughey, B. (2005). The most infectious prion protein particles. Nature *437*, 257-261.

Sitia, R., and Braakman, I. (2003). Quality control in the endoplasmic reticulum protein factory. Nature *426*, 891-894.

Sleigh, J.N., Buckingham, S.D., Esmaeili, B., Viswanathan, M., Cuppen, E., Westlund, B.M., and Sattelle, D.B. (2011). A novel Caenorhabditis elegans allele, smn-1(cb131), mimicking a mild form of spinal muscular atrophy, provides a convenient drug screening platform highlighting new and pre-approved compounds. Hum Mol Genet *20*, 245-260.

Smith, W.W., Jiang, H., Pei, Z., Tanaka, Y., Morita, H., Sawa, A., Dawson, V.L., Dawson, T.M., and Ross, C.A. (2005). Endoplasmic reticulum stress and mitochondrial cell death pathways mediate A53T mutant alpha-synuclein-induced toxicity. Hum Mol Genet *14*, 3801-3811.

Solforosi, L., Criado, J.R., McGavern, D.B., Wirz, S., Sanchez-Alavez, M., Sugama, S., DeGiorgio, L.A., Volpe, B.T., Wiseman, E., Abalos, G.*, et al.* (2004). Cross-linking cellular prion protein triggers neuronal apoptosis in vivo. Science *303*, 1514-1516.

Sonati, T., Reimann, R.R., Falsig, J., Baral, P.K., O'Connor, T., Hornemann, S., Yaganoglu, S., Li, B., Herrmann, U.S., Wieland, B.*, et al.* (2013). The toxicity of antiprion antibodies is mediated by the flexible tail of the prion protein. Nature.

Sood, R., Porter, A.C., Ma, K., Quilliam, L.A., and Wek, R.C. (2000). Pancreatic eukaryotic initiation factor-2alpha kinase (PEK) homologues in humans, Drosophila melanogaster and Caenorhabditis elegans that mediate translational control in response to endoplasmic reticulum stress. Biochem J *346 Pt 2*, 281-293.

Spriggs, K.A., Bushell, M., and Willis, A.E. (2010). Translational regulation of gene expression during conditions of cell stress. Mol Cell *40*, 228-237.

Spudich, A., Frigg, R., Kilic, E., Kilic, U., Oesch, B., Raeber, A., Bassetti, C.L., and Hermann, D.M. (2005). Aggravation of ischemic brain injury by prion protein deficiency: role of ERK-1/-2 and STAT-1. Neurobiol Dis *20*, 442-449.

Sreenan, S., Pick, A.J., Levisetti, M., Baldwin, A.C., Pugh, W., and Polonsky, K.S. (1999). Increased beta-cell proliferation and reduced mass before diabetes onset in the nonobese diabetic mouse. Diabetes *48*, 989-996.

Stahl, S.M. (2009). Mechanism of action of trazodone: a multifunctional drug. CNS spectrums *14*, 536-546.

Takano, K., Kitao, Y., Tabata, Y., Miura, H., Sato, K., Takuma, K., Yamada, K., Hibino, S., Choshi, T., Iinuma, M.*, et al.* (2007). A dibenzoylmethane derivative protects dopaminergic neurons against both oxidative stress and endoplasmic reticulum stress. American journal of physiology Cell physiology *293*, C1884-1894.

Tateishi, J., Brown, P., Kitamoto, T., Hoque, Z.M., Roos, R., Wollman, R., Cervenakova, L., and Gajdusek, D.C. (1995). First experimental transmission of fatal familial insomnia. Nature *376*, 434-435.

Thastrup, O., Cullen, P.J., Drobak, B.K., Hanley, M.R., and Dawson, A.P. (1990). Thapsigargin, a tumor promoter, discharges intracellular Ca2+ stores by specific inhibition of the endoplasmic reticulum Ca2(+)-ATPase. Proc Natl Acad Sci U S A *87*, 2466-2470.

Thimmulappa, R.K., Rangasamy, T., Alam, J., and Biswal, S. (2008). Dibenzoylmethane activates Nrf2-dependent detoxification pathway and inhibits benzo(a)pyrene induced DNA adducts in lungs. Medicinal chemistry *4*, 473-481.

Thomas, J.H. (2001). Nematodes are smarter than you think. Neuron *30*, 7-8.

Tobler, I., Gaus, S.E., Deboer, T., Achermann, P., Fischer, M., Rulicke, T., Moser, M., Oesch, B., McBride, P.A., and Manson, J.C. (1996). Altered circadian activity rhythms and sleep in mice devoid of prion protein. Nature *380*, 639-642.

Todd, N.V., Morrow, J., Doh-ura, K., Dealler, S., O'Hare, S., Farling, P., Duddy, M., and Rainov, N.G. (2005). Cerebroventricular infusion of pentosan polysulphate in human variant Creutzfeldt-Jakob disease. J Infect *50*, 394-396.

Tong, Y., Yamaguchi, H., Giaime, E., Boyle, S., Kopan, R., Kelleher, R.J., 3rd, and Shen, J. (2010). Loss of leucine-rich repeat kinase 2 causes impairment of protein degradation pathways, accumulation of alpha-synuclein, and apoptotic cell death in aged mice. Proc Natl Acad Sci U S A *107*, 9879-9884.

Torres, M., Castillo, K., Armisen, R., Stutzin, A., Soto, C., and Hetz, C. (2010). Prion protein misfolding affects calcium homeostasis and sensitizes cells to endoplasmic reticulum stress. PLoS One *5*, e15658.

Trevitt, C.R., and Collinge, J. (2006). A systematic review of prion therapeutics in experimental models. Brain *129*, 2241-2265.

Tsao, S.M., and Yin, M.C. (2001). In-vitro antimicrobial activity of four diallyl sulphides occurring naturally in garlic and Chinese leek oils. Journal of medical microbiology *50*, 646-649.

Unterberger, U., Hoftberger, R., Gelpi, E., Flicker, H., Budka, H., and Voigtlander, T. (2006). Endoplasmic reticulum stress features are prominent in Alzheimer disease but not in prion diseases in vivo. J Neuropathol Exp Neurol *65*, 348-357.

Urano, F., Calfon, M., Yoneda, T., Yun, C., Kiraly, M., Clark, S.G., and Ron, D. (2002). A survival pathway for Caenorhabditis elegans with a blocked unfolded protein response. J Cell Biol *158*, 639-646.

van Delft, M.F., and Huang, D.C. (2006). How the Bcl-2 family of proteins interact to regulate apoptosis. Cell Res *16*, 203-213.

Wang, X., Shi, Q., Xu, K., Gao, C., CHen, C., Li, X.L., Wang, G.R., Tian, C., Han, J., and Dong, X.P. (2011). Familial CJD Associated PrP Mutants within Transmembrane Region Induced Ctm-PrP Retention in ER and Triggered Apoptosis by ER Stress in SH-SY5Y Cells. PLoS One *6*, e14602.

Wang, X., Wang, X., Li, L., and Wang, D. (2010). Lifespan extension in Caenorhabditis elegans by DMSO is dependent on sir-2.1 and daf-16. Biochem Biophys Res Commun *400*, 613-618.

Wang, X.Z., Harding, H.P., Zhang, Y., Jolicoeur, E.M., Kuroda, M., and Ron, D. (1998). Cloning of mammalian Ire1 reveals diversity in the ER stress responses. EMBO J *17*, 5708-5717.

Weissmann, C. (1996). The Ninth Datta Lecture. Molecular biology of transmissible spongiform encephalopathies. FEBS Lett *389*, 3-11.

White, A.R., Enever, P., Tayebi, M., Mushens, R., Linehan, J., Brandner, S., Anstee, D., Collinge, J., and Hawke, S. (2003). Monoclonal antibodies inhibit prion replication and delay the development of prion disease. Nature *422*, 80-83.

White, J.G.S., J.N. Brenner, S. (1986). The structure of the nervous system of the nematode Caenorhabditis Elegans. Philos Trans R Soc Lond B Biol Sci *314*.

White, M.D., Farmer, M., Mirabile, I., Brandner, S., Collinge, J., and Mallucci, G.R. (2008). Single treatment with RNAi against prion protein rescues early neuronal dysfunction and prolongs survival in mice with prion disease. Proc Natl Acad Sci U S A *105*, 10238-10243.

Wickner, R.B., Taylor, K.L., Edskes, H.K., Maddelein, M.L., Moriyama, H., and Roberts, B.T. (2001). Yeast prions act as genes composed of self-propagating protein amyloids. Adv Protein Chem *57*, 313-334.

Will, R.G., Ironside, J.W., Zeidler, M., Cousens, S.N., Estibeiro, K., Alperovitch, A., Poser, S., Pocchiari, M., Hofman, A., and Smith, P.G. (1996). A new variant of Creutzfeldt-Jakob disease in the UK. Lancet *347*, 921-925.

Williams, E.S., and Young, S. (1993). Neuropathology of chronic wasting disease of mule deer (Odocoileus hemionus) and elk (Cervus elaphus nelsoni). Vet Pathol *30*, 36-45.

Wimo, A., Winblad, B., Aguero-Torres, H., and von Strauss, E. (2003). The magnitude of dementia occurrence in the world. Alzheimer Dis Assoc Disord *17*, 63-67.

Wong, B.S., Liu, T., Li, R., Pan, T., Petersen, R.B., Smith, M.A., Gambetti, P., Perry, G., Manson, J.C., Brown, D.R.*, et al.* (2001). Increased levels of oxidative stress markers detected in the brains of mice devoid of prion protein. J Neurochem *76*, 565-572.

Woo, C.W., Kutzler, L., Kimball, S.R., and Tabas, I. (2012). Toll-like receptor activation suppresses ER stress factor CHOP and translation inhibition through activation of eIF2B. Nat Cell Biol *14*, 192-200.

Wyatt, J.M., Pearson, G.R., Smerdon, T.N., Gruffydd-Jones, T.J., Wells, G.A., and Wilesmith, J.W. (1991). Naturally occurring scrapie-like spongiform encephalopathy in five domestic cats. Vet Rec *129*, 233-236.

Yan, X., Xing, J., Lorin-Nebel, C., Estevez, A.Y., Nehrke, K., Lamitina, T., and Strange, K. (2006). Function of a STIM1 homologue in C. elegans: evidence that store-operated Ca2+ entry is not essential for oscillatory Ca2+ signaling and ER Ca2+ homeostasis. The Journal of general physiology *128*, 443-459.

Yang, C.S., Chhabra, S.K., Hong, J.Y., and Smith, T.J. (2001). Mechanisms of inhibition of chemical toxicity and carcinogenesis by diallyl sulfide (DAS) and related compounds from garlic. The Journal of nutrition *131*, 1041S-1045S.

Yoo, B.C., Krapfenbauer, K., Cairns, N., Belay, G., Bajo, M., and Lubec, G. (2002). Overexpressed protein disulfide isomerase in brains of patients with sporadic Creutzfeldt-Jakob disease. Neurosci Lett *334*, 196-200.

Yu, W., and Lu, B. (2012). Synapses and dendritic spines as pathogenic targets in Alzheimer's disease. Neural Plast *2012*, 247150.

Zamarbide, M., Martinez-Pinilla, E., Ricobaraza, A., Aragon, T., Franco, R., and Perez-Mediavilla, A. (2013). Phenyl acyl acids attenuate the unfolded protein response in tunicamycin-treated neuroblastoma cells. PLoS One *8*, e71082.

Zhang, L., Yu, J., Pan, H., Hu, P., Hao, Y., Cai, W., Zhu, H., Yu, A.D., Xie, X., Ma, D., *et al.* (2007). Small molecule regulators of autophagy identified by an image-based high-throughput screen. Proc Natl Acad Sci U S A *104*, 19023-19028.

Zhang, P., McGrath, B., Li, S., Frank, A., Zambito, F., Reinert, J., Gannon, M., Ma, K., McNaughton, K., and Cavener, D.R. (2002). The PERK eukaryotic initiation factor 2 alpha kinase is required for the development of the skeletal system, postnatal growth, and the function and viability of the pancreas. Mol Cell Biol *22*, 3864-3874.

Zhao, L., and Ackerman, S.L. (2006). Endoplasmic reticulum stress in health and disease. Curr Opin Cell Biol *18*, 444-452.